

**DESIGN OF AN ORGANIC-LIQUID-PHASE/IMMOBILIZED-CELL REACTOR  
FOR THE MICROBIAL EPOXIDATION OF PROPENE**



CENTRALE LANDBOUWCATALOGUS

0000 0174 6037

Promotoren: dr.ir. K. van 't Riet, hoogleraar in de proceskunde  
ir. K.Ch.A.M. Luyben, hoogleraar in de bioprocestechnologie  
aan de Technische Universiteit Delft  
Co-promotor: dr.ir. J. Tramper, universitair hoofddocent

BIBLIOTHEEK  
DER  
TECHNISCHE HOOGESCHOOL  
DELFT

L.E.S. Brink

# **DESIGN OF AN ORGANIC-LIQUID-PHASE/IMMOBILIZED-CELL REACTOR FOR THE MICROBIAL EPOXIDATION OF PROPENE**

Proefschrift  
ter verkrijging van de graad van  
doctor in de landbouwwetenschappen,  
op gezag van de rector magnificus,  
dr. C.C. Oosterlee,  
in het openbaar te verdedigen  
op woensdag 5 november 1986  
des namiddags te vier uur in de aula  
van de Landbouwuniversiteit te Wageningen

## STELLINGEN

1. Het door Yamané et al. gehanteerde model, waarbij wordt uitgegaan van het bestaan van in een organisch solvent gesuspendeerde, vrije cellen, lijkt onrealistisch.
  - T. Yamané, H. Nakatani, E. Sada, T. Omata, A. Tanaka en S. Fukui *Biotechnol. Bioeng.* 1979, **21**, 2133–2145
2. Maximalisering van het verschil in polariteit tussen substraat en organisch solvent brengt, zeker in geval van immobilisatie in waterige gelen, de optimale situatie niet altijd dichterbij.
  - C. Laane, S. Boeren, K. Vos en C. Veeger, *Biotechnol. Bioeng.* (ter perse)
  - dit proefschrift, hoofdstuk 8
3. De heterogene biokatalyse verstrekt enige goede voorbeelden van de brede toepasbaarheid van chemisch-technologische principes.
  - dit proefschrift, hoofdstukken 4 en 6
4. Het uitdrukken van effectieve diffusiecoëfficiënten van zuurstof in dragermaterialen als percentage van de zuurstofdiffusiecoëfficiënt in water leidt tot verwarring als er niet van een gestandaardiseerde waarde voor de diffusiesnelheid van zuurstof in water gebruik wordt gemaakt.
  - P. Adlercreutz *Biotechnol. Bioeng.* 1986, **28**, 223–232
5. Bij het toekennen van betekenis aan biokinetiek- en stoftransportconstanten, die verkregen zijn door multi-parameter modellen te fitten aan experimentele waarnemingen, dient uiterste voorzichtigheid betracht te worden.
  - W.N. Marrazzo, R.L. Merson en B.J. McCoy *Biotechnol. Bioeng.* 1975, **17**, 1515–1528
  - T. Tsukamoto, S. Morita en J. Okada *Chem. Pharm. Bull.* 1982, **30**, 782–788
  - Y.H. Park, M.H. Han en H.-K. Rhee *J. Chem. Tech. Biotechnol.* 1984, **34B**, 57–69
  - J.M.S. Cabral, J.P. Cardoso, J.M. Novais en J.F. Kennedy *Enzyme Microb. Technol.* 1984, **6**, 365–370
  - R. Lortie en D. Thomas *Biotechnol. Bioeng.* (ter perse)
6. De niet in dit proefschrift beschreven, 'mislukte' experimenten hebben toch een belangrijke bijdrage geleverd aan het uiteindelijke resultaat.
7. Met behulp van computers vervaardigde presentaties van wetenschappelijke resultaten wekken vaak ten onrechte de indruk dat deze in een handomdraai gemaakt kunnen worden. Integendeel, de computer is bij wetenschappelijk onderzoek in belangrijke mate een hulpmiddel om werk van een hoger kwaliteitsniveau af te kunnen leveren, hetgeen zeker niet hetzelfde is als 'meer in minder tijd'.

8. Sommige ftalaat testers kunnen inmiddels ook tot de groep stoffen worden gerekend, waarvan de carcinogene en mutagene eigenschappen pijnlijk laat aan het licht zijn gekomen.
  - T. Wams, Xenobiotika en Beleid, Deel II: Voorbeeldstudie Ftalaat testers, doctoraalverslag biologie, Groningen, 1986
9. De terecht door vrijwel iedereen als verfoeilijk beoordeelde relatie tussen blank en zwart in Zuid-Afrika vertoont helaas nog al wat overeenkomsten met die tussen de Westerse ('Eerste') Wereld en de 'Derde Wereld'.
10. De titel van Pirsigs boek 'Zen and the art of motorcycle maintenance' had evengoed 'Zen and the art of writing of scientific papers' kunnen luiden.

L.E.S. Brink

Design of an Organic-Liquid-Phase/Immobilized-Cell Reactor for the Microbial Epoxidation of Propene

Wageningen, 5 november 1986

**Voor mijn vriendin**

Omslagillustratie uit 'Trends in Biotechnology' (1984, 2, 103).

# CONTENTS

1. General introduction	9
2. Automation of an experimental system for the microbial epoxidation of propene and 1-butene	19
3. Optimization of organic solvent in multiphase biocatalysis	31
4. Modelling the effects of mass transfer on kinetics of propene epoxidation of immobilized <i>Mycobacterium</i> cells: pseudo-one-substrate conditions and negligible product inhibition	43
5. Modelling the effects of mass transfer on kinetics of propene epoxidation of immobilized <i>Mycobacterium</i> cells: product inhibition	51
6. Facilitated mass transfer in a packed-bed immobilized-cell reactor by using an organic solvent as substrate reservoir	59
7. Production of propene oxide in an organic-liquid-phase/immobilized-cell reactor	83
8. Discussion	97
Summary	111
Samenvatting	113
Dankwoord	115
Curriculum vitae	117



The main part of this thesis has been published in the literature:

- chapter 2 L.E.S. Brink, J. Tramper, K. van 't Riet and K.Ch.A.M. Luyben, *Anal. Chim. Acta* 1984, **163**, 207–217
- chapter 3 L.E.S. Brink and J. Tramper, *Biotechnol. Bioeng.* 1985, **27**, 1258–1269
- chapter 4 L.E.S. Brink and J. Tramper, *Enzyme Microb. Technol.* 1986, **8**, 281–288
- chapter 5 L.E.S. Brink and J. Tramper, *Enzyme Microb. Technol.* 1986, **8**, 334–340
- chapter 6 L.E.S. Brink and J. Tramper, *J. Chem. Tech. Biotechnol.* (in press)
- chapter 7 L.E.S. Brink and J. Tramper, (submitted)

# 1. GENERAL INTRODUCTION

## 1.1 Non-Aqueous Solvent Systems in Biotechnological Processes

One of the main, current breakthroughs in biotechnology is catalysis in media, which are significantly less polar than aqueous solutions. The use of enzymes, cell organelles or whole cells (in short: biocatalysts) in these apparently anomalous environments is, however, not as amazing as it might seem. In their natural state many enzymes are associated with more or less non-polar, cellular elements, especially membranes [1]. Therefore, a strictly aqueous, highly polar microenvironment could often be more hostile to the biocatalyst than a less polar medium and, thus, could result in a reduced activity, specificity and/or stability. From this point of view, the at times remarkable reports on bioconversions in non-aqueous solvent systems, e.g. of Klibanov and co-workers, who carried out successfully enzymatic reactions at sometimes elevated temperatures in nearly anhydrous solvents [2, 3], can be more easily understood.

There could be many reasons to justify the use of organic media instead of aqueous solutions. The most important of these are:

- possibility of high concentrations of poorly water-soluble substrates/products
- shift of reaction equilibria as a result of the altered partitioning of substrates and products between the phases of interest
- shift of reaction equilibria (with water as one of the products) as a result of a substantially reduced water activity [4]
- reduction of substrate and/or product inhibition
- prevention of hydrolysis of substrates/products
- facilitated recovery of products and biocatalyst, even when the latter is not immobilized
- less risk of microbial contamination
- stabilization of the biocatalyst [1, 3].

It is, however, not likely that all the mentioned, advantageous effects will be relevant for one particular bioconversion. Disadvantages are primarily biocatalyst denaturation and/or inhibition by the organic solvent and the increasing complexity of the reaction system.

The degree of miscibility of an organic solvent with water will be highly decisive for the attractiveness of the solvent system. Water/organic solvent two-phase systems (with the biocatalyst in the aqueous phase) are generally believed to be more promising than water/water-miscible organic solvent systems. The latter do not show the advantages of reduced substrate/product inhibition and facilitated product/biocatalyst recovery. Also, the chance of inhibition or denaturation by the solvent is markedly smaller in biphasic systems as a result of the low concentration of the water-immiscible solvent in the aqueous biocatalyst phase. A potential danger for the biocatalyst in a solvent/water biphasic system is denaturation at the liquid/liquid interface. However, if required, this problem can be overcome by immobilizing the biocatalyst in the aqueous phase. Two-liquid-phase bioreactions, the central idea on which this thesis is based, will be considered in more detail in the following sections.

## 1.2 Water/Organic Solvent Two-Phase Bioreactions

In the first part of the seventies the earliest accounts of the since then ever growing literature on two-liquid-phase bioreactions started to appear. Not surprisingly, the transformation of steroids, with their very low solubility in water, was often chosen in these studies to demonstrate the usefulness of an additional organic phase. Pioneering work on biphasic systems was done by Antonini and co-workers [5-8]. Other innovating studies on steroid bioconversions in two-liquid-phase systems were performed by Buckland et al. [9], Duarte and Lilly [10], Omata et al. [11] and Yamané et al. [12]. Klibanov et al. [13] showed that biphasic systems could also successfully be used for the synthesis of ester bonds. Reviews on the subject of water/organic solvent two-phase systems were given by Antonini et al. [14], Lilly [15], Carrea [16] and Lilly and Woodley [17]. This research field is still attracting much attention as witness the many recent reports on biphasic and related systems (e.g. [18-23]).

The choice of the water-immiscible solvent will probably have the most far-reaching consequences for the design of a suitable water/organic solvent two-phase bioprocess [14, 15]. A significant effect of the type of solvent can be expected on the kinetics and stability of the biocatalyst [10, 24]. The solubility of reactants and products in the organic phase and the partitioning of these compounds between the different phases will be influenced by the character of the organic solvent. Also, recovery of the product can be facilitated by a proper choice of the type of solvent. Finally, the safety of the ultimate process, and hence operation costs, will be determined in part by solvent properties like flammability and toxicity. Choosing a truly optimal solvent is likely to be a complicated process. The number of employable, water-immiscible solvents, and of mixtures of such solvents, is almost unlimited. Furthermore, as it is improbable that an ideal solvent would exist, weighing of the various effects of solvent type against each other will be needed.

Immobilization of the biocatalyst has certain, well-proven benefits, like facilitated product/biocatalyst separation, continuous processing and, sometimes, increased stability [25-27]. As a consequence, the use of immobilized biocatalysts in two-liquid-phase systems is an interesting combination of two developing technologies. In two-liquid-phase/immobilized-biocatalyst systems immobilization could provide additional stability to the biocatalyst by protecting it against denaturing effects of the organic solvent. However, complications could arise from unwanted interactions between the solvent and the support material used in the immobilization technique. The type of support material is determining not only for the activity and stability of the biocatalyst, but also, in case of entrapment of the biocatalyst in natural or synthetic gels, for the hydrophilicity-hydrophobicity balance of the gel. The latter is, like the type of solvent employed, of importance for the partitioning of substrates and products between the biocatalyst phase and the liquid phases [28-30].

Inherent to the nature of the reaction system, water/organic solvent bioreactions are usually carried out in media involving two liquid phases. In case of an insoluble (immobilized) biocatalyst, a third, solid phase is present. Sometimes even a fourth phase, containing gaseous substrates and/or products, can be part of the multiphase reaction system. An elucidating classification of these, potentially very complex systems has been proposed by Lilly and Woodley [17]. The authors distinguished three forms of theoretical concentration profiles (Figure 1) in addition to three types of aqueous phase configurations (1: discrete continuous, 2: discrete discontinuous,

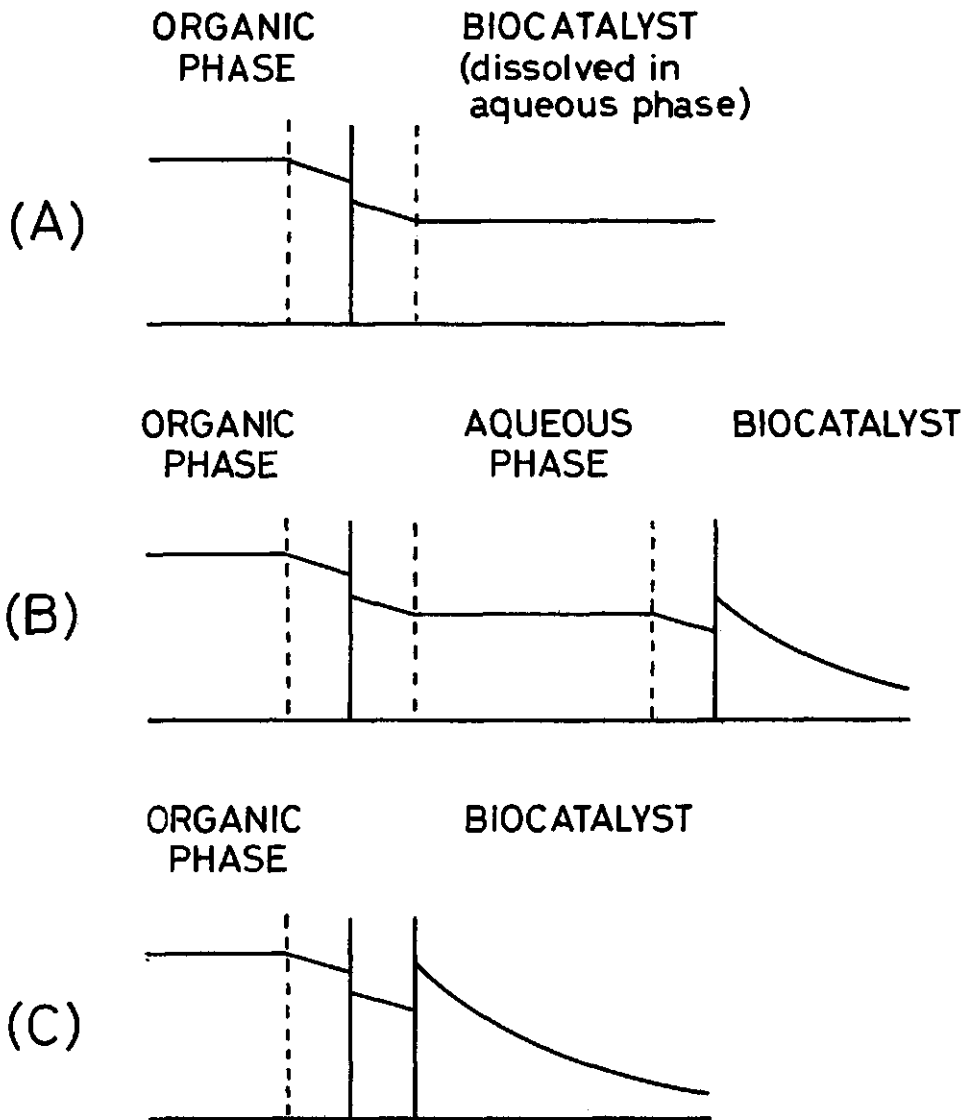


**Figure 1.** The three theoretical concentration profiles possible in water/organic solvent two-phase biocatalytic systems (reproduced from reference 17 with permission).

3: non-discrete). The five reaction systems, which are theoretically possible if these two discriminations are made, are schematically shown in Figure 2. The combination

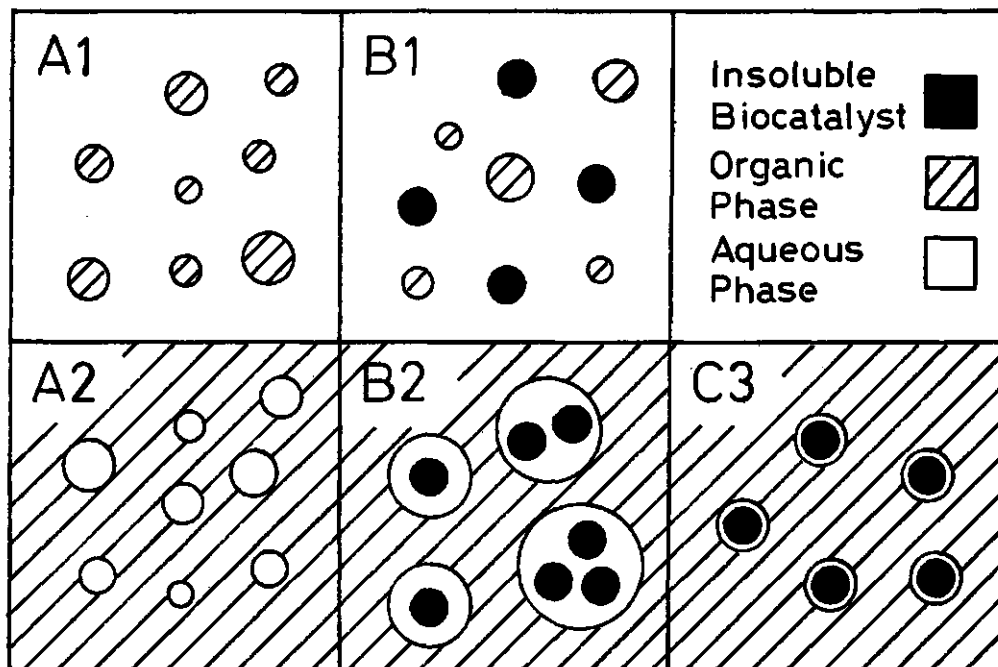


**Figure 2.** The five two-liquid-phase reaction systems distinguished by Lilly and Woodley (reproduced from reference 17 with permission).

profile C/non-discrete aqueous phase (C3 in Figure 2) is somewhat different from the other four systems (A1, B1, A2, B2), as the interfacial area available for mass transfer is solely determined by the liquid/solid specific surface area of the biocatalyst. Therefore, it is not necessary to disperse a liquid phase in an other liquid. Furthermore, water activities significantly lower than unity, desirable for e.g. esterification reactions, are probably easiest obtained in a class C3 system (e.g. [31, 32]).

Certain, special two-liquid-phase bioreaction systems bear resemblance to the above described water/organic solvent systems, but possess specific characteristics. An example is the aqueous two-liquid-phase system proposed by Kula [33] and Mattiasson [34]. By using the incompatibility of two water-soluble polymers, e.g. polyethene glycol and dextran, it is possible to create two separate, aqueous phases. As the surface tension between these two phases is very low, much lower than that of water/solvent two-phase systems, a very high interfacial liquid/liquid area can be easily obtained, while the chance of biocatalyst inactivation is reduced. The distribution of substrates, products and the biocatalyst (mostly suspended) between the two phases can be used to shift reaction equilibria and to remove toxic products from the biocatalyst-rich phase. Reversed micelles (e.g. [35]) provide another example of exceptional biphasic systems. The biocatalyst (up to now usually enzymes) is located in very small water 'pools', which are dispersed in an organic

solvent with the aid of ionic surfactants. This bioreaction system may thus be classified under A2 in the scheme of Figure 2. The main advantage of employing reversed micelles is the possibility of very high rates of mass transfer between the water droplets and the solvent phase. An alternative procedure to solubilize enzymes in organic solvents was recently proposed by Takahashi et al. [18]. Polyethylene glycol was attached covalently to the surface of lipases, and the resulting composite was found to be soluble in solvents like benzene, toluene and chloroform, containing trace amounts of water, with retention of catalytic activity. It will be of interest to learn, whether these new approaches will be applicable to a broad range of biocatalysts.

### 1.3 Implications for Bioreactor Design

Despite ever increasing research efforts, it still takes many years to develop new technological approaches and concepts from idea to practical utility. An example in the field of chemical reaction engineering is the effectiveness factor concept [36]. Though the basic fundamentals of the process of simultaneous diffusion and chemical transformation in catalyst particles were already understood in the late thirties [37, 38], it took some decades before this theory was developed to and applied at advanced levels (e.g. [39, 40]). Similar phenomena are observed in the design of immobilized-biocatalyst reactors. The immobilization of enzymes and the employment of different types of immobilized-enzyme reactors became customary in the late sixties and early seventies [41, 42]. However, this research area is at present still making tremendous progress, as illustrated by the current trend to use immobilized, growing or non-growing, whole cells [43-45]. It can be expected that a similar development will also apply for the only recently initiated research on two-liquid-phase biocatalytic reactors (using freely suspended or immobilized biocatalysts).

Immobilization of the biocatalyst in water/solvent two-phase systems might be advantageous, but is not crucial, as the product can be removed from the bioreactor via the organic solvent, while the aqueous biocatalyst phase is retained. A problem, that may arise if soluble biocatalysts are employed (class A1 and A2 in Figure 2), is the emulsification of one of the two liquid phases in the other to create sufficient interfacial area between the two liquid phases for high mass-transfer rates [17]. The stirred tank is an obvious reactor type for this purpose. The emulsion should, however, not become too stable, as this would result in unacceptably large liquid/liquid separators. The complexity of class A1 and A2 systems may thus be considerable. This was recently illustrated by Harbron et al. [46] and Brookes et al. [47]. Reaction rates in the used stirred-tank reactors were found to be dependent on the degree of agitation and the ratio of the organic and aqueous phases. Also, the cell concentration in the aqueous phase, which was related to the viscosity of the cell phase, appeared to influence the reaction rate. These effects were attributed to mass-transfer limitations across the water/solvent interface and/or in the aqueous phase.

In case of biocatalyst immobilization (class B1, B2 and C3 in Figure 2) two possibilities exist with regard to the mobility of the catalyst particles: moving or fixed. Moving particles will be found in slurry reactors like the stirred tank and the gas or liquid-fluidized bed. Reaction systems with unmoving particles are commonly called fixed-bed reactors. The design of two-liquid-phase slurry bioreactors, in

which a discrete aqueous phase is present (B1, B2), is likely to be even more complex than that of class A1 and A2 reactors. Not only the above mentioned mass-transfer phenomena will occur, but also diffusion to and in biocatalyst particles could become rate-controlling. The situation for reaction systems without a discrete water phase (C3 in Figure 2), often found in fixed-bed reactors, seems, however, more manageable. As the amount of water in this system is reduced to only a thin, adherent film covering the particles, the liquid/liquid mass-transfer limitations may disappear leaving only the external (organic liquid/solid) and internal diffusion limitations to be dealt with. Description of the latter phenomena will be facilitated by the availability of well-proven models of coupled diffusion and chemical reaction in liquid/solid systems. These models were already applied successfully to immobilized-biocatalyst systems involving water-soluble reactants [42-45, 48-50].

#### 1.4 Epoxidation of Alkenes in Two-Liquid-Phase Biocatalytic Systems

The production of propene oxide from propene and oxygen by immobilized cells is used in this thesis as a model to gain fundamental insights into the optimal design of immobilized-biocatalyst reactors, in which a water-immiscible organic solvent occupies a large part of the total reactor volume. In this section the reasons for the choice of this particular model system will be expounded.

Propene oxide can be considered a typical bulk commodity of the chemical industry. Its annual world production is about  $2 \times 10^6$  metric tons, of which more than 95% is again converted to other products, like urethane polyether polyols, propene glycol, lubricants, surfactants and emulsion breakers [51]. Due to its toxic nature, one of the commercial uses of propene oxide itself is as a sterilizing agent. The two major routes for the production of propene oxide are the chlorohydrin process and the hydroperoxide process [51, 52]. Both oxidations make use of oxygen carriers (HOCl and ROOH, respectively) to epoxidize propene, as it appeared not possible to develop a commercial direct-oxidation route. In case of ethene oxide such a process does exist. In the chlorohydrin process propene is reacted with an aqueous chlorine solution in a packed-bed reactor (40 to 90°C), after which the reaction products, two propene chlorohydrin isomers, are treated with a base to produce the epoxide and a chloride salt. The formation of chlorinated hydrocarbons (especially propene dichloride) as byproducts reduces the overall selectivity of the propene epoxidation to about 90%. In the hydroperoxide process propene is reacted with an organic hydroperoxide, which must be produced first from oxidation of isobutane or ethylbenzene. The produced coproducts are in this case *t*-butyl alcohol and  $\alpha$ -methylbenzyl alcohol, respectively. The manufacture of the peroxide as well as the epoxidation are carried out under elevated pressures and temperatures (2 to 5 MPa, 80 to 140°C). Both processes demand high operational costs as a result of high energy demands, epoxide purification, treatment of byproducts, coproducts and effluent, corrosion problems and safety measures. Therefore, much research was and is directed at finding more economic alternatives. Only recently, biotechnological epoxidation processes are being considered as possibly realistic options. The phenomenon that some biotechnologically obtained epoxides are optical active [53] could make bioprocesses especially interesting.

Many proposed, biotechnological processes for the direct conversion of alkenes to the corresponding alkene epoxides are carried out with free or immobilized cells [54-62]. A multi-enzyme process for the synthesis of alkene oxides was developed

by Neidleman et al. [63, 64]. Some groups have investigated the potentials of the use of water/organic solvent two-phase systems for epoxidation reactions [65–67]. Many of the above listed advantages (paragraph 1.1) of employing biphasic systems could be relevant. For instance, the solubility of alkenes and alkene oxides in suitable solvents is often much higher than that in water, making high concentrations of reactant and product in the bioreactor possible, and reducing the effect of any substrate and/or product inhibition in the aqueous biocatalyst phase. The innovating study of Schwartz and McCoy [65] gives a clear illustration of these phenomena. The addition of a 20% (vol/vol) cyclohexane phase to a fermentation broth of *Pseudomonas oleovorans* increased the conversion of 1,7-octadiene to epoxyoctene and diepoxyoctane from ~19% to ~90%. The extraction of about 95% of the formed monoepoxide in the organic phase reduced inhibition by this product in the cell phase, and this caused the higher substrate conversion. A similar conclusion was also reported by de Smet [66]. High 1,2-epoxyoctane concentrations could be reached by extracting the toxic product from the growing *Pseudomonas oleovorans* cells into a 1-octene phase. In this case a substrate phase (1-octene) performs the function of the substrate and product reservoir. Several aspects of the epoxidation of 1,7-octadiene by non-growing, free *Pseudomonas putida* cells in a two-liquid-phase system were studied by Harbron et al. [46]. The volumetric epoxide production rates were claimed to be higher than those of growing cells reported in the work of Schwartz and McCoy [65] and de Smet [66] as a result of the higher cell concentrations used. Propene epoxidation by immobilized *Nocardia corallina* cells in a biphasic system was recently reported by Miyawaki et al. [67]. The cells could be 'solubilized' in a liquid paraffin phase, like biocatalysts in reversed micelles [35], by emulsification with the paraffin and an antifoam agent. The hydrophobic environment of the immobilized cells resulted in an improved activity and stability.

Though the economic feasibility of epoxidation processes using (two-liquid-phase) biocatalytic reactors is still questionable, the huge amount of research directed to this subject makes it conceivable, that commercial units may be in operation in the next decade. Therefore, considering the fundamental importance of two-liquid-phase systems, the design of a biocatalytic, biphasic epoxidation process provides an interesting mixture of basic research and commercial relevance. In this work the epoxidation of a gaseous alkene, propene, by non-growing *Mycobacterium* cells [68] was chosen as the model reaction. This epoxidation is suited for fundamental studies as the reactants (propene and oxygen) and the product of this bioconversion are relatively simple molecules. This facilitates the estimation of chemical, physical and thermodynamic properties of these substances. The main advantages of using two-liquid-phase systems are also very relevant to propene epoxidation. The formed epoxide is very inhibitory [69], and the gaseous substrates are only slightly soluble in water. The presence of an organic phase could reduce product inhibition by extraction of the epoxide and, furthermore, could facilitate the transport of the two substrates from the gas phase to the cell phase. Also, hydrolysis of propene oxide in water, reported to occur to some extent [70], can be prevented by keeping the epoxide in an organic product reservoir. The economic feasibility of the process is enhanced by the high optical activity of the formed propene oxide [53]. Many of the above listed incentives, except stereospecificity, could also be applicable to ethene epoxidation. However, in this case a gas-solid bioreactor may be more feasible than a multiphase bioreactor [61].



## 1.5 Review of the Work to be presented

In this thesis the results of a fundamental investigation of water/organic solvent two-phase biocatalytic systems are described using the microbial epoxidation of propene as a model. Emphasis will be placed on the design of immobilized-biocatalyst reactors without a discrete aqueous phase (class C3 in Figure 2). Microbial aspects of the *Mycobacterium* strain used for the epoxidation, like the screening of cell strains, activity, specificity, stability, genetic work, cell-growth conditions and stereospecificity of the formed epoxides, were studied in a parallel research project [53, 68, 69].

An automated experimental set-up was employed to facilitate the measurement of the rates of propene and oxygen consumption and epoxide production under varying conditions (chapter 2). The importance of a proper choice of the solvent type will be discussed in chapter 3. Criteria are given to guide this decision. The microkinetics of the product-inhibited epoxidation with gel-entrapped cells, reaction kinetics and mass-transfer effects, are modelled in chapters 4 and 5. In chapter 6 this microkinetic model is incorporated in an integral model of a packed-bed organic-liquid-phase/immobilized-cell reactor. The influence of the substrate solubility in the reaction medium is quantified. Limitations of the production of propene oxide in an organic-liquid-phase/immobilized-cell reactor are treated in chapter 7. Finally, concluding observations are made in the last chapter of this thesis.

## 1.6 References

1. Butler, L.G. *Enzyme Microb. Technol.* 1979, **1**, 253-259.
2. Cambou, B. and Klivanov, A.M. *J. Am. Chem. Soc.* 1984, **106**, 2687-2692.
3. Zaks, A. and Klivanov, A.M. *Science* 1984, **224**, 1249-1251.
4. Halling, P.J. *Enzyme Microb. Technol.* 1984, **6**, 513-516.
5. Lugaro, G., Carrea, G., Cremonesi, P., Casellato, M.M. and Antonini, E. *Arch. Biochem. Biophys.* 1973, **159**, 1-6.
6. Cremonesi, P., Carrea, G., Sportoletti, G. and Antonini, E. *Arch. Biochem. Biophys.* 1973, **159**, 7-10.
7. Cremonesi, P., Carrea, G., Ferrara, L. and Antonini, E. *Eur. J. Biochem.* 1974, **44**, 401-405.
8. Cremonesi, P., Carrea, G., Ferrara, L. and Antonini, E. *Biotechnol. Bioeng.* 1975, **17**, 1101-1108.
9. Buckland, B.C., Dunnill, P. and Lilly, M.D. *Biotechnol. Bioeng.* 1975, **17**, 815-826.
10. Duarte, J.M.C. and Lilly, M.D. in *Enzyme Engineering* (Weetall, H.H. and Royer, G.P., eds), Plenum Press, New York, 1980, vol. 5, pp. 363-367.
11. Omata, T., Iida, T., Tanaka, A. and Fukui, S. *Eur. J. Appl. Microbiol. Biotechnol.* 1979, **8**, 143-155.
12. Yamané, T., Nakatani, H., Sada, E., Omata, T., Tanaka, A. and Fukui, S. *Biotechnol. Bioeng.* 1979, **21**, 2133-2145.
13. Klivanov, A.M., Samokhin, G.P., Martinek, K. and Berezin, I.V. *Biotechnol. Bioeng.* 1977, **19**, 1351-1361.
14. Antonini, E., Carrea, G. and Cremonesi, P. *Enzyme Microb. Technol.* 1981, **3**, 291-296.
15. Lilly, M.D. *J. Chem. Tech. Biotechnol.* 1982, **32**, 162-169.
16. Carrea, G. *Trends in Biotechnol.* 1984, **2**, 102-106.
17. Lilly, M.D. and Woodley, J.M. in *Biocatalysts in Organic Syntheses* (Tramper, J., van der Plas, H.C. and Linko, P., eds), Elsevier, Amsterdam, 1985, pp. 179-192.
18. Takahashi, K., Nishimura, H., Yoshimoto, T., Okada, M., Ajima, A., Matsushima, A., Tamaura, Y., Saito, Y. and Inada, Y. *Biotechnol. Lett.* 1984, **6**, 765-770.
19. Randolph, T.W., Blanch, H.W., Prausnitz, J.M. and Wilke, C.R. *Biotechnol. Lett.* 1985, **7**, 325-328.
20. Schutt, H., Schmidt-Kastner, G., Arens, A. and Preiss, M. *Biotechnol. Bioeng.* 1985, **27**, 420-433.

21. Leonhardt, A., Szwajcer, E. and Mosbach, K. *Appl. Microbiol. Biotechnol.* 1985, **21**, 162–166.
22. Saunders, R.P., Hardman, R. and Cheetham, P.S.J. *Biotechnol. Bioeng.* 1985, **27**, 825–831.
23. Damiano, D. and Wang, S.S. *Biotechnol. Lett.* 1985, **7**, 81–86.
24. Playne, M.J. and Smith, B.R. *Biotechnol. Bioeng.* 1983, **25**, 1251–1265.
25. Klein, J. and Wagner, F. in *Applied Biochemistry and Bioengineering* (Wingard, L.B., Katchalski-Katzir, E. and Goldstein, L., eds), Academic Press, New York, 1983, vol. 4, pp. 11–51.
26. Rosevear, A. *J. Chem. Tech. Biotechnol.* 1984, **34B**, 127–150.
27. Tramper, J. *Trends in Biotechnol.* 1985, **3**, 45–50.
28. Fukui, S., Ahmed, S.A., Omata, T. and Tanaka, A. *Eur. J. Appl. Microbiol. Biotechnol.* 1980, **10**, 289–301.
29. Omata, T., Tanaka, A. and Fukui, S. *J. Ferment. Technol.* 1980, **58**, 339–343.
30. Fukui, S. and Tanaka, A. *Adv. Biochem. Eng.* 1984, **29**, 1–33.
31. Bell, G., Todd, J.R., Blain, J.A., Patterson, J.D.E. and Shaw, C.E.L. *Biotechnol. Bioeng.* 1981, **23**, 1703–1719.
32. Macrae, A.R. *J. Amer. Oil Chem. Soc.* 1983, **60**, 291–294.
33. Kula, M.-R. in *Applied Biochemistry and Bioengineering* (Wingard, L.B., Katchalski-Katzir, E. and Goldstein, L., eds), Academic Press, New York, 1983, vol. 2, pp. 71–95.
34. Mattiasson, B. *Trends in Biotechnol.* 1983, **1**, 16–20.
35. Luisi, P.L. and Laane, C. *Trends in Biotechnol.* 1986, **4**, 153–161.
36. Weisz, P.B. *Science* 1973, **179**, 433–440.
37. Thiele, E.W. *Ind. Eng. Chem.* 1939, **31**, 916–920.
38. Zeldovich, J.B. *Acta Physicochim. USSR* 1939, **10**, 583–592.
39. Bischoff, K.B. *AIChE J.* 1965, **11**, 351–355.
40. Aris, B. in *The Mathematical Theory of Diffusion and Reaction in Permeable Catalysts*, Clarendon Press, Oxford, 1975, 2 vols.
41. Lilly, M.D. and Dunnill, P. in *Methods in Enzymology* (Mosbach, K., ed.), Academic Press, New York, 1976, vol. 44, 717–738.
42. Vieth, W.R., Venkatasubramanian, K., Constantinides, A. and Davidson, B. in *Applied Biochemistry and Bioengineering* (Wingard, L.B., Katchalski-Katzir, E. and Goldstein, L., eds), Academic Press, New York, 1976, vol. 1, pp. 221–327.
43. Venkatasubramanian, K., Karkare, S.B. and Vieth, W.R. in *Applied Biochemistry and Bioengineering* (Wingard, L.B., Katchalski-Katzir, E. and Goldstein, L., eds), Academic Press, New York, 1983, vol. 4, pp. 311–349.
44. Radovich, J.M. *Enzyme Microb. Technol.* 1985, **7**, 2–10.
45. Karel, S.F., Libicki, S.B. and Robertson, C.R. *Chem. Eng. Sci.* 1985, **40**, 1321–1354.
46. Harbron, S., Smith, B.W. and Lilly, M.D. *Enzyme Microb. Technol.* 1986, **8**, 85–88.
47. Brookes, I.K., Lilly, M.D. and Drozd, J.W. *Enzyme Microb. Technol.* 1986, **8**, 53–57.
48. Buchholz, K. *Adv. Biochem. Eng.* 1982, **24**, 39–71.
49. Kasche, V. *Enzyme Microb. Technol.* 1983, **5**, 2–13.
50. Klein, J. and Vorlop, K.-D. *Am. Chem. Soc. Symp. Ser.* 1983, **207**, 376–392.
51. Kirk, R.O. and Dempsey, T.J. in *Kirk—Othmer Encyclopedia of Chemical Technology*, John Wiley and Sons, New York, 1982, vol. 19, pp. 246–274.
52. Van den Berg, P.J. and de Jong, W.A. in *Introduction to Chemical Process Technology*, Delft University Press, Delft, The Netherlands, 1980, pp. 203–207.
53. Habets-Crützen, A.Q.H., Carlier, S.J.N., de Bont, J.A.M., Wistuba, D., Schurig, V., Hartmans, S. and Tramper, J. *Enzyme Microb. Technol.* 1985, **7**, 17–21.
54. Furuhashi, K., Taoka, A., Uchida, S. and Urawa, S. (1980) *Ger. Offen.* No. 2 931 148.
55. Furuhashi, K., Taoka, A., Uchida, S., Karube, I. and Suzuki, S. *Eur. J. Appl. Microbiol. Biotechnol.* 1981, **12**, 39–45.
56. Hou, C.T. (1981) *Eur. Patent* No. 42 306.
57. Hou, C.T. and Edison, N.J. (1982) *U.S. Patent* No. 4 348 476.
58. Hou, C.T., Patel, R.N., Laskin, A.I., Barnabe, N. and Barist, I. *Appl. Environ. Microbiol.* 1983, **46**, 171–177.
59. Drozd, J.W. and Balley, M.L. (1984) *Eur. Patent* No. 99 609.
60. Wiegant, W.M. and de Bont, J.A.M. *J. Gen. Microbiol.* 1980, **120**, 325–331.
61. De Bont, J.A.M., van Ginkel, C.G., Tramper, J. and Luyben, K.Ch.A.M. *Enzyme Microb. Technol.* 1983, **5**, 55–59.

62. Wingard, L.B., Roach, R.P., Miyawaki, O., Egler, K.A., Klinzing, G.E., Silver, R.S. and Brackin, J.S. *Enzyme Microb. Technol.* 1985, **7**, 503–509.
63. Neidleman, S.L., Amon, W.F. and Geigert, J. (1980) *Eur. Patent* No. 7 176.
64. Neidleman, S.L. and Geigert, J. in *Biotechnology* (Phelps, C.F. and Clarke, P.H., eds), The Biochemical Society, London, 1983, Symp. No. 48, pp. 39–52.
65. Schwartz, R.D. and McCoy, C.J. *Appl. Environ. Microbiol.* 1977, **34**, 47–49.
66. De Smet, M.-J. in *A Biotechnological Approach to the Synthesis of Epoxides*, PhD Thesis, University of Groningen, Groningen, The Netherlands, 1982.
67. Miyawaki, O., Wingard, L.B., Brackin, J.S. and Silver, R.S. *Biotechnol. Bioeng.* 1986, **28**, 343–348.
68. Habets–Crützen, A.Q.H., Brink, L.E.S., van Ginkel, C.G., de Bont, J.A.M. and Tramper, J. *Appl. Microbiol. Biotechnol.* 1984, **20**, 245–250.
69. Habets–Crützen, A.Q.H. and de Bont, J.A.M. *Appl. Microbiol. Biotechnol.* 1985, **22**, 428–433.
70. Carrà, S., Santacesaria, E., Morbidelli, M. and Cavalli, L. *Chem. Eng. Sci.* 1979, **34**, 1123–1132.

## 2. AUTOMATION OF AN EXPERIMENTAL SYSTEM FOR THE MICROBIAL EPOXIDATION OF PROPENE AND 1-BUTENE

L. E. S. BRINK\*, J. TRAMPER and K. VAN 'T RIET

*Department of Food Science, Food and Bioengineering Group, Agricultural University Wageningen, De Dreyen 12, 6703 BC Wageningen (The Netherlands)*

K. CH. A. M. LUYBEN

*Laboratory of Bioengineering, Delft University of Technology, Julianalaan 67, 2628 BC Delft (The Netherlands)*

(Received 14th April 1984)

### SUMMARY

An experimental set-up for automatic gas chromatographic analysis of circulation gas in a batch-reactor system is described. Gas sampling, substrate addition, data acquisition and data reduction are done with a coupled programmable integrator and microcomputer. On-line monitoring of the microbial oxidation of the gaseous alkenes, propene and 1-butene, to the corresponding epoxides is used to illustrate the operation of the experimental system. Measured gas concentrations of alkene and alkene oxide can be converted readily to quantify the reaction course in the liquid phase(s) of the circulation system. Results are presented for both one liquid phase (water) and two liquid phases (water and organic solvent) present in the reactor. The operational stability of the immobilized-cell system used for the epoxidations can be assessed by computer-controlled addition of gaseous alkene.

The use of water-immiscible organic solvents has recently been given increasing attention as a possible approach to diminishing the fundamental restrictions often inherent in biotechnological processes. Some of these restrictions are the low solubility of (gaseous) substrates and/or products in water, product inhibition, product hydrolysis and laborious product recovery [1, 2]. In order to study the potential of an additional organic phase, the epoxidation of the gaseous alkenes, propene and 1-butene, by immobilized cells in a multiphase bioreactor has been studied as a model. The system consists of a solid biocatalyst, an aqueous phase, an organic solvent, and a gas phase containing the gaseous substrates oxygen and propene or 1-butene [3]. Selecting an optimal composition for this multiphase system involves careful weighing of many different factors and their possible mutual interactions. Factors such as the technique of immobilization, type of organic solvent, microbial aspects (bacterial strain, co-factor regeneration) and process engineering aspects (hydrodynamics, reactor design) allow a vast number of combinations, which requires automation of the experiments, especially the monitoring of alkene and alkene oxide concentrations in the liquid phases.

The choice of a well-established technique like gas chromatography (g.c.) for separation and determination of the various components in the multi-phase system is obvious. Gas chromatography may be used for on-line monitoring by using a small sampling interval in combination with the proper chromatographic conditions. Direct g.c. of the aqueous and/or organic liquid phase has several disadvantages: it is difficult to quantify small quantities of organic compounds in water because of overloading the column and the detector by water; the various solvents (and their impurities) used may interfere seriously and contaminate the g.c. column; and the automation of liquid-sample withdrawal is expensive. The need for intimate contact between gas and liquid phases to supply the gaseous substrates, however, makes it feasible to follow the reaction course in the reactor by measuring the gas-phase concentrations. The easily detectable gaseous substrates and volatile alkene oxides and the low concentrations of water, solvent and impurities in the gas phase, and the simple automation of a gas-sampling valve, are further considerations which make gas analysis preferable to liquid analysis. This technique, head-space gas chromatography (h.s.g.c.), has found practical applications in trace analysis and in the measurement of thermodynamic data [4], and has been used recently to monitor batch and continuous alcoholic fermentations with ethanol concentrations in the liquid phase up to 110 g l<sup>-1</sup>, and acetone/butanol fermentation with acetone and butanol concentrations in the liquid phase up to 20 g l<sup>-1</sup> [5, 6].

An inherent disadvantage of quantitative h.s.g.c., compared with direct g.c., stems from the need to convert the measured gas concentrations to liquid concentrations so that additional parameters must be considered [4]. The conversion is mostly based on the assumption of thermodynamic equilibrium between the gas and liquid phase(s). Henry's law may be used for poorly soluble gases like oxygen and propene to correlate the partial vapour pressure ( $p_i$ ) of a component  $i$  in the gas phase and its mole fraction ( $x_i$ ) in the liquid (aqueous or organic) phase:  $p_i = H_i x_i$ , where  $H_i$  is the Henry constant of component  $i$ . For less volatile, better soluble compounds like alkene oxides, non-ideality in the liquid phase is taken into account by specifying an activity coefficient  $\gamma_i$  of the dissolved component  $i$ . If ideal behaviour of the gas phase can be assumed, the activity coefficient relates the partial vapour pressure to liquid mole fraction by the equation

$$p_i = p_i^0 \gamma_i x_i \quad (1)$$

in which  $p_i^0$  is the vapour pressure of the pure component  $i$ . The activity coefficient depends not only on temperature and, to a lesser extent, on pressure, but also on the interaction between component  $i$  and the other components present. Successful quantitative interpretation based on the  $p_i$  equation, and the experimental determination of the calibration factor  $p_i^0 \gamma_i$ , must therefore take into account possible changes in the activity coefficient caused by variations in the composition of the liquid phase. At low concentrations of the component of interest, a linear relation between signal ( $p_i$ )

and the mole fraction in the liquid ( $x_i$ ) is expected, because the activity coefficient of a very dilute solution is nearly constant [4, 7]. Comberbach and Bu'Lock [5] found that for ethanol/distilled water mixtures, a linear relation exists between the h.s.g.c. signal and the actual ethanol concentration in the liquid phase from 2 to 80 g l<sup>-1</sup>.

## EXPERIMENTAL

### Batch reactor with gas circuit

Cells were entrapped in calcium alginate gel for immobilization. Details of the immobilization technique and of microbial aspects such as substrate specificity of the *Mycobacterium* strain E3 used for the epoxidations, are reported elsewhere [3]. Experiments with the biocatalyst beads (ca. 25 ml) were done with a small bubble-column bioreactor, containing an aqueous 0.05 M calcium chloride solution and in some cases an organic solvent phase (total volume of beads and liquid phases, 250 ml). An aerated flask containing 250 ml of (0.05 M) potassium phosphate buffer of pH 7.0 was used in measurements with suspended cells. Air (25 ml s<sup>-1</sup>) from a gas supply vessel (300 ml) containing 1.7% alkene (v/v) was circulated through the suspension of immobilized or free cells by means of a gas diaphragm pump (Fig. 1). Reaction and gas supply vessel (total gas volume 570 ml) were thermostated at 30°C in a water bath. Errors produced by leakage of gaseous components were minimized by using only materials with low gas permeability, like glass,

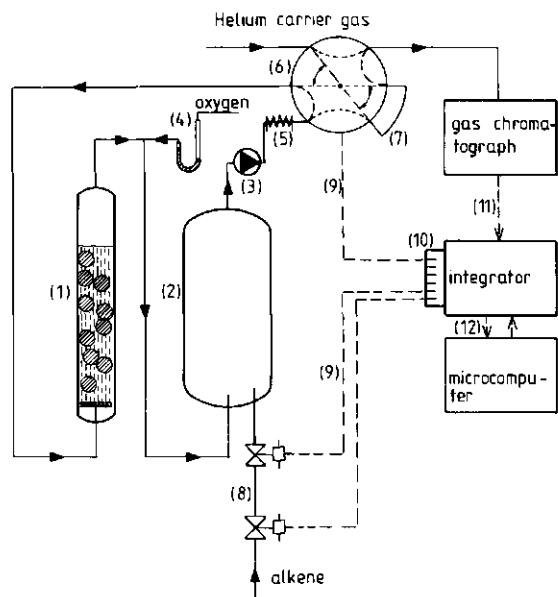


Fig. 1. Schematic representation of circulation batch reactor and control system: (1) bubble-column bioreactor; (2) gas-supply vessel; (3) diaphragm pump; (4) oxygen inlet with water seal; (5) heating; (6) two-position gas-sampling valve showing the normal (---) and inject (---) mode; (7) sample loop; (8) magnetic valves; (9) control signals; (10) external-control option; (11) analog g.c. signal; (12) digital communication. See also text and Fig. 2.

teflon (compared with other plastics) and viton for tubing. As the gaseous substrates were consumed in the reaction, the pressure in the system decreased; atmospheric pressure was maintained by introducing pure oxygen through a water seal, which also maintained an excess of oxygen.

Gas samples (0.48 ml) were withdrawn from the gas circuit every 30 min by a computer-controlled electropneumatic two-position gas-sampling valve. Problems of water condensation were averted simply by heating the gas entering the valve to 50°C and isolating the sampling valve and sample loop, which resulted in a reasonably constant valve temperature (about 35°C).

Measurements of the operational stability of the immobilized-cell system were facilitated by controlling the substrate level in the circulation system. Gaseous alkene was added by sequential computer-controlled opening and closing of two magnetic valves. The amount of gas added per sequence was determined by separate calibration.

### *Gas chromatograph*

A gas chromatograph (Carlo Erba 4200) equipped with flame-ionization and thermal-conductivity detectors was used. Helium was used as carrier gas (0.33 ml s<sup>-1</sup>); the column (2 m, 3 mm o.d.) was packed with Porapak-Q (80–100 mesh). Oven and flame-ionization detectors were held at 200 and 210°C, respectively. Alkene and alkene oxide were quantified regularly by computer-controlled switching of the two-position valve into the inject mode, upon which the content (0.48 ml) of the sample loop was carried into the column.

The partial vapour pressures of (excess) oxygen and nitrogen were verified by manual injection of gas samples (50 μl) onto a column packed with molecular sieve 13X (60–80 mesh) and using the thermal-conductivity detector. This column was positioned outside the gas chromatograph and used at ambient temperatures.

Response factors relating peak areas to gas phase concentrations were evaluated by adding known quantities of alkene or alkene oxide to the system described above (without biocatalyst), and/or to known gas volumes (not in contact with a condensed phase), and subsequent analysis of the gas phase. Likewise, addition of a known quantity of alkene oxide to the batch-reactor system (also no biocatalyst) made it possible to establish relationships between liquid and gas phase concentrations of the epoxide in question.

### *Integrator and microcomputer*

Processing of the analog g.c. signals and control of the electropneumatic and magnetic valves were done with a programmable integrator (Spectra-Physics 4270) coupled to a microcomputer (Hewlett-Packard 86-B). The integrator was equipped with an interface (RS-232) for serial communication with the computer, and with external controls (6 per channel of integration) for on/off-switching of valves and, if necessary, of other equipment (see Fig. 2). Implementation of a second channel for peak integration is optional. The interfacing capabilities could be extended for data acquisition from various instruments (e.g., pH and oxygen electrodes).

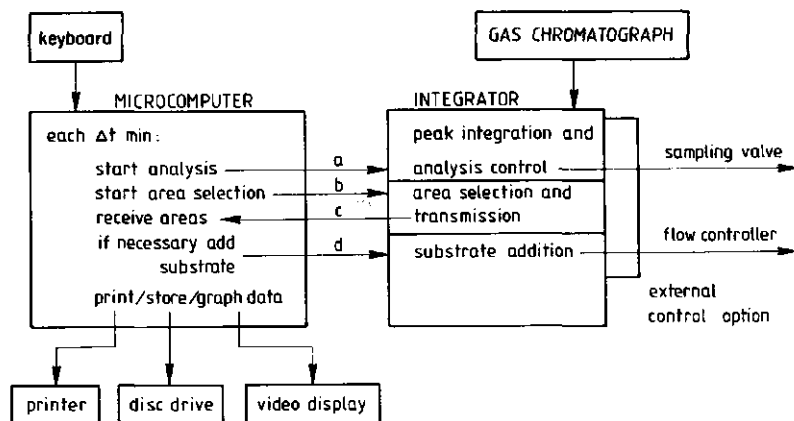


Fig. 2. Signal flow diagram showing the coupling of integrator and microcomputer. Serial interfaces (RS-232) were used for the communication signals (a, b, c, d). See text for discussion.

### Data handling

At regular time intervals  $\Delta t$  (e.g., 30 min) the sampling sequence (Fig. 2) is initiated by the built-in timer of the microcomputer. The analysis is started (arrow *a* in Fig. 2) by transmitting an inject command to the integrator; this has the same effect as pressing the "start" or "inject" knob of the integrator. The analysis and peak integration are controlled by built-in standard programs. The parameters needed are stored in the integrator memory before the experiment. Typical values are: at 0.01 min (almost zero), switch gas-sampling valve to the inject mode; at 4.9 min, switch gas-sampling valve to the normal mode; at 5 min, terminate the signal integration. The main program in the microcomputer then initiates a simple user-written program for area selection at 5.2 min (step *b*); only the areas of the required components are selected and subsequently transmitted (step *c*) back to the computer. Required unit conversions (e.g., area to partial vapour pressure) and calculations are then done. In experiments with a constant level of alkene, the alkene area or concentration of the latest sample and, if wanted, of previous samples are compared with a user-defined setpoint. If the deviation exceeds a certain value, a small quantity of substrate is added to the batch-reactor system by initiating (step *d*) another user-written program section in the integrator memory, which in turn activates the substrate valve(s). Sample number, sampling time, areas or concentrations, number of substrate additions and total amount of substrate consumed are then printed and stored (computer memory and/or disc drive) and can be reproduced graphically on the video display (e.g., alkene (oxide) concentration versus time).



## RESULTS AND DISCUSSION

### Quantitative h.s.g.c.

The consumption of the alkene substrates could be quantified by using as reference the first measurement taken very shortly after the addition of a known amount of alkene (10 ml). The conversion factor between peak area and total amount of gaseous alkene present in the various phases of the circulation system was determined thus. The peak areas during the remainder of the experiment were converted to ml of alkene by using this factor. It was assumed that decreasing alkene concentrations did not affect the value of the Henry constants of interest (alkene/water, alkene/solvent). Gas and liquid concentrations were calculated with the absolute values of the Henry constants. For example, from the constant for propene in water ( $1.24 \times 10^6$  kPa at  $30^\circ\text{C}$  [8]), it was calculated that 4.6% of the total amount of propene present would dissolve in the 250-ml aqueous phase (water and hydrophilic gel), while the rest remained in the 570-ml gas phase. The low salt concentrations used (0.05 M calcium chloride) showed no significant effect on the fraction of propene present in the gas phase.

Activity coefficients are needed to convert the measured gas concentrations to liquid concentrations of the produced alkene oxides. In experiments with only one (aqueous) liquid phase (no organic solvent), propene oxide was quantified by addition of a known quantity of propene oxide  $N_{\text{PO}}$  to the circulation system. Separate calibration (only gas phase present) of the measured peak areas of propene oxide for conversion of areas to gas mole fractions  $y_{\text{PO}}$  (see Table 1) made it possible to determine the liquid mole fraction  $x_{\text{PO}}$  by using a simple mass balance

$$x_{\text{PO}} = (N_{\text{PO}} - y_{\text{PO}}N_{\text{g}})/N_{\text{l}} \quad (2)$$

TABLE 1

Equilibrium data for propene oxide

$N_{\text{PO}}^{\text{a}}$ ( $10^{-6}$ mol)	$y_{\text{PO}}^{\text{b}}$ ( $10^{-3}$ )	$y_{\text{PO}}N_{\text{g}}/N_{\text{PO}}^{\text{c}}$	$x_{\text{PO}}^{\text{d}}$ ( $10^{-4}$ )	$\gamma_{\text{PO}}^{\text{e}}$
713	0.795	0.026	0.50	18.2
1426	1.52	0.024	1.00	17.4
2139	2.23	0.024	1.50	17.0
2852	3.08	0.025	2.00	17.6
3565	3.84	0.025	2.50	17.6
4278	4.63	0.025	3.00	17.7
			Average	17.6

<sup>a</sup>Total number of moles of propene oxide present in the circulation system. <sup>b</sup>Gas-phase mole fraction (h.s.g.c. signal). <sup>c</sup>Fraction of propene oxide in the gas phase. <sup>d</sup>Liquid mole fraction. <sup>e</sup>Activity coefficients.

in which  $N_g$  and  $N_l$  are the total number of moles in the gas and liquid phase, respectively (570 ml or 0.0229 mol of gas phase and 250 ml or 13.9 mol of demineralized water). Activity coefficients,  $\gamma_{PO}$ , were estimated by using the equation (obtained from Eqn. 1)

$$\gamma_{PO} = p_{PO}/x_{PO}p_{PO}^0 = y_{PO}P_t/x_{PO}p_{PO}^0 \quad (3)$$

with the system pressure  $P_t = 100$  kPa, and the vapour pressure of pure propene oxide at  $30^\circ\text{C}$ ,  $p_{PO}^0 = 87.25$  kPa [9].

From Table 1 it may be concluded that for the dilute aqueous solutions of propene oxide considered ( $\leq 3 \times 10^{-4}$ ), the activity coefficient is independent of epoxide concentrations, and that there is a linear relationship between  $y_{PO}$  (h.s.g.c. signal) and the liquid-phase mole fraction  $x_{PO}$ . Quantification of the propene oxide is also facilitated by the linear relationship between the h.s.g.c. signal or gas-phase mole fraction  $y_{PO}$  and the total number of moles of propene oxide  $N_{PO}$  present in the batch-reactor system (Table 1):  $y_{PO} = 1.08 N_{PO} - 2 \times 10^{-5}$  (standard error of estimate  $0.04 \times 10^{-3}$ ; correlation coefficient 0.999). In most of the tests, the total amount of biologically produced liquid propene oxide did not exceed  $29.2 \mu\text{l}$  ( $416 \mu\text{mol}$ , the maximum theoretical production from 10 ml of gaseous propene), thus Table 1 shows that a single factor suffices for the conversion of peak areas to produced amounts of epoxide, and also to liquid epoxide concentrations.

Similar behaviour has already been found for dilute aqueous solutions of alcohols, ketones, aldehydes, esters and sulfides [7], thus it can be assumed that the same linear relationship will hold for 1-butene oxide. It was found that the small fraction of the total amount of this epoxide that was contained in the gas phase (3.2%) was slightly higher than the corresponding fraction of propene oxide (2.5%).

As the solubility of propene oxide and 1-butene oxide in the water-immiscible organic solvents used is mostly higher than the corresponding solubility in water, replacement of part of the aqueous phase by these solvents will decrease the gas-phase and aqueous phase concentrations of the epoxide. The epoxide activity coefficients will be affected considerably by the mutual solubility of water and the organic solvent. Accordingly, conversion of gas concentrations to aqueous and organic liquid concentrations, and the distribution of the epoxide between the two liquid phases, cannot be evaluated from activity coefficients of separate gas/water and gas/solvent calibrations. Although not required in the present investigation, epoxide concentrations in the liquid phases may be deduced from separate gas/water/solvent calibrations.

#### *Monitoring alkene consumption and alkene oxide production*

The microbial epoxidation of propene and 1-butene was investigated as described above. Typical gas chromatograms for the propene epoxidation, at the start and finish of the experiment, are shown in Fig. 3. Methane was used to check the sealing of the recirculation system. Separate blank mea-

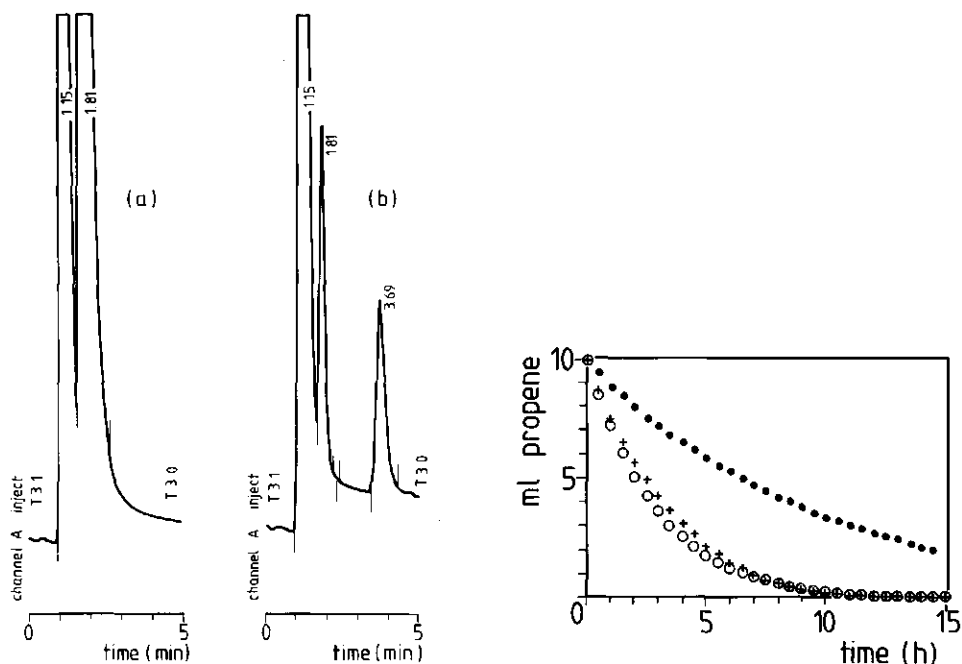


Fig. 3. Typical chromatograms from a propene epoxidation experiment: (a) only methane (1.15 min) and propene (1.81 min) are present at the start; (b) at the end, propene was mostly converted to propene oxide (3.69 min). Peak markers show the start and end of peak integration. Switching of the gas-sampling valve is indicated by "T3 1" (inject mode) and "T3 0" (normal mode).

Fig. 4. Amount of unconverted propene in the system versus time: (○) free cells; (+) cells immobilized in 0.7-mm alginate beads; (●) cells immobilized in 2.5-mm alginate beads.

surements, without biocatalyst, showed that the leakage rate of propene at the maximum propene level (1.7% v/v) was several times higher than the leakage rate of methane (also 1.7% v/v). In these experiments, alkene leakage rates were always less than 5% of the alkene consumption rates. Retention times of 1-butene and 1-butene oxide for the same chromatographic conditions were 2.5 and 6.4 min, respectively. The total time required for one sampling sequence was about 5.5 min for propene epoxidation, but may be reduced to 2 min or even less by increasing carrier flow and oven temperature and/or reducing column length and diameter.

Results of propene consumption by free and immobilized cells in an aqueous environment are given in Fig. 4. Equal amounts of cells (ca. 1 g dry weight) were used in each case. Propene levels are given in ml (gaseous) propene present in the total circulation system. Multiplication by appropriate factors would give the number of moles present, partial vapour pressure, gas or liquid mole fraction as the unit of the Y-axis. Compared to the curve for 2.5 ( $\pm 0.2$ )-mm beads, there is only a small difference in propene consumption

rate between free suspended cells and cells immobilized in alginate beads with an average diameter of  $0.7 \pm 0.1$  mm, obviously because of diffusion limitation.

The kinetic parameters can be estimated by different methods, including non-linear regression, and the diffusion limitation can be modelled by using the same microcomputer system; details will be given elsewhere. For example, the kinetic parameters of the integrated Michaelis–Menten equation, estimated by a non-linear regression of substrate versus time, were used to characterize the alkene consumption rates. Illustrations of this regression method are given in Figs. 5 and 6. It did not seem necessary to make these calculations during the experiments.

Measured values of propene oxide and 1-butene oxide production by cells immobilized in alginate beads are compared with values calculated from propene and 1-butene consumption rates in Fig. 7 (1 ml of gaseous propene gives  $2.92 \mu\text{l}$  of liquid propene oxide; 1 ml of gaseous 1-butene gives  $3.58 \mu\text{l}$  of liquid 1-butene oxide). Epoxide levels are given as the total amount in the circulation system, but most of it is in the aqueous phase (see above). Despite the small quantities of propene oxide and 1-butene oxide in the gas phase, the trend of the epoxide concentrations is clear. The increasing difference between the epoxide concentrations found and those calculated from alkene consumption rates confirms that the bacterial strain used can consume the alkene oxides [3]. Decreasing the sampling time interval will improve the reliability even further. The relative influence of the experimental error in the alkene oxide concentrations (10–20% in Fig. 7) is smaller at higher epoxide levels (see below).

Propene epoxidation was also monitored in the presence of a second liquid phase consisting of a water-immiscible organic solvent (10 ml). Some results are summarized in Fig. 8. As reported for other cells [10], the very inert perfluoro compound used (FC-40; 3M, St. Paul, MN) caused little or no

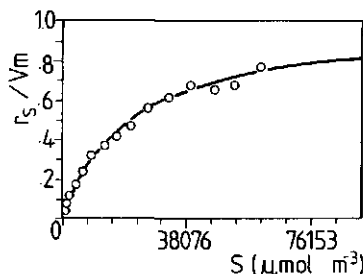
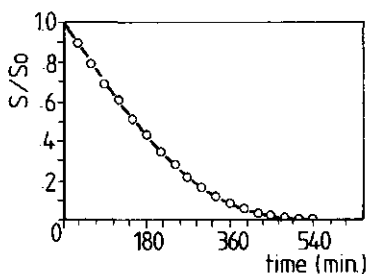


Fig. 5. Dimensionless substrate (propene) concentrations,  $S/S_0$ , versus time for cells (0.8 g dry weight) immobilized in 1.0-mm alginate beads. Smooth line depicts the Michaelis–Menten model approximation ( $V_m = 2.30 \mu\text{mol min}^{-1} \text{ g dry weight}^{-1}$ ;  $K_m = 20900 \mu\text{mol m}^{-3}$ ).

Fig. 6. Dimensionless propene consumption rates  $r_s/V_m$  versus substrate (propene) concentration  $S$  for immobilized cells (as in Fig. 5). Smooth line depicts Michaelis–Menten model approximation as in Fig. 5.

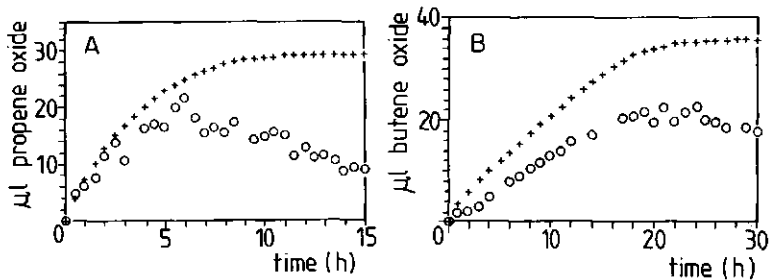


Fig. 7. Amount of liquid epoxide produced in the circulation system versus time: (A) propene oxide with 0.7-mm beads; (B) butene oxide with 0.8-mm beads. (○) Measured values, (+) values calculated from substrate consumption.

inactivation of the cells compared to a blank measurement without solvent. Commoner solvents (phthalic acid dibutyl ester and di-isopentyl ether) caused some cell inhibition, and hexane and trioctylamine rapidly inactivate the immobilized-cell system.

#### Substrate level control

The operational stability of the immobilized cells was verified by monitoring the substrate level. The propene concentration was held constant within about 10% of a user-defined setpoint (10 ml in these tests) by computer-controlled opening and closing of two magnetic valves each time the measured propene concentrations of two consecutive analyses both fell below the setpoint. Such variations in propene level are unlikely to affect the substrate consumption rate as the enzymatic reaction order at this substrate level is close to zero. Again, an increasing difference was found between the measured

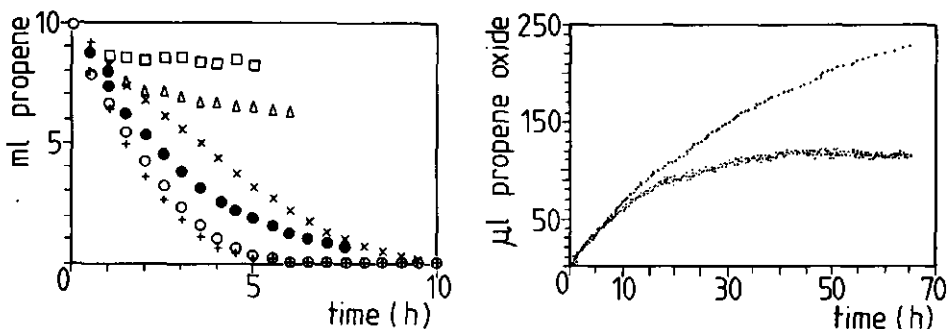


Fig. 8. Amount of unconverted propene in the system versus time with 10 ml of organic liquid phase present (cells immobilized in alginate): (+) blank measurement; (○) FC-40; (•) phthalic acid dibutyl ester; (x) di-isopentyl ether; (Δ) n-hexane; (◻) trioctylamine.

Fig. 9. Amount of propene oxide produced in the reactor with control of propene level (cells immobilized in alginate). Lower points represent measured values; upper points represent values calculated from cumulative amount of propene addition.

amount of liquid propene oxide and the calculated production, obtained by multiplying the number of substrate additions by the amount of propene added (0.74 ml) in one valve-switching sequence (Fig. 9).

From the number of analyses (each 10 min), the volume of the gas phase in the circulation system, and the internal volume of the sample loop of the gas-sampling valve (0.48 ml), it can be deduced that the maximum cumulative experimental error arising from sampling losses of propene is about 5%. Minimizing this error, and preventing the oxygen partial vapour pressure from becoming too low, is possible by increasing the interval between sampling times, reducing the sample loop volume and/or increasing the volume of the gas phase.

Further research will concentrate on factors of importance for the optimization of this multiphase system.

#### REFERENCES

- 1 E. Antonini, G. Carrea and P. Cremonesi, *Enzyme Microb. Technol.*, 3 (1981) 291.
- 2 M. D. Lilly, *J. Chem. Technol. Biotechnol.*, 32 (1982) 162.
- 3 A. Q. H. Habets-Crützen, L. E. S. Brink, C. G. van Ginkel, J. A. M. de Bont and J. Tramper, *Eur. J. Appl. Microbiol. Biotechnol.*, in press.
- 4 H. Hachenberg and A. P. Schmidt, *Gas Chromatographic Headspace Analysis*, Heyden, London, 1977.
- 5 D. M. Comberbach and J. D. Bu'Lock, *Biotechnol. Bioeng.*, 25 (1983) 2503.
- 6 D. M. Comberbach, J. M. Scharer and M. Moo-Young, *Biotechnol. Lett.*, 6 (1984) 91.
- 7 S. Özeris and R. Bassette, *Anal. Chem.*, 35 (1963) 1091.
- 8 Landolt-Börnstein, *Gleichgewicht der Absorption von Gasen in Flüssigkeiten*, IV. Band, 4. Teil, Bandteil c, Springer-Verlag, Berlin, 1976.
- 9 B. Gutsche and H. Knapp, *Polish J. Chem.*, 54 (1980) 2261.
- 10 P. Adlercreutz and B. Mattiasson, *Eur. J. Appl. Microbiol. Biotechnol.*, 16 (1982) 165.

# 3. OPTIMIZATION OF ORGANIC SOLVENT IN MULTIPHASE BIOCATALYSIS

L. E. S. Brink and J. Tramper

Department of Food Science, Food and Bioengineering Group,  
Agricultural University Wageningen, De Dreyen 12, 6703 BC Wageningen,  
The Netherlands

Accepted for Publication January 4, 1985

The microbial epoxidation of propene and 1-butene was used to study some fundamental aspects of two-liquid-phase biocatalytic conversions. Introduction of a water-immiscible organic solvent phase in a free-cell suspension gave rise to a series of undesired phenomena, e.g., inactivation by the solvent, clotting of biomass, and aggregation of cells at the liquid-liquid interface. Immobilization of the cells in hydrophilic gels, e.g., calcium alginate, prevented direct cell-organic solvent contact and the related clotting and aggregation of biomass. However, the gel entrapment did not seem to provide additional protection against the organic solvent. The influence of various organic solvents on the retention of immobilized-cell activity was related to solvent properties like the polarity (as expressed by the Hildebrand solubility parameter) and the molecular size (as expressed by the molecular weight or molar volume). High activity retention was favored by a low polarity in combination with a high molecular weight. The solubility parameter also proved useful to describe the capacity of various organic solvents for oxygen and alkene oxides. This facilitated the optimization of the solvent polarity.

## INTRODUCTION

The immobilization of enzymes, cell organelles, and whole cells has become a widely applied and commonly accepted technique in the field of biocatalysis. A state-of-the-art review concerning the many different aspects of this fast expanding area has recently been given by Mattiasson.<sup>1</sup> The great interest in immobilized biocatalysts is based on well-known advantages inherent to the immobilization, that is, improved biocatalyst separation, continuous processing and sometimes enhanced operational stability. Immobilization has not changed the situation that bioconversions are still mostly performed in aqueous environments. Replacement of part of the aqueous phase by an organic phase, however, might prove to be as important as the immobilization technique for broadening the scope of practical applications.<sup>2,3</sup>

Two classes of water-organic solvent systems can roughly be distinguished: (1) water-water-miscible organic solvent homogeneous liquid system<sup>4</sup> and (2) water-water-immiscible organic solvent two-liquid-

phase system.<sup>2,3</sup> In the latter case the free, or immobilized biocatalysts are present in the aqueous phase, whereas the main part of the substrates and products are contained in the organic phase. The presence of a substantial amount of organic solvent in the biocatalytic reaction medium may offer certain important advantages in comparison to the aqueous reaction medium. High concentrations of poorly water-soluble substrates and/or products are possible in organic-solvent-containing media. The chance of microbial contamination is reduced. Furthermore, reaction equilibria may be shifted favorably, and substrate and/or product hydrolysis can be largely prevented. In case of two-liquid-phase systems extra advantageous phenomena could occur. Substrate or product inhibition may be reduced as a consequence of a lower inhibitor concentration in the aqueous environment of the enzyme or cell, and recovery of product and biocatalyst is facilitated. The main drawback of introducing an organic solvent is denaturation of the enzymes responsible for the desired bioconversion. The influence of this denaturation by the solvent might be reduced, and consequently the biocatalyst stability enhanced, by immobilizing the biocatalysts at or in a protective support. In that case one also benefits from the intrinsic advantages provided by immobilization itself.

Though an additional liquid phase tends to complicate the process, e.g., hydrodynamics, bioreactor design, handling, separation, the two-liquid-phase system might often be preferable to the homogeneous liquid system. In the latter system high organic solvent concentrations in the aqueous biocatalyst phase may lead to inhibition, denaturation, and loss of substrate specificity. Similarly, high substrate and/or product concentrations can also give rise to inhibition. Furthermore, the first type of system is never very hydrophobic and therefore not suited for very lipophilic substrates. The work described in this article will concentrate only on the water-organic solvent two-liquid-phase reactions. The special case of aqueous two-liquid-phase systems<sup>1,5</sup> in which the incompatibility of two different water-soluble poly-

mers creates two separate aqueous phases will also not be considered.

Until now a main part of the research on two-liquid-phase biocatalytic reactions deals with the transformations of the very water-insoluble steroids. Much work concerning this type of bioconversion has been carried out by Antonini and co-workers.<sup>2</sup> Free or immobilized enzymes and solvents like ethyl and butyl acetate were used for the biotransformation of different steroids. The oxidation of the steroid cholesterol by free and immobilized cells suspended in various organic phases has been studied by Lilly and co-workers.<sup>3,6-8</sup> Several steroid conversions were investigated by Fukui and Tanaka.<sup>9</sup> Cells were entrapped in gels of various degrees of hydrophilicity/hydrophobicity. The immobilized biocatalysts were contacted with organic solvents, like mixtures of benzene and *n*-heptane, containing the steroid substrates. Some examples of bio-reactions not involving steroids have also been reported. Omata et al.<sup>10</sup> demonstrated the hydrolysis of methyl succinate by gel-entrapped cells in water-saturated *n*-heptane. In another study a favorable shift in the reaction equilibrium of an esterification was established by using an enzyme covalently bound to porous glass in chloroform.<sup>11</sup> In this case the low water activity strongly increased the yield of the ester. Schwartz and McCoy<sup>12</sup> showed that the presence of a cyclohexane phase during the fermentation of octane and 1,7-octadiene greatly increased the conversion of the diene to epoxy-octene. This increase was attributed to the lower concentration of the monoepoxide, and hence reduced product inhibition, in the aqueous fermentation broth. Adlercreutz et al.<sup>13</sup> used emulsions of perfluoro chemicals to enhance the oxygen supply to cells entrapped in calcium alginate. Completely fluorinated organic compounds were applied in relation to their very nonpolar and inert properties and their high solvent capacity for gases. From the above work it can be concluded that uniform rules for the design of two-liquid-phase systems are still insufficiently available.

Two characteristics of two-liquid-phase systems seem to play a predominant role in process design and optimization, that is, type of organic solvent, and (if applicable) technique of immobilization. The nature of the organic solvent can markedly affect the reaction kinetics and stability of the biocatalyst, the chemical and mechanical stability of the carrier material, and finally the partition of substrates and products between the different phases. The polarity of the solvent has been used to qualify some of the mentioned effects.<sup>2,9,10</sup> Omata et al.<sup>10</sup> reported that a high solvent polarity promoted the penetration of a hydrophobic substrate in a hydrophilic gel but also inactivated the entrapped cells. This example illustrates that the various solvent effects on the efficiency of the bioconversion are often contradictory and that optimization is necessary when choosing an organic solvent.

The technique of immobilization and the amount of water surrounding the biocatalyst both may influence the rate of mass transfer of substrates and products between the different phases in the two-liquid-phase system. Furthermore the retention of activity and stability of the biocatalyst will be affected by the immobilization. A minimal degree of enzyme hydration will always be necessary for the maintenance of catalytic activity.<sup>4</sup> An optimum in this amount of water seems likely.<sup>14</sup> A thick "layer" of protective water will cause little or no denaturation by the solvent. However, diffusion limitations may occur as a consequence of the long diffusion path through water, the small interfacial specific surface area, and/or the low solubility of lipophilic or gaseous substrates in water (e.g., oxygen). High mass transfer rates are more likely when the amount of water is minimized (e.g., reversed micelles,<sup>14</sup> but the number of practical examples is still limited.

When gel entrapment is used as the immobilization technique, the quantity of surrounding water is determined by the size of the gel particle and by the hydrophobicity-hydrophilicity balance of the gel. A very hydrophilic gel, like calcium alginate, will have a high water content, which in turn leads to a high retention of activity. Again, however, low diffusion rates of substrates and products through such an aqueous gel may cause an undesirable low overall reaction rate. It has indeed been shown that increasing the hydrophobicity of the gel used for entrapment may result in higher activities.<sup>9</sup> Higher gel-solvent partition coefficients of the substrates were found to correlate with these higher conversion rates.

In this work a study is presented concerning some of the fundamental aspects of two-liquid-phase bioconversions mentioned above. We are investigating as a model the microbial epoxidation of propene and 1-butene in a system containing a water-immiscible organic solvent.<sup>15-17</sup> In addition to the two liquid phases, this multiphase system also consists of a solid, immobilized-cell phase and a gas phase containing the two gaseous substrates oxygen and alkene. Many of the above-stated advantages of immobilization and of an additional organic phase are applicable to this model reaction. The very inhibitory effects of propene oxide and 1-butene oxide on the catalytic activity of the cells<sup>18</sup> can be averted by *in situ* extraction of these products into the organic phase. The solubility of the gaseous substrates, only sparingly soluble in water, is relatively high in a suitable organic solvent. Recovery of the immobilized biocatalyst and the epoxide is facilitated. A possible lowering of the yield due to hydrolysis of propene oxide<sup>19</sup> can be prevented.

The design and optimization of the multiphase system will be expounded in relation to the microbial epoxidation of gaseous alkenes. It is shown, however, that the derived design criteria, especially with respect to



the organic solvent and its interactions with other system elements, can be helpful in various applications of two-liquid-phase bioconversions.

## MATERIALS AND METHODS

### Chemicals and Microorganism

Solvent source, purity, molecular weight, and specific gravity are presented in Table I. Liquid propene oxide

and 1-butene oxide were obtained from Merck. Mixtures of different perfluoro chemicals (FC-40, FC-70) were purchased from 3M, St. Paul, MN. Propene and 1-butene were of commercial purity and obtained from the Matheson company, East Rutherford, NY. Alginate Industries, London, the United Kingdom, and the Copenhagen Pectin Factory Ltd., Denmark, provided sodium alginate (Manucol DM) and sodium K-carrageenan (Genugel type X-0828), respectively. Microbial aspects, like substrate specificity, of the *Mycobacterium* strain

Table I. Physical properties, solubility parameters, and immobilized-cell activity retentions of organic solvents used.

Solvent	Solvent number	Source	Purity (%)	Molecular weight (g/mol)	Specific gravity (20°C) (g/cm <sup>3</sup> )	Solubility in water <sup>a</sup> (20°C) (% w)	Solubility parameter [(cal/cm <sup>3</sup> ) <sup>1/2</sup> ]	Activity retention (%)
<b>Saturated aliphatic hydrocarbons</b>								
n-Hexane	1	Merck	97	86.18	0.660	0.00095	7.3	39
n-Hexadecane	2	Baker	>99	226.45	0.7733	—	8.0	85
<b>Aromatic hydrocarbons</b>								
Toluene	3	Merck	99.5	92.15	0.8669	0.052	8.9	~0
Ethylbenzene	4	Merck	99	106.17	0.867	0.0152	8.8	29
<b>Unsaturated hydrocarbons</b>								
Styrene	5	Merck	99.5	104.15	0.906	0.031	9.3	45
<b>Aliphatic alcohols</b>								
1-Butanol	6	Merck	98	74.12	0.8098	9	11.4	~0
1-Hexanol	7	Merck	98	102.18	0.814	0.594	10.7	6
<b>Aliphatic ethers</b>								
Diisopropyl ether	8	Merck	98	102.18	0.723	1.197	7.1 <sup>b</sup>	56
Diisopentyl ether	9	Merck	97	158.29	0.777	0.020	7.2 <sup>b</sup>	77
<b>Aromatic ethers</b>								
Methyl phenyl ether	10	Merck	99	108.13	0.993	1.04	9.5 <sup>b</sup>	5
Diphenyl ether	11	Fluka	>98	170.21	1.0748	0.39	9.6 <sup>b</sup>	~95
<b>Aliphatic aldehydes</b>								
Hexanal	12	Merck	98	100.16	0.815	0.5	9.2 <sup>c</sup>	~0
<b>Aliphatic ketones</b>								
Methyl isobutyl ketone	13	Merck	99	100.16	0.798	1.693	9.4 <sup>b</sup>	~0
Methyl octyl ketone	14	Fluka	>95	156.27	0.825	—	7.8	53
<b>Esters of saturated aliphatic monocarboxylic acids</b>								
Butyl acetate	15	Merck	99	116.16	0.883	0.43	8.5	3
Ethyl trichloro acetate	16	Pfaltz B.	—	191.44	1.3836	—	8.9 <sup>b</sup>	16
<b>Esters of unsaturated aliphatic monocarboxylic acids</b>								
Butyl acrylate	17	Merck	99	128.17	0.898	—	8.4	~0
<b>Esters of aromatic monocarboxylic acids</b>								
Butyl benzoate	18	Merck	99	178.23	1.004	—	8.4 <sup>b</sup>	14
<b>Esters of dicarboxylic acids</b>								
Diethyl maleate	19	Merck	97	172.18	1.065	1.4	8.7 <sup>b</sup>	1
Dibutyl adipate	20	Fluka	>99	258.36	0.962	—	8.9 <sup>c</sup>	7
Dimethyl phthalate	21	Merck	99	194.19	1.188	0.43	10.7	19
Diethyl phthalate	22	Merck	99	222.24	1.117	—	10.0	74
Dibutyl phthalate	23	Merck	99	278.35	1.045	0.040	9.3	76
Diocetyl phthalate	24	L&I	99	390.54	0.985	—	7.9	108
Didecyl phthalate	25	Fluka	>95	446.68	0.966	—	7.2	101
Di-(2-methoxyethyl) phthalate	26	Fluka	>98	282.30	1.171	—	10.2 <sup>c</sup>	22
Diallyl phthalate	27	Fluka	~97	246.27	1.119	—	10.1 <sup>c</sup>	43
<b>Esters of polybasic acids</b>								
Tri-n-butyl phosphate	28	Fluka	99	266.32	0.976	0.039	8.6 <sup>c</sup>	12
Tri-2-tolyl phosphate	29	BDH	—	368.37	~1.16	0.000050	8.4	55
<b>Aliphatic chlorinated hydrocarbons</b>								
Chloroform	30	Merck	99	119.38	1.4832	0.815	9.3	~0
Tetrachloro methane	31	Merck	99	153.82	1.5940	0.077	8.6	~22
1,1,2,2-Tetrachloro ethane	32	Merck	98	167.85	1.594	0.287	9.7	10
<b>Fluorinated hydrocarbons</b>								
FC-40	33	3M	—	~650	~1.87	—	5.9 <sup>d</sup>	94
FC-70	34	3M	—	~820	~1.94	—	5.9 <sup>d</sup>	94

<sup>a</sup> From refs. 20 and 30.

<sup>b</sup> From experimental molar heat of vaporization.

<sup>c</sup> From Small's molar attraction constants (ref. 26).

<sup>d</sup> Estimated from the solubility parameters of other perfluoro chemicals.

E3 used for the epoxidation reactions, have been published elsewhere.<sup>15</sup>

### Immobilization Procedures

The technique of immobilization in calcium alginate and potassium K-carrageenan have been reported elsewhere.<sup>15</sup> The shape and size of the gel beads were examined microscopically.

### Cell Activity Measurements

The experimental setup used for investigation of the epoxidation reactions consisted of a batch reactor system with gas circuit, a computer-controlled gas sampling valve, an on-line gas chromatograph, and an integrator coupled to a microcomputer. Full details of this experimental system and the quantitative application of the headspace gas chromatography technique will be published.<sup>16</sup>

A small bubble column bioreactor (4.5 cm i.d.) was used for contacting the biocatalyst beads and the liquid phase(s) with the circulating gas. At the start of an experiment this air stream contained 1.7% propene or 1-butene (v/v). The total volume of beads and liquid phase(s) was always 250 cm<sup>3</sup> (~15 cm<sup>3</sup> gel beads, an aqueous salt solution and, if applicable, 10 cm<sup>3</sup> organic solvent). An aqueous (0.05M) solution of CaCl<sub>2</sub> was used in case of cells immobilized in calcium alginate. Potassium carrageenan beads were suspended in an aqueous 1% (w/w) solution of KCl. The ionic strength of these two salt solutions (0.15 and 0.13, respectively) resembles that of a 0.9% (w/w) NaCl solution (physiological salt solution, ionic strength 0.15). Experiments with free cells were carried out in an aerated flask containing 250 cm<sup>3</sup> (0.05M) CaCl<sub>2</sub> solution. A portion (10 cm<sup>3</sup>) of this CaCl<sub>2</sub> solution was replaced by an equal volume of organic solvent when the solvent influence on free-cell activity was to be examined.

### Epoxide Partition

The distribution of propene oxide over a water phase and a water-immiscible organic phase was examined. Equal volumes (20 cm<sup>3</sup>) of these phases were equilibrated at 30°C in 40-cm<sup>3</sup> screw-cap bottles after addition of 10 mm<sup>3</sup> propene oxide. Epoxide concentrations in the two liquid phases were then determined gas chromatographically by measuring peak heights.

The partition of propene oxide and 1-butene oxide in air-solvent and air-water systems was also established. The liquid phase (25 cm<sup>3</sup> water or solvent and 100 mm<sup>3</sup> propene oxide or 1-butene oxide) and an air phase were brought in equilibrium at 30°C in 75-cm<sup>3</sup> screw-cap bottles. The headspace gas was then analyzed using a gas chromatograph coupled to an integrator.

## RESULTS AND DISCUSSION

### General

As pointed out in the introduction, several interactions and phenomena, which may occur in and between the different elements of the multiphase system, must be considered and, if necessary, verified experimentally before a meaningful choice of these system elements can be made. The retention of catalytic activity as influenced by the technique of immobilization was determined. Furthermore, the influence of the organic solvent on catalytic activity and carrier stability was established. Solubility data of the substrates and epoxides in organic solvents (relative to water) were sought for in the literature or, if not available, were determined experimentally. Solvent properties, like boiling point, toxicity, and flammability, and economic aspects will not be considered here.

More than 30 organic solvents were investigated to test the suitability for application in the multiphase system (Table I). The solvents are subdivided according to a classification given by Riddick et al.<sup>20</sup> Initially, each solvent class was represented by one or two compounds. Additional solvents were selected using the information gained from the experiments on the activity retention of immobilized cells (see below). Furthermore, the selection was partly based on experimental results concerning the toxicity of organic extraction reagents to anaerobic bacteria.<sup>21</sup>

Entrapment of the cells in calcium alginate and potassium K-carrageenan, apart from being very workable, appeared to be successful immobilization techniques with respect to retention of catalytic activity. The immobilized cells proved not to be inferior to the free cells (Fig. 1). The somewhat lower stability of the suspended cells in this figure can be attributed to the phenomenon of cells spurted out of the suspension by the gas stream. The use of small gel particles (~0.7

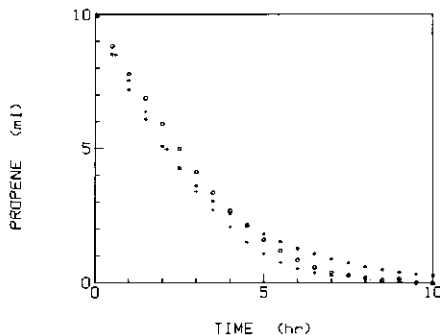


Figure 1. Amount of unconverted propene versus time: (\*) free cells, (O) cells immobilized in calcium alginate, (+) cells immobilized in potassium K-carrageenan.

mm) in combination with small cell load (~1 g dry weight cells in 30 g alginate or K-carrageenan gel) avoided diffusional processes to become rate limiting. When the experiments with immobilized cells were performed with larger particles and/or higher cell loads, lower reaction rates were measured as a result of these diffusion limitations.<sup>16,22</sup>

As the reaction proceeds, an increasing difference is found between experimental epoxide concentrations and calculated values from alkene consumption rates.<sup>16</sup> Hydrolysis of the produced propene oxide to 1,2-propanediol cannot explain the difference. Literature values<sup>19</sup> ( $2.3 \times 10^{-6} \text{ s}^{-1}$ ) as well as experimentally determined values ( $1.5 \times 10^{-6} \text{ s}^{-1}$ ) of the first-order reaction constant for hydrolysis at the experimental conditions used (30°C, pH ~6) are an order of magnitude too small to explain this discrepancy. Since it was found that leakage can be excluded, the only resulting possibility is enzymic activity. This confirms the previously found ability of the bacteria used to consume the alkene oxides.<sup>15</sup> Immobilization in alginate or K-carrageenan lowers the rate of this propene oxide consumption (Fig. 2), indicating an additional advantage of using immobilized cells.

The structure of the calcium alginate gel appeared to be stable in all the solvents tested (for solvents, see Table I), provided the organic solvents were saturated with water. No visible deleterious effects like disintegration, excessive attrition, dissolution, or chemical reaction could be observed. The K-carrageenan gel also did not seem to be affected by solvents like dibutyl phthalate and diisopentyl ether. These observations directly seem to correlate with the low to very low solubility of water-immiscible solvents in hydrophilic gels. Immobilization in calcium alginate was used for further work, because the shapes of the alginate particles appeared more spherical than those of K-carrageenan particles.

### Influence of the Organic Solvent on the Retention of Activity

#### Free Cells

From various preparatory experiments concerning the oxygen, ethene, and propene consumption rates of free cells in a solvent-containing system (mostly phosphate buffer saturated with the solvent), it became clear that the number of usable solvents is very limited indeed.<sup>17</sup> Many solvents caused almost instant inactivation of the suspended cells. Examples of these are chloroform, toluene, 1-butanol, butyl acetate, tetrachloro ethane, and hexanoic acid.

Furthermore, it became evident that the presence or absence of a separate organic liquid phase could be a decisive factor in the measurements with free cells. Many undefined physical phenomena and often rapid loss of catalytic activity occurred when a water-

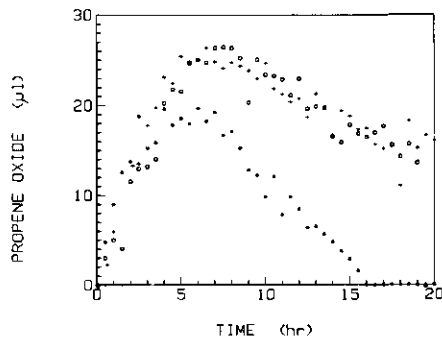


Figure 2. Amount of produced propene oxide versus time: (\*) free cells, (○) cells immobilized in calcium alginate, (+) cells immobilized in potassium K-carrageenan.

immiscible solvent was added to an aqueous cell suspension in such quantity that a separate liquid phase formed. The very high surface tension between the two liquid phases and the large difference in dielectric constants may well explain some of these phenomena.<sup>5</sup> Aggregation of cells at the water-organic interface appeared sometimes to be the reason for loss of activity (e.g., butyl acetate). The introduction of the solvent can have a positive or a negative overall effect on the propene consumption rate of free cells (Fig. 3). When no organic solvent was added, an increasing part of the biomass was spurted out of the suspension by gas bubbles breaking up at the surface. The presence of a dibutyl phthalate phase largely prevented this kind of biomass loss, resulting in an apparent increase of catalytic activity. However, after about 10 h in suspension the formation of biomass clots appeared in the water-dibutyl phthalate mixture. In case of diisopentyl ether, spurring out and clotting of cells was not observed. The epoxidation rate was nevertheless re-

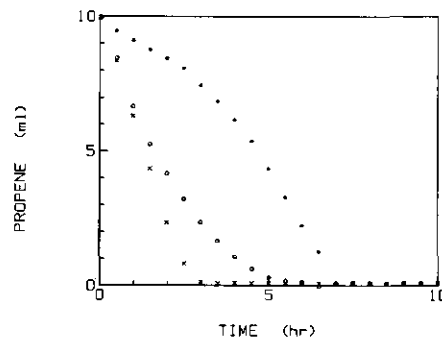


Figure 3. Amount of unconverted propene versus time (free cells, 10 mL organic liquid phase present): (○) blank measurement, (×) dibutyl phthalate, (+) diisopentyl ether.

duced (Fig. 3), but after a few hours of reaction, the consumption rate inexplicably increased.

In general, one could say that the introduction of an organic solvent in a free-cell suspension gives rise to a series of physical, microbial, and/or biochemical effects on the catalytic activity. The resulting, often undesirable and inexplicable effects can hamper greatly the development, scaling up, and control of the biotechnological process. Immobilization may prove useful as a way to overcome these problems.

### Immobilized Cells

The choice of the organic solvent also appeared critical when cells were immobilized in calcium alginate gel.<sup>16,17</sup> A first selection of the solvents under investigation (Table I) was made by measuring the retention of immobilized-cell activity in the presence of a separate organic liquid phase (Table I). Quantification of the retention of activity took place by relating the amount of propene consumed by the immobilized cells after 3 h reaction to the corresponding amount of a blank measurement (no organic phase present). The given percentages in Table I must only be seen as a rough guide for the influence of a specific organic solvent. Solvent impurities and activity loss during storage of biomass (necessary in view of the duration of the experiments and the method of measurement) could sometimes give rise to experimental errors. Despite the entrapment of the cells in the alginate gel, many organic solvents caused rapid loss of activity. Solvents like *n*-hexane, diisopropyl ether, methyl octyl ketone, diallyl phthalate, and tritolyol phosphate resulted in a low activity retention (Table I). Little loss of activity was only measured when the following solvents were present: *n*-hexadecane, diisopentyl ether, diphenyl ether, di-*n*-alkyl phthalates (except the dimethyl ester), and finally two perfluoro chemicals (FC-40, FC-70). Entrapment did, however, prevent the occurrence of above-discussed phenomena like aggregation, clotting, and spurting out of biomass.

The very divergent effects established for the various solvents (Fig. 4) underlines the importance of a careful choice of the solvent. However, it would be very time consuming and expensive to test the large number of solvents that could, in theory, be used in the multiphase system. In this context it would be very desirable to relate the measured activity retentions of the immobilized biocatalyst to readily available solvent properties. The resulting (semiempirical) rules could then be applied to exclude many solvents in advance.

The solvent polarity has already been mentioned in a qualitative manner to explain the inactivation of enzymes or cells under the influence of an organic solvent.<sup>2,10</sup> In this work the solubility parameter was taken as a semi-quantitative measure for the polar character of the organic solvent. Other means of quantification, like dielectric constant, dipole moment, and

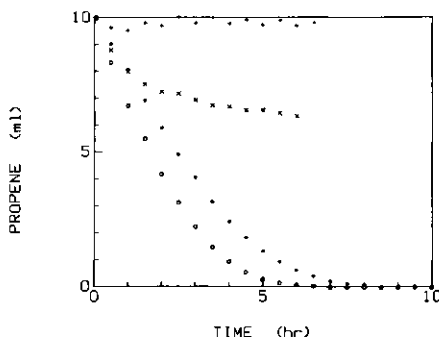


Figure 4. Amount of unconverted propene versus time (cells immobilized in calcium alginate, 10 mL organic liquid phase present); (O) blank measurement, (\*) diisopentyl ether, (x) *n*-hexane, (+) butyl acetate.

polarizability, were not used, as the data availability of these quantities is rather limited. The solubility parameter, denoted by the symbol  $\delta$ , is the Hildebrand expression for the square root of the cohesive energy density<sup>23,24</sup> [in (cal/cm<sup>3</sup>)<sup>0.5</sup>] and is suited for describing intermolecular forces and solubility:

$$\delta = \left( \frac{-E}{v} \right)^{0.5} = \left( \frac{\Delta H_v - RT}{v} \right)^{0.5} = \left( \frac{\rho(\Delta H_v - RT)}{M} \right)^{0.5}$$

A higher value of  $\delta$  normally corresponds with a higher polarity of the solvent. Solubility parameter values of the solvents under investigation are listed in Table I. Parameter values not given directly in the literature<sup>23-25</sup> could be calculated from experimental values of the molar heat of vaporization  $\Delta H_v$  (see equation above) or by using Small's molar attraction constants.<sup>26</sup> Only a weak, negative correlation was established between the measured activity retentions of immobilized cells and the solubility parameters of the corresponding solvents (both in Table I). Thus, a low polarity (low  $\delta$ ) tends to give a high retention of biocatalytic activity, but not pronouncedly.

Another solvent characteristic that might be important with respect to the measured immobilized-cell activities is dimension of the solvent molecule. Larger molecules could be more susceptible to (steric) hindrances on their way from the organic bulk phase to the catalyzing enzymes in the immobilized cells. Such obstruction could arise from the low solvent solubility in water and from the transport of solvent through the aqueous matrix structure of the (alginate) gel and through the (outer) cell membranes. A rough measure for these hindrances may be given by the solubility in water, molecular weight  $M$ , or the molar volume ( $v = M/\rho$ ) of the organic solvent (Table I). McAuliffe<sup>27</sup> found that for certain homologous series of hydrocarbons the logarithm of the solubility in water is a linear function of the hydrocarbon molar volume. Not surprisingly, however, no clear relation could be dem-

onstrated between the molar volumes (or molecular weights) and solubilities in water of the very different solvents investigated in this work. These two quantities can therefore not be treated as one and the same parameter.

Very weak, positive (+) or negative (-) correlations exist between on the one hand activity retention and on the other solubility in water (-), molecular weight (+), or molar volume (+). However, a more significant relation emerges when the retention of cell activity was considered as a function of both the solubility parameter (polarity) and the molecular weight (Fig. 5). Each box in this figure corresponds to one of the solvents in Table I. Many of the low activities can be found in an area of high polarity ( $\delta > \sim 8$ ) and small molecular weight ( $M < \sim 200$ ). The higher retentions of activity are found outside this area, which appears especially to be true for the two perfluoro chemicals (both 94%) and the two largest di-*n*-alkyl phthalates (101 and 108%). The latter compounds have all in common a low polarity in combination with a high molecular weight.

The picture of Figure 5 does not change significantly when the molecular weight is replaced by the molar volume of the solvent. Furthermore, it must be noted that both parameters of Figure 5 are required for a satisfactory explanation of the differences in activity. Though molecular weight (molar volume) and  $\delta$  may be related to each other in case of one specific, homologous series of organic solvents, it can be deduced from Figures 5 and 6 that no simple relation exists between  $M$  and  $\delta$  when different solvents classes are considered.

When the logarithm of the solubility in water is plotted versus the solubility parameter, an area of inactivation may also be distinguished (high polarity and high solvent solubility in water). The use of the solubility in water is, however, less attractive than

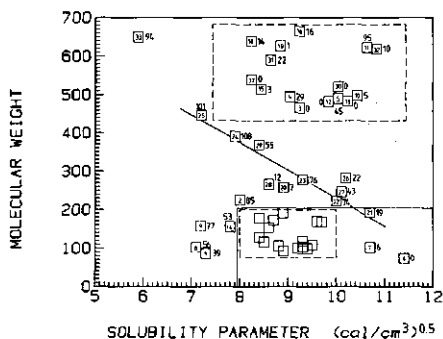


Figure 5. Measured activity retentions (%; large figures) of immobilized cells exposed to organic solvents as function of molecular weight and solubility parameter of solvents. Each box and number (small figure) corresponds to one of the solvents in Table I; line: di-*n*-alkyl phthalates.

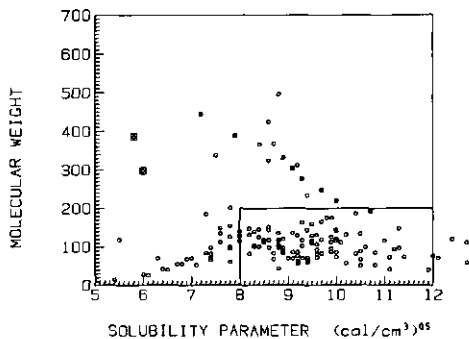


Figure 6. The distribution of commonly used organic solvents in a molecular weight versus solubility parameter plot: (□) perfluoro *n*-heptane and perfluoro cyclohexane, (×) dialkyl phthalates.

molecular weight or molar volume in view of lacking experimental solubility data.

The effects of molecular size and polarity can be illustrated by considering the homologous series of the di-*n*-alkyl phthalates (see also Fig. 5). As mentioned above, inactivation did not occur when the dioctyl and didecyl esters (large molecules, nonpolar) were used as the organic phase. Some loss of activity was measured when comparing the propene consumption in the presence of a dibutyl phthalate or a diethyl phthalate phase (smaller alkyl chains, moderately polar) with the blank experiments (76 and 74%, respectively, see Table I). Hardly any activity was found when dimethyl phthalate (relatively small molecule, polar) was present in the multiphase system.

Similar phenomena can be distinguished in Table I. The higher activity in case of *n*-hexadecane and tritoyl phosphate, in comparison to *n*-hexane and tributyl phosphate, respectively, could be a molecular size effect. Larger size and a lower polarity may explain the higher activity in case of diisopentyl ether, diphenyl ether, and methyl octyl ketone in comparison to diisopropyl ether, methyl phenyl ether and methyl isobutyl ketone, respectively.

The situation of about 150 commonly used organic solvents<sup>25</sup> in a plot of  $M$  versus  $\delta$  (Fig. 6) affirms the experimentally established observation that many solvents cause strong inactivation of the immobilized cells. More than two-thirds of the total number of solvents in Figure 6 can be found in the above-mentioned area of inactivation ( $\delta > \sim 8$  and  $M < \sim 200$ ). Also, it can clearly be seen in this figure that the dialkyl phthalates and perfluoro chemicals, which cause almost no inactivation (Table I), are relatively exceptional organic solvents. Organic compounds with still higher values for  $M$  and  $\delta$  (top right in Fig. 6) are very likely solid at 30°C and are therefore not suited for our purposes.

To test the applicability of the above-described relations between solvent polarity, molecular size, and immobilized-cell activity, the experimental results of

**Table II.** Molecular weights, solubility parameters, and free-cell activity retentions of the organic solvents of Playne et al.<sup>4</sup>

Solvent	Solvent number	Molecular weight (g/mol)	Solubility parameter [(cal/cm <sup>3</sup> ) <sup>0.5</sup> ]	Activity retention (%)
<i>n</i> -Hexane	1	86.18	7.3	62
Isooctane	35	114.22	6.9 <sup>b</sup>	71
<i>n</i> -Decane	36	142.28	8.0	84
Freon 113	37	187.39	7.3	100
Isopentyl alcohol	38	88.15	10.5 <sup>b</sup>	3
1-Hexanol	7	102.18	10.7	1
1-Octanol	39	130.22	9.3 <sup>b</sup>	8
2-Ethyl hexanol	40	130.22	9.5	27
1-Dodecanol	41	186.33	8.1	70
Isopentyl acetate	42	130.18	8.1 <sup>b</sup>	14
Tri- <i>n</i> -butyl phosphate	28	266.32	8.6 <sup>c</sup>	100
Tri-2-tolyl phosphate	29	368.37	8.4	109
Dibutyl phthalate	23	278.35	9.3	88
Diisopentyl phthalate	43	306.39	9.1 <sup>d</sup>	85
Diethyl ketone	44	86.13	10.0 <sup>b</sup>	1
Methyl isobutyl ketone	13	100.16	9.4 <sup>b</sup>	3
Dipropyl ketone	45	114.18	9.6 <sup>b</sup>	1
Methyl hexyl ketone	46	128.21	8.4 <sup>b</sup>	0
Diisopropyl ether	8	102.18	7.1 <sup>b</sup>	9
Diisopentyl ether	9	158.29	7.2 <sup>b</sup>	62
Benzene	47	78.11	9.2	0
Toluene	3	92.15	8.9	3
<i>o</i> -Xylene	48	106.16	8.8 <sup>b</sup>	0
Nitrobenzene	49	123.11	10.0	0

<sup>a</sup> From ref. 21.

<sup>b</sup> From experimental molar heat of vaporization.

<sup>c</sup> From Small's molar attraction constants (ref. 26).

<sup>d</sup> Estimated from the solubility parameter of di-*n*-pentyl phthalate.

Playne et al.<sup>21</sup> were used. The influence of 24 organic solvents (test concentrations 25 mm<sup>3</sup>/cm<sup>3</sup>) on the relative gas production of suspended anaerobic cells was correlated with solvent polarity and size in the same manner as above (Table II and Fig. 7). Again, low cell activities occurred in an area of high polarity ( $\delta > \sim 8$ ) and low molecular weights ( $M < \sim 200$ ).

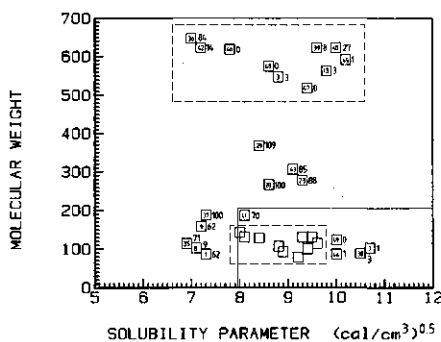


**Figure 7.** Activity retentions (%; large figures) of free cells exposed to organic solvents<sup>21</sup> as a function of molecular weight and solubility parameter of the solvents. Each box and number (small figure) corresponds to one of the solvents in Table II.

A conclusion that could be drawn from comparing Figures 5 and 7 is the similar response of free (Fig. 7) and immobilized (Fig. 5) cells to the presence of an organic solvent. Likewise, many similarities exist between free and immobilized propene-consuming cells, both used in this work, with respect to the toxicity of organic solvents (see Table I and the section on free cells). From these observations it could be deduced that immobilization in calcium alginate provides no additional cell protection against organic solvents.

The results of Duarte et al.<sup>7</sup> can also be used to test the significance of solvent polarity and molecular size to cell activity retention (Table III and Fig. 8). Notwithstanding the small differences between the measured activities and the limited number of solvents tested, the lower activities seem again more likely with solvents situated in the lower right section of Figure 8.

### Solubility of Gaseous Substrates and Epoxide Extraction Capacity

The Hildebrand solubility parameter not only proved useful for predicting the solvent effect on cell activity but may also be applied to describe the solubilities of oxygen and epoxides in various organic solvents.

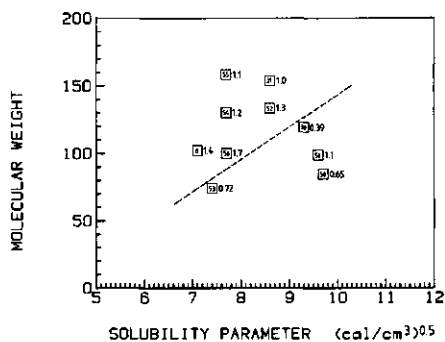


Figure 8. Comparative rates (tetrachloro methane = 1.0; large figures) of free cells exposed to organic solvents<sup>a</sup> as a function of molecular weight and solubility parameter of the solvents. Each box and number (small figure) corresponds to one of the solvents in Table III.

### Gaseous Substrates

A significant change of the gas solubility in a hydrophilic carrier gel (like calcium alginate) under the influence of a water-immiscible organic solvent seems unlikely. Thus, the solubility of the gaseous substrates in the aqueous gel remains essentially that in water, and the solubility in the organic solvent itself may not be of dominant importance. In certain applications, however, the gas solubility in the solvent might play a decisive role. When gas-liquid transfer is a limiting factor in the substrate transport from the gas phase to the biocatalyst phase, a higher substrate solubility in the solvent will increase the reaction rate. A high solvent capacity for the gaseous substrates can also be advantageous when a bioreactor packed with biocatalyst beads is continuously fed with an organic solvent for supply of dissolved substrates (and removal of products).

As shown by Hildebrand et al.<sup>23</sup>, a good correlation

exists between the oxygen solubility in various organic solvents (expressed in mole fractions) and the solubility parameters of these solvents. High solubilities of oxygen are found in solvents with a low polarity (low  $\delta$ ), and vice versa. Extreme examples of this are perfluoro *n*-heptane ( $\delta$  5.9) and water ( $\delta$  ~23), in which the oxygen solubilities, expressed in mole fractions, are  $55.1 \times 10^{-4}$ <sup>28</sup> and  $0.21 \times 10^{-4}$ , respectively. A similar, though somewhat weaker, correlation was found when the oxygen solubilities<sup>28</sup> were expressed in mmol oxygen/L solvent (Fig. 9). From the foregoing it can be deduced that activity retention under the influence of an organic solvent and a high oxygen solubility in the solvent are not contradictory, as they are both favored by a low solvent polarity. Perfluoro chemicals provide a very good illustration of this finding.

Values of the propene solubility in solvents were obtained by extrapolating from partial pressure/mole fraction data.<sup>29</sup> The thus calculated solubilities (expressed in millimolars) did not seem to correlate with the solubility parameter. The capacity of the solvents for propene is, however, always about two orders of magnitude higher than that of water.

### Epoxides

The partition of propene oxide between equal volumes of organic solvent and water was measured (Table IV). The standard deviations in these experimental values is rather high (5–10%) due to the interfering influences of water, solvent, and impurities on the gas chromatography analysis.

The percentage of the total amount of epoxide extracted into the solvent correlated with the polarity of the extractant as expressed by the solubility parameter (Fig. 10). High propene oxide ( $\delta$  9.2) extraction capacities, much better than that of water (50%), were found only at rather high solvent polarities ( $\sim 9 < \delta < \sim 10$ ). However, a too high polarity ( $\delta > \sim 10$ ) also

Table III. Molecular weights, solubility parameters, and free-cell comparative rates (tetrachloro methane = 1.0) of the organic solvents used by Duarte et al.<sup>a</sup>

Solvent	Solvent number	Molecular weight (g/mol)	Solubility parameter [(cal/cm <sup>3</sup> ) <sup>0.5</sup> ]	Comparative rate (-)
Dichloro methane	50	84.93	9.7	0.65
Chloroform	30	119.38	9.3	0.39
Tetrachloro methane	31	153.82	8.6	1.0
1,2-Dichloro ethane	51	98.96	9.6 <sup>b</sup>	1.1
1,1,1-Trichloro ethane	52	133.41	8.6 <sup>b</sup>	1.3
Diethyl ether	53	74.12	7.4	0.72
Diisopropyl ether	8	102.18	7.1 <sup>b</sup>	1.4
Di- <i>n</i> -butyl ether	54	130.23	7.7 <sup>c</sup>	1.2
Di- <i>n</i> -pentyl ether	55	158.29	7.7 <sup>c</sup>	1.1
Butyl ethenyl ether	56	100.16	7.7 <sup>c</sup>	1.7

<sup>a</sup> From ref. 7.

<sup>b</sup> From experimental molar heat of vaporization.

<sup>c</sup> From Small's molar attraction constants (ref. 26).

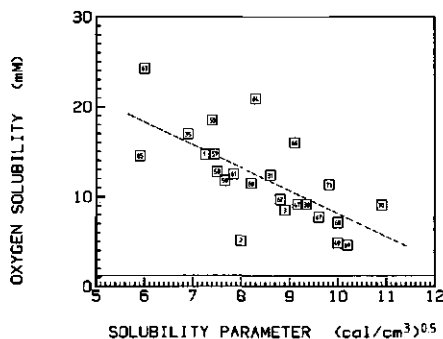


Figure 9. Capacities for oxygen of organic solvents (water: 1.2mM) as a function of solubility parameter (1 = *n*-hexane, 2 = *n*-hexadecane, 3 = toluene, 30 = chloroform, 31 = tetrachloromethane, 35 = isooctane, 47 = benzene, 49 = nitrobenzene, 53 = diethyl ether, 57 = *n*-heptane, 58 = *n*-octane, 59 = *n*-nonane, 60 = cyclohexane, 61 = methyl cyclohexane, 62 = *m*-xylene, 63 = perfluoro-*n*-heptane, 64 = perfluorobenzene, 65 = perfluoro tri-*n*-butyl amine, 66 = fluorobenzene, 67 = chlorobenzene, 68 = bromobenzene, 69 = iodobenzene, 70 = 2-methyl 1-propanol, 71 = acetone).

seems unfavorable for epoxide extraction. The high extraction capacity of 1,1,2,2-tetrachloroethane (98%) may be a result of strong hydrogen bonding between molecules of this solvent and propene oxide.

Another measure for the extraction capacity was obtained by determining the partition of propene oxide and 1-butene oxide between a gas phase (air) and a solvent phase (Table V). The choice of the solvents used in these experiments was partly based on the cell activity measurements (Table I). An error of about

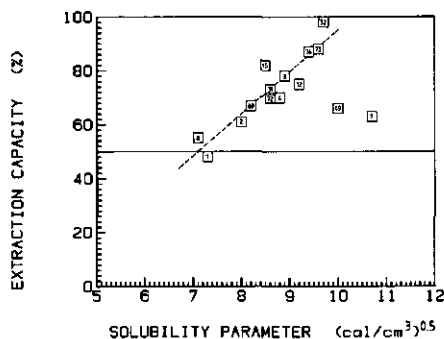


Figure 10. Extraction capacities for propene oxide of organic solvents (water 50%) as a function of the solubility parameter. Each box and number (small figure) corresponds to one of the solvents in Table IV.

5% in the values of Table V was estimated from duplicate measurements.

The percent propene oxide that was found present in the gas phase also related to the solubility parameter. Again, only solvents with a high polarity ( $\sim 8.5 < \delta < \sim 10$ ) possess a capacity for propene oxide ( $\delta$  9.2) significantly higher than that of water (Table V). The capacity of the organic solvents for the more nonpolar 1-butene oxide is not a clear function of  $\delta$  but is mostly an order of magnitude higher than the capacity of water for this epoxide. The extreme nonpolar perfluoro chemicals (FC-40, FC-70) showed a remarkable low capacity for the relatively polar propene oxide and also, to a somewhat lesser extent, for 1-butene oxide.

From the water-solvent, as well as from the gas-solvent, measurements it can be concluded that a suc-

Table IV. Extraction capacity for propene oxide of various solvents in the water-solvent equilibrium experiments.

Solvent	Solvent number	Solubility parameter [(cal/cm <sup>3</sup> ) <sup>0.5</sup> ]	Extraction capacity (%)
Water	—	~23	50*
<i>n</i> -Hexane	1	7.3	48
<i>n</i> -Hexadecane	2	8.0	61
Cyclohexane	60	8.2	67
Toluene	3	8.9	78
Ethylbenzene	4	8.8	70
1-Hexanol	7	10.7	63
Diisopropyl ether	8	7.1 <sup>b</sup>	55
Hexanal	12	9.2 <sup>c</sup>	75
Methyl pentyl ketone	72	8.6	70
Butyl acetate	15	8.5	82
Tetrachloro methane	31	8.6	73
1,1,2-Trichloro ethane	73	9.6	88
1,1,2,2-Tetrachloro ethane	32	9.7	98
Pentachloro ethane	74	9.4	87
Nitrobenzene	49	10.0	66

\* Theoretical.

<sup>b</sup> From experimental molar heat of vaporization.

<sup>c</sup> From Small's molar attraction constants (ref. 26).



Table V. Percent of epoxide amount not dissolved in the gas-solvent equilibrium experiments.

Solvent	Solvent number	Solubility parameter [(cal/cm <sup>3</sup> ) <sup>0.5</sup> ]	Epoxide not dissolved	
			Propene oxide (%)	1-Butene oxide (%)
Water	—	~23	1.81	2.28
n-Hexane	1	7.3	1.88	—
Toluene	3	8.9	0.80	0.19
Diisopentyl ether	9	7.2 <sup>a</sup>	1.48	0.41
Dimethyl phthalate	21	10.7	2.82	0.42
Diethyl phthalate	22	10.0	1.06	0.40
Dibutyl phthalate	23	9.3	1.31	0.45
Dioctyl phthalate	24	7.9	1.73	0.62
Tetrachloro methane	31	8.6	0.84	0.13
1,1,2,2-Tetrachloro ethane	32	9.7	0.13	0.039
FC-40	33	5.9 <sup>b</sup>	11.7	5.80
FC-70	34	5.9 <sup>b</sup>	12.0	—

<sup>a</sup> From experimental molar heat of vaporization.

<sup>b</sup> Estimated from the solubility parameters of other perfluoro chemicals.

cessful propene oxide extraction from the aqueous (gel) phase may require a high polarity of the extractant (e.g., tetrachloro ethane). This can contradict the previously found findings concerning oxygen solubility and especially activity retention. Thus, an optimum in the solvent polarity may be likely. In case of the less polar 1-butene oxide, a nonpolar extractant (e.g. dioctyl phthalate) can still have a high capacity for this epoxide as compared to the capacity of water. Cell denaturation could then be the decisive factor in the choice of the extractant. However, extreme non-polarity (e.g., perfluoro chemicals) can still cause unacceptably low extraction rates.

## CONCLUSIONS

The suitability of a water-immiscible organic solvent for use in multiphase biocatalysis can be predicted by evaluating the polarity (as expressed by the Hildebrand solubility parameter) and the molecular size (as expressed by the molecular weight or molar volume) of the organic solvent. The combination of a low polarity and a high molecular weight often leads to a high activity retention of the free or immobilized cells. Furthermore, the solubility parameter is helpful to assess the capacity of the organic solvent for the (co-) substrates and products involved in the bioconversion. In case of the microbial epoxidation of propene an organic solvent with a high molecular weight and a medium solubility parameter should be used (e.g., dibutyl phthalate). A too low polarity, though favorable for a high activity retention and a high solvent capacity for oxygen, can give an unacceptable low propene oxide extraction rate (e.g., perfluoro chemicals).

The authors wish to thank Professor Ir. K. Ch. A. M. Luyben and Dr. Ir. K. Van't Riet for helpful discussions. These investigations were supported (in part) by the Netherlands Foundation for Technical Research (STW), future Technical Science Branch/Division of the

Netherlands Organization for the Advancement of Pure Research (ZWO).

## NOMENCLATURE

<i>E</i>	molar cohesive energy (J/mol)
<i>M</i>	molecular weight (g/mol)
<i>R</i>	gas constant (J/mol K)
<i>T</i>	temperature (K)
<i>v</i>	molar volume (cm <sup>3</sup> /mol)
$\Delta H_v$	molar heat of vaporization (J/mol)
$\delta$	Hildebrand solubility parameter [(J/cm <sup>3</sup> ) <sup>0.5</sup> ]
$\rho$	specific gravity (g/cm <sup>3</sup> )

## References

1. B. Mattiasson, *Immobilized Cells and Organelles*, 2 vols. (CRC Press, Boca Raton, Florida 1983).
2. E. Antonini, G. Carrea, and P. Cremonesi, *Enz. Microb. Technol.*, **3**, 291 (1981).
3. M. D. Lilly, *J. Chem. Tech. Biotechnol.*, **32**, 162 (1982).
4. L. G. Butler, *Enz. Microb. Technol.*, **1**, 253 (1979).
5. B. Mattiasson, *Trends in Biotechnol.*, **1**, 16 (1983).
6. B. C. Buckland, P. Dunnill, and M. D. Lilly, *Biotechnol. Bioeng.*, **17**, 815 (1975).
7. J. M. C. Duarte and M. D. Lilly, *Enzyme Engineering*, Vol. 5 (Plenum Press, New York, 1980), p. 363.
8. U. K. Patent 1 555 004.
9. S. Fukui and A. Tanaka, *Advances in Biochemical Engineering/Biotechnology*, Vol. 29 (Springer-Verlag, Berlin, 1984), p. 1.
10. T. Omata, A. Tanaka, and S. Fukui, *J. Ferment. Technol.*, **58**, 339 (1980).
11. A. M. Kilbanov, G. P. Samokhin, K. Martinek, and I. V. Berezin, *Biotechnol. Bioeng.*, **19**, 1351 (1977).
12. R. D. Schwartz and C. J. McCoy, *Appl. Environ. Microbiol.*, **34**, 47 (1977).
13. P. Adlercreutz and B. Mattiasson, *Eur. J. Appl. Microbiol. Biotechnol.*, **16**, 165 (1982).
14. M. H. Hilhorst, "Enzymic Reactions in Reversed Micelles" Ph.D. Thesis, Agricultural University, Wageningen, 1984.
15. A. Q. H. Habets-Crutzen, L. E. S. Brink, C. G. van Ginkel, J. A. M. de Bont, and J. Tramper, *Appl. Microbiol. Biotechnol.*, **20**, 245 (1984).

16. L. E. S. Brink, J. Tramper, K. Van't Riet, and K. Ch. A. M. Luyben, *Anal. Chim. Acta*, **163**, 207 (1984).
17. J. Tramper, L. E. S. Brink, R. S. Hamstra, J. A. M. de Bont, A. Q. H. Habets-Crützen, and C. G. van Ginkel. Preprints of the 3rd European Congress on Biotechnology, München, West Germany (1984).
18. A. Q. H. Habets-Crützen and J. A. M. de Bont, *Appl. Microbiol. Biotechnol.*, in press.
19. S. Carrà, E. Santacesaria, M. Morbidelli, and L. Cavalli, *Chem. Eng. Sci.*, **34**, 1123 (1979).
20. J. A. Riddick and W. B. Bunger, in *Techniques of Chemistry*, Vol. 2, 3rd ed. (Wiley, New York, 1970), p. 1.
21. M. J. Playne and B. R. Smith, *Biotechnol. Bioeng.*, **25**, 1251 (1983).
22. L. E. S. Brink and J. Tramper (submitted).
23. J. H. Hildebrand, J. M. Prausnitz, and R. L. Scott. *Regular and Related Solutions* (Van Nostrand Reinhold Co., New York, 1970).
24. K. Shinoda and P. Becher. *Principles of Solution and Solubility* (Marcel Dekker, New York, 1978).
25. R. C. Weast, Ed., *Handbook of Chemistry and Physics*, 57th ed. (CRC Press, Cleveland, OH, 1976).
26. P. A. Small, *J. Appl. Chem.*, **3**, 71 (1953).
27. C. McAuliffe, *J. Phys. Chem.*, **70**, 1267 (1966).
28. E. Wilhelm and R. Battino, *Chem. Rev.*, **73**, 1 (1973).
29. B. I. Konobeev and V. V. Lyapin, *Khim. Prom.*, **43**, 114 (1967).
30. N. A. Lange, *Handbook of Chemistry* (Handbook Publishers, Sandusky, OH, 1934).

# 4. MODELLING THE EFFECTS OF MASS TRANSFER ON KINETICS OF PROPENE EPOXIDATION OF IMMOBILIZED MYCOBACTERIUM CELLS: PSEUDO-ONE-SUBSTRATE CONDITIONS AND NEGLIGIBLE PRODUCT INHIBITION

L.E.S. Brink and J. Tramper

Department of Food Science, Food and Bioengineering Group, Agricultural University Wageningen, De Dreyen 12, 6703 BC Wageningen, The Netherlands

(Received 9 September 1985; revised 12 December 1985)

*Experimental verification of the internal pore and external film diffusion model is presented using the oxidation of propene to propene oxide by calcium alginate-entrapped Mycobacterium cells as a model system. Assuming pseudo-one-substrate Michaelis-Menten kinetics and negligible product inhibition, theoretical consumption rates for oxygen and propene of the immobilized cells were compared to experimental values obtained in a circulation batch reactor system. The diameter of the spherical gel particles, immobilized cell density and the intrinsic kinetic parameters were measured independently. Internal pore diffusion of the limiting substrate was found the main mass-transfer resistance. A good agreement was observed between predicted and experimental epoxidation rates.*

**Keywords:** Immobilized cells; mass transfer modelling; alginate; propene epoxidation

## Introduction

The theoretical analysis of the external and internal mass-transfer resistances, often encountered in microbial aggregates, mould pellets and immobilized biocatalysts, has made considerable advances.<sup>1-7b</sup> In a recent review Kasche<sup>6</sup> pointed out that, in contrast to the numerous theoretical studies, the number of investigations with correlations between model predictions and experimental data is only limited. Therefore, instead of developing new, purely mathematical diffusion models, existing models should be verified experimentally. A similar conclusion has been stated by Radovich<sup>7a</sup> and Karel *et al.*<sup>7b</sup> for immobilized, whole-cell systems.

The Thiele effectiveness factor concept<sup>8,9</sup> is mostly used for describing the coupled diffusion and reaction in immobilized biocatalysts. Accordingly, comparisons between experimental and predicted data are often presented as graphs of external ( $\eta_e$ ), internal ( $\eta_i$ ) or overall effectiveness factor ( $\eta$ ) plotted as a function of a Thiele-type modulus ( $\phi$ ) or, alternatively, as a function of particle size, cell density or bulk substrate concentration. Marsh *et al.*<sup>10</sup> and Rovito and Kittrell<sup>11</sup> used Thiele analyses in combination with zero and first-order reaction kinetics, respectively, of immobilized enzymes on porous glass to correlate favourably a limited number of experimental  $\eta$  values with calculated values. A similar approach was followed by Bunting and Laidler<sup>12</sup> for first-order asymptotic approxi-

mation of Michaelis-Menten kinetics of a  $\beta$ -galactosidase enzyme entrapped in polyacrylamide discs. The eight measured points agreed very well with theoretical values for  $\eta$ . The partition and diffusion coefficients used were determined independently. Interparticle and intraparticle mass-transfer effects on substrate-inhibited Michaelis-Menten kinetics of immobilized invertase were examined by Kobayashi and Moo-Young.<sup>13</sup> Experimentally obtained internal  $\eta$  values (some even exceeded unity) compared favourably with calculated values. Korus and O'Driscoll<sup>14</sup> investigated the influence of internal diffusion on Michaelis-Menten kinetics of several gel-entrapped enzymes. Both the experimental data and the shape of theoretical curves of  $\eta$  plotted versus particle size showed the same trend. The quantitative disagreement that existed they attributed to uncertainties in the assumptions concerning the partition coefficient and the intrinsic kinetic constants, and to the use of an arithmetical mean for the particle size. Pore diffusion and two-substrate reaction in porous glass particles were studied by Dahodwala *et al.*<sup>15</sup> The effective diffusion coefficients of the two substrates, oxygen and galactose, were approximated by the diffusion coefficients in water and immobilization was assumed not to influence the intrinsic kinetic properties of the galactose oxidase enzyme. Despite these and other simplifications, theoretical  $\eta$  values were in rather good agreement with experimental values. Kasche *et al.*<sup>16,17</sup> used operational effective-

## Papers

ness factors to estimate the time required to obtain 90% substrate conversion in immobilized chymotrypsin and trypsin enzyme reactors. From a large number of comparisons between calculated and experimental  $\eta$  values it was concluded that the applied procedure for solving the pore diffusion equation, the collocation method, can be used for predicting the performance of immobilized enzyme reactors. Boersma *et al.*<sup>18</sup> fitted the pore diffusion model to experimental  $\eta$  values of an immobilized *Arthrobacter* cell preparation in a plot of  $\eta$  as a function of a generalized Thiele modulus. A good fit was obtained when the effective diffusion coefficient of glucose in the support material (a mixture of two polyelectrolytes) was given a value about one seventh of the molecular diffusion coefficient of glucose in water. In another study the effective diffusion coefficient for oxygen in barium alginate gel was estimated from comparing experimental and calculated values in a graph of  $\eta$  versus cell density of immobilized *Hansenula polymorpha*.<sup>19</sup> The diffusion rate in the gel was found to be 25% of that in water (the latter estimated at  $2.6 \times 10^{-9} \text{ m}^2 \text{ s}^{-1}$ ). Excellent agreement was reached between experimental and predicted data in a plot of  $\eta/\phi$  by Klein and Vorlop<sup>20</sup> for immobilized *Escherichia coli* cells in epoxy resin beads. An independently determined, effective pore diffusion coefficient was used in making these predictions. They also provided some experimental verifications of the pore diffusion model in graphs of  $\eta$ /particle size and  $\eta$ /cell density for the oxidation of glucose to gluconic acid by calcium alginate-entrapped *Acetobacter simplex* cells. In other studies of Klein and coworkers a large number of experimental  $\eta$  values for the degradation of phenol by *Candida tropicalis* cells entrapped in several polymeric ionic networks were all found to be considerably smaller than the corresponding calculated values.<sup>21,22</sup> These deviations were ascribed to inaccuracies in the several, simplifying assumptions made, such as zero-order reaction kinetics and the estimation of the effective diffusion coefficient from the polymer concentration and the diffusivity in water.<sup>21</sup> Better results were, however, obtained when external mass transfer, partitioning and Michaelis-Menten kinetics were included in the modelling of the diffusional resistances.<sup>23</sup> In a recent study Jain and Ghose<sup>24</sup> investigated the product-inhibited cellobiose hydrolysis by calcium alginate-entrapped *Pichia etchellsii* cells. The four experimental  $\eta$  values were shown to coincide with the theoretical curve representing  $\eta$  as a function of particle size.

From the divergent work discussed above, it can be concluded that some experimental proof of the relatively simple pore diffusion model (sometimes in combination with external mass-transfer relations) does exist. The availability of accurate estimations for the effective diffusion constant and for the intrinsic kinetics of the immobilized biocatalyst seems to play a dominant role in the reliable prediction of diffusion resistances.

In this study additional, experimental verification of the pore diffusion model with Michaelis-Menten kinetics is presented. The oxidation of propene to propene oxide by non-growing *Mycobacterium* cells entrapped in calcium alginate is used as the model reaction. This system is suited for fundamental studies because of the relatively simple molecules involved in the epoxidation (propene, oxygen, propene oxide). This facilitates quantitative gas analysis<sup>25</sup> and the prediction of thermodynamic properties and diffusion coefficients. Furthermore, the work is part of our efforts to produce propene oxide stereospecifically in an organic liquid phase/immobilized cell system.<sup>26-28</sup> After

optimizing the two main elements of this multiphase system, technique of immobilization and type of organic solvent,<sup>29,30</sup> attention is at present focused on the choice and design of a suitable multiphase bioreactor. However, independent of the type of immobilized cell reactor, knowledge of the performance of the immobilized biocatalyst preparation as a function of particle size, microbial activity, cell density and substrate concentration levels, will be indispensable. In this and the following paper the mass-transfer effects on propene epoxidation kinetics of calcium alginate-entrapped cells are quantified. In this paper the modelling of the diffusion resistances is given using two simplifying assumptions: pseudo-one-substrate reaction kinetics and negligible product inhibition. Under these conditions the influence of particle size, cell density and substrate levels on the epoxidation rates of the gel-entrapped cells was established in a quantitative manner. The observed rates are correlated with theoretical values, obtained by approximate solutions (e.g. the collocation method) to the problem of coupled reaction and pore diffusion in permeable biocatalysts in series with external gas-liquid and liquid-solid film diffusion. This one-substrate porediffusion model is found to give accurate predictions of the mass-transfer effects of propene as well as of oxygen on the kinetic behaviour of the immobilized cells. A second paper<sup>34</sup> deals with the more complex case of product-inhibited epoxidation kinetics.

## Materials and methods

### Chemicals and microorganism

The support material, sodium alginate (Manucol DM), was obtained from Alginate Industries, London, UK. The description of the *Mycobacterium* strain E3 used for the epoxidation reaction is given elsewhere.<sup>26</sup>

### Immobilization

The procedure of immobilization in calcium alginate has been described earlier.<sup>26</sup> The mean diameter of the spherical gel particles was determined by microscopic measurement of about 40 bead diameters.

### Measurement of epoxidation kinetics and mass-transfer effects

The propene and oxygen consumption rates of the calcium alginate-entrapped cells were measured in a laboratory-scale batch reactor system with gas circuit. The details of this experimental set-up have been reported previously.<sup>25,30</sup> The gel particles were suspended by the circulating gas in a bubble-column bioreactor (4.5 cm i.d.), containing an aqueous 0.05 M calcium chloride solution (total volume of beads and liquid, 250 cm<sup>3</sup>). The total amount of biocatalyst used in one experiment was always about 1 g dry weight of cells. The time course of the reaction in the immobilized cell phase was followed by on-line gas chromatographic analysis of the two gaseous substrates and the volatile propene oxide in the circulating gas stream. The liquid concentrations of the substrates, in equilibrium with the gas phase, could then be calculated using Henry's law.<sup>25</sup> Automatic operation of a gas-sampling valve in conjunction with a g.c. column-switching valve was enabled by coupling the on-line gas chromatograph to an integrator and a microcomputer. This also made it possible to perform data acquisition and reduction and, furthermore, to control the gas concentration of propene or oxygen in

the experimental system at a high, constant level by computer-controlled opening of a mass-flow controller. The latter permitted the measurement of kinetic and mass-transfer rates of one of the two substrates under pseudo-one-substrate conditions (excess liquid concentrations of propene and oxygen: 160 and 240  $\mu\text{M}$ , respectively).

## Theoretical

Various transport phenomena in the multiphase system ( $\text{SL}_1\text{L}_2\text{G}$ ) may limit the kinetic epoxidation rate of the gel-entrapped cells.<sup>4</sup> Mass-transfer resistances with respect to the transport of the two substrates and the produced propene oxide could occur in a gas film, in aqueous and/or organic liquid films at the gas-liquid and the liquid-solid interfaces and, finally, in the solid gel phase.<sup>30</sup> In the absence of a water-immiscible organic solvent three resistances are likely to prevail: external diffusion limitations in the water film adjacent to the gas-liquid interface and in an aqueous film surrounding the hydrophilic gel particle and, lastly, internal diffusion limitation in the porous gel. These limitations are often expressed in terms of external and internal effectiveness factors,  $\eta_e$  and  $\eta_i$ , which, in the case of a one-substrate Michaelis-Menten reaction with intrinsic kinetic constants  $V_m$  and  $K_m$ , can be represented by the following equations:

$$\eta_e = \left( \frac{V_m S_S}{K_m + S_S} \right) / \left( \frac{V_m S^*}{K_m + S^*} \right) \quad (1)$$

$$\eta_i = \nu_R / \left( \frac{V_m S_S}{K_m + S_S} \right) \quad (2)$$

with  $\nu_R$  the overall substrate consumption rate,  $S_S$  and  $S^*$  the substrate concentrations at the gel surface and at the gas-liquid interface, respectively. Hence, the overall effectiveness of the biocatalyst particle is:

$$\eta = \eta_e \eta_i = \nu_R / \left( \frac{V_m S^*}{K_m + S^*} \right) \quad (3)$$

It is assumed in these equations that no partitioning occurs between the uncharged substrates in the aqueous phase and the gel phase.

The effectiveness factors can be derived from the solution of Fick's second law, describing the coupled one-substrate pore diffusion and reaction in a porous medium. Assuming pseudo steady-state, isothermal conditions, homogeneous cell density  $X$ , concentration-independent effective diffusion coefficient  $D_e$ , spherical geometry with diameter  $d_p$  and Michaelis-Menten kinetics, this well known differential equation can be written as:<sup>1</sup>

$$D_e \left( \frac{d^2 S}{dr^2} + \frac{2}{r} \frac{dS}{dr} \right) = \frac{X V_m S}{K_m + S} \quad (4)$$

with the boundary conditions:

$$D_e \frac{dS}{dr} = \beta (S^* - S_S) \text{ at } r = 0.5 d_p \quad (5)$$

$$\frac{dS}{dr} = 0 \quad \text{at } r = 0 \quad (6)$$

and the overall external mass-transfer coefficient  $\beta$ :<sup>31</sup>

$$\beta = \{ a_S [1/(k_L a) + 1/(k_S a_S)] \}^{-1} \quad (7)$$

where  $r$  is the radial distance from the centre of the particle;  $k_L$  and  $k_S$  are the mass-transfer coefficients in the stagnant liquid films adjacent to the gas-liquid and liquid-solid interfaces, respectively;  $a$  and  $a_S$  are the gas-liquid and liquid-solid specific surface areas, respectively;

$a_S = 6 X_V / (d_p X)$  for spherical particles, with  $X_V$  the reactor-volume-based cell density.

As equation (4) cannot be solved analytically, several, sometimes complex integration methods have been applied to derive the substrate concentration profile in the bead and from this the internal and external stationary effectiveness factors.<sup>6</sup> In this work the three-point collocation method<sup>16,32,33</sup> is applied to obtain approximate solutions to the diffusion equation. This method can be used to calculate the overall effectiveness factor,  $\eta$ , of the biocatalyst bead and the substrate concentration at the gel surface,  $S_S$ , if values for  $V_m$ ,  $K_m$ ,  $X$ ,  $d_p$ ,  $D_e$ ,  $\beta$  and  $S^*$  are available. The overall consumption rate,  $\nu_R$ , and  $\eta_i$  and  $\eta_e$  can then easily be calculated using equations (1) to (3).

## Results and discussion

### Evaluation of model parameters

**Intrinsic kinetics.** Under pseudo-one-substrate conditions the consumption rates for propene ( $S_1$ ) and oxygen ( $S_2$ ) of the calcium alginate-entrapped cells were found to obey Michaelis-Menten kinetics:<sup>30,34</sup>

$$-\frac{dS_1}{dt} = \frac{V_{m,1} S_1}{K_{m,1} + S_1} \quad (8)$$

$$-\frac{dS_2}{dt} = \frac{V_{m,2} S_2}{K_{m,2} + S_2} \quad (9)$$

The intrinsic kinetic parameters in these two equations were determined by fitting the integrated forms of equation (8) and (9) to experimental time-course data [ $S_1(t)$  and  $S_2(t)$ , respectively] utilizing a non-linear regression technique. The use of small particle diameters ( $d_p \approx 0.7$  mm) in combination with low biocatalytic activity [ $X V_m \approx 5 \times 10^4 \mu\text{mol min}^{-1} (\text{m}^3 \text{particle})^{-1}$ ] avoided diffusional masking of the resulting parameters.<sup>34</sup> The (pseudo)-equilibrium constants,  $K_{m,1}$  and  $K_{m,2}$ , were assigned average values ( $5 \pm 3$  and  $15 \pm 5 \mu\text{M}$ , respectively) using 12 time-course experiments. The relatively high variation in these values does not lead to inaccurate model predictions, in view of the small effect of the two parameters on the predicted consumption rates. This is not the case for the maximum rate parameters,  $V_{m,1}$  and  $V_{m,2}$ . As considerable variations were found between obtained maximum rates of the various cell batches used, specific estimates for these parameters are necessary for each cell batch.

**Particle diameter.** Microscopic examination of the calcium alginate beads formed revealed that the shape of the particles, especially of the larger ones ( $> 1$  mm), resembles a spherical geometry. Buchholz<sup>35</sup> and Kasche<sup>16</sup> used average diameters ( $\sum d_{pi}^2 / \sum d_{pi}$  and  $(\sum d_{pi}^3 / n)^{0.5}$ , respectively;  $n$  is the total number of particles), both differing from the arithmetical mean  $\sum d_{pi} / n$ , to give increased weight to the larger particles. These two corrections were not applied here, as the differences between the mentioned averages of the experimentally obtained diameter distributions were found negligible ( $\approx 0.02$  mm). The particle diameters appeared to be normally distributed with a standard deviation of 0.1 to 0.2 mm.

**Cell density.** The cell density,  $X$ , is expressed as g dry weight per  $\text{m}^3$  gel particle. It was observed experimentally that 1  $\text{cm}^3$  of the initial cell suspension/sodium alginate mixture yielded about 0.50 ( $\pm 0.04$ )  $\text{cm}^3$  calcium alginate gel (corresponding to  $\approx 4\%$ , w/v, calcium alginate). It is

assumed that the immobilized cells are homogeneously distributed in the gel beads. The reactor-volume-based cell density,  $X_V$ , was mostly 6% of the biocatalyst-volume-based cell density,  $X$ .

**Effective diffusion coefficients.** Some relations have been proposed to correlate the effective diffusion coefficient,  $D_e$ , to the diffusivity in water,  $D$ . However, the applicability is often limited. The porosity and tortuosity of the support material, used by Satterfield,<sup>36</sup> are mostly unknown. Klein and coworkers<sup>37,38</sup> related effective diffusion coefficients in polymeric carriers, like chitosan and polymethacrylamide, to the volume fraction of polymer, the cell-mass concentration or the volume fraction of cells and, finally, a coefficient determined by the molecular size of the substrate. It is, however, uncertain whether the latter relations would give reliable estimates of the required diffusion coefficients in the alginate carrier used in this study.

As the water content of the ( $\approx 4\%$ , w/v) calcium alginate gel (volume fraction of the wet cells mostly  $< \approx 0.3$ ) is very high and the molecular sizes of the two substrates are small, the effective diffusion coefficients of the substrates in the gel material are not likely to be much lower than the corresponding diffusion coefficients in water. This consideration is confirmed by two recent, experimental studies. Tanaka *et al.*<sup>39</sup> investigated the substrate diffusion characteristics in calcium alginate gel beads (without biocatalyst). The effective diffusivities of substrates with molecular weights smaller than  $2 \times 10^4$  ( $\text{g mol}^{-1}$ ) were found equal to the corresponding values in water and, furthermore, independent of the calcium alginate concentration in the beads. Adlercreutz<sup>40</sup> determined that the effective diffusivity of oxygen in calcium alginate gel [ $X \leq 48 \times 10^3$  g dry weight ( $\text{m}^3$  particle) $^{-1}$ ] at  $30^\circ\text{C}$  was  $\approx 2.1 \times 10^{-9} \text{ m}^2 \text{ s}^{-1}$ , which is  $\approx 90\%$  of the diffusivity in water ( $\approx 2.4 \times 10^{-9} \text{ m}^2 \text{ s}^{-1}$ , see below). In another study the maximum pore size of alginate beads (gel type Manucol LD) was estimated  $1.4 \times 10^{-6} \text{ m}$ .<sup>41</sup> This also indicates a limited influence of the gel matrix structure on the internal diffusion rates of propene and oxygen, since the dimensions of these substrate molecules are much smaller than the mentioned pore diameter. Accordingly, in this study the estimated diffusivities at  $30^\circ\text{C}$  of propene and oxygen in water,  $D_1$  and  $D_2$ , respectively, were used to predict the substrate diffusion rates in the calcium alginate beads ( $D_1 \approx 1.5 \times 10^{-9} \text{ m}^2 \text{ s}^{-1}$ ,<sup>42,43</sup>  $D_2 \approx 2.4 \times 10^{-9} \text{ m}^2 \text{ s}^{-1}$ ).<sup>43</sup> A possible influence of cell density on the effective diffusion coefficients is assumed not to be significant. It is recognized that the true, effective diffusion coefficients of the substrates in the alginate gel will be somewhat lower than the corresponding coefficients in water, due to the alginate network and partial blocking of pores by the immobilized cells. However, to our knowledge, no reliable, general method is available yet to quantify these effects for gaseous substrates.

**External mass-transfer coefficients.** The volumetric gas-liquid oxygen transfer coefficient,  $(k_L a)_2$ , was found to equal  $0.05 \text{ s}^{-1}$  using a dynamic oxygen electrode method. The propene transfer coefficient at the gas-liquid interface,  $(k_L a)_1$ , can then be estimated from:<sup>44</sup>

$$(k_L a)_1 = (D_1/D_2)^{0.5} (k_L a)_2 \quad (10)$$

which yields  $(k_L a)_1 \approx 0.04 \text{ s}^{-1}$ .

The mass-transfer coefficient,  $k_S$ , in the aqueous film surrounding the alginate bead can be obtained from dimen-

sionless number equations relating Sherwood ( $\text{Sh} = k_S d_p / D$ ) to Reynolds ( $\text{Re} = \rho_L U d_p / \mu_L$ ) and Schmidt ( $\text{Sc} = \mu_L / (\rho_L D)$ ). ( $D$  is the propene or oxygen diffusion coefficient in the water film,  $\rho_L$  and  $\mu_L$  are the density and viscosity of the fluid, respectively, and  $U$  is the velocity of the liquid relative to the particle). For laminar flow ( $\text{Re} < 30$ ) a correlation derived by Brian and Hales can be used:<sup>45</sup>

$$\text{Sh} = (4.0 + 1.21 \text{Re}^{2/3} \text{Sc}^{2/3})^{0.5} \quad (11)$$

while at more turbulent flow conditions ( $\text{Re} > 30$ ) the well known relationship of Ranz and Marshall can be applied:<sup>46</sup>

$$\text{Sh} = 2.0 + 0.60 \text{Re}^{1/2} \text{Sc}^{1/3} \quad (12)$$

In this work the slip velocity,  $U$ , was equated to three times the terminal velocity,  $U_T$ .<sup>47</sup> This constant velocity of a particle falling in a fluid phase under the action of gravity is usually calculated as follows:<sup>48</sup>

$$U_T = [4g d_p \Delta\rho / (3\rho_L C)]^{0.5} \quad (13)$$

In this equation  $g$  is the gravitational acceleration constant ( $9.81 \text{ m s}^{-2}$ ),  $\Delta\rho$  the density difference between the alginate beads and the aqueous phase (about  $50 \text{ kg m}^{-3}$ ) and  $C$  the drag coefficient of a spherical, rigid particle falling in a fluid phase. The drag coefficient and the terminal velocity can be iteratively calculated using the relation between  $C$  and the Reynolds number ( $\rho_L U_T d_p / \mu_L$ ).<sup>48</sup>

The propene and oxygen liquid-solid mass-transfer coefficients thus calculated (about  $5.5 \times 10^{-5}$  and  $7.5 \times 10^{-5} \text{ m s}^{-1}$ , respectively) are only weak functions of the particle diameter. Hence, the smallest diameters used in this work ( $\approx 0.7 \text{ mm}$ ) yield the lowest Sherwood numbers ( $k_S d_p / D \approx 20$ , for propene as well as for oxygen). From these relatively high Sherwood numbers ( $\text{Sh} > 20$ ) it can be derived that the resistance due to the liquid-solid mass transfer will be limited.<sup>5,16</sup>

#### Comparisons between experimental and theoretical reaction rates

The theoretical external and internal diffusion analysis and the above derived set of model parameters were combined to calculate the influences of propene or oxygen diffusion on the epoxidation kinetics of the immobilized cells. The predicted substrate consumption rates were compared to experimental rates obtained from two types of time-course data. At a constant, high oxygen concentration ( $240 \mu\text{M}$ ) the decrease in propene level was measured at regular time intervals, whereas at a constant, high propene concentration ( $160 \mu\text{M}$ ) the oxygen level in the experimental system was monitored. For both cases it was verified experimentally that pseudo-one-substrate conditions were approached by varying the excess level of the non-limiting substrate. An example of this is given in *Figure 1*. The oxygen-consumption rate was strongly diffusion-limited (experimental  $\eta < 0.4$  for  $S_2 < 80 \mu\text{M}$ ) in this particular case for particle beads of  $\approx 2.6 \text{ mm}$ . However, as can be seen from *Figure 1*, increasing the constant propene level from  $160$  to  $320 \mu\text{M}$  does not significantly alter the oxygen consumption rate, which indicates that only oxygen is rate limiting.

The determination of reaction rates from time-course data is only correct when inhibition by the formed propene oxide and cell inactivation do not occur. The measured epoxide concentrations were always smaller than  $3 \text{ mM}$ , and mostly smaller than  $1.5 \text{ mM}$ . At these low concentrations the inhibitory effect of the propene oxide on propene and oxygen consumption rates of free and immobilized

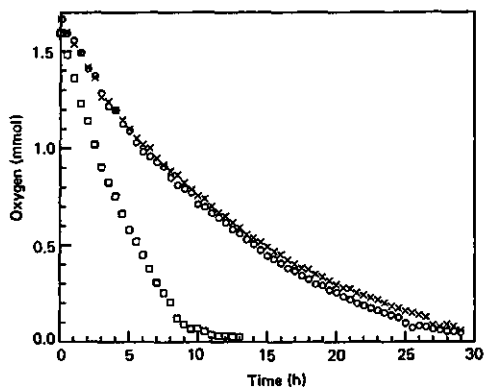


Figure 1 Amount of unconverted oxygen in the experimental system versus time showing pseudo-one-substrate conditions (1 mmol oxygen corresponds to  $S_1^* = 48.1 \mu\text{M}$ ); (o) kinetic control,  $S_1 = 160 \mu\text{M}$  [ $V_{m,2} = 9.0 \mu\text{mol min}^{-1}$  (g dry weight) $^{-1}$ ,  $X = 0.80 \times 10^4$  g dry weight ( $\text{m}^3$  particle) $^{-1}$ ,  $d_p = 0.8$  mm]; (□)  $S_1 = 160 \mu\text{M}$  [ $V_{m,2} = 9.0 \mu\text{mol min}^{-1}$  (g dry weight) $^{-1}$ ,  $X = 3.6 \times 10^4$  g dry weight ( $\text{m}^3$  particle) $^{-1}$ ,  $d_p = 2.6$  mm]; (x)  $S_1 = 320 \mu\text{M}$  [ $V_{m,2} = 9.0 \mu\text{mol min}^{-1}$  (g dry weight) $^{-1}$ ,  $X = 3.6 \times 10^4$  g dry weight ( $\text{m}^3$  particle) $^{-1}$ ,  $d_p = 2.7$  mm]

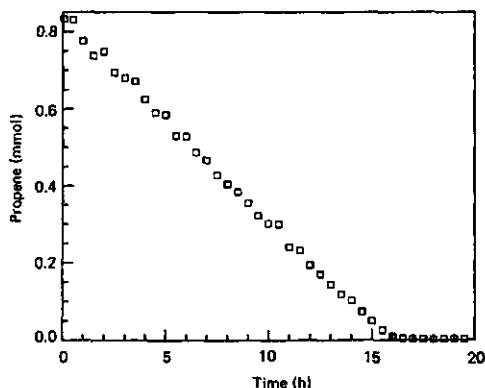


Figure 2 Amount of unconverted propene in the experimental system versus time showing the operational stability of the immobilized cells (1 mmol propene corresponds to  $S_1^* = 192 \mu\text{M}$ ,  $S_2 = 240 \mu\text{M}$ ); (□) kinetic control [ $V_{m,1} = 1.1 \mu\text{mol min}^{-1}$  (g dry weight) $^{-1}$ ,  $X = 0.96 \times 10^4$  g dry weight ( $\text{m}^3$  particle) $^{-1}$ ,  $d_p = 0.7$  mm]

cells was found to be small.<sup>34,49</sup> Furthermore, it was demonstrated that hydrolysis of the produced epoxide in a sulphuric acid solution during the time-course experiments (removal from the circulating gas stream) did not alter the immobilized cell activity for propene and oxygen.

The operational stability of the immobilized cells also did not interfere significantly with the diffusion measurements. Some experiments were repeated by addition of a fresh amount of the limiting substrate to the reaction system. Only small reductions in immobilized cell activity were observed. Likewise, under diffusion-free experimental conditions and at high concentrations ( $S^* \gg K_m$ ), an almost time-independent consumption rate of the substrate was obtained (Figure 2).

Increasing the cell density and/or the diameter of the biocatalyst particles (while holding the total amount of biocatalyst in the bioreactor constant) reduces the propene epoxidation rate considerably (Figures 3 and 4). This appears to be especially true at high biocatalytic activities,  $X V_{m,1}$  (Figure 5). Similar results were obtained for the coupled diffusion and oxygen consumption (Figure 6). The experimental reaction rates were extracted from these data of concentration versus time by fitting second-order polynomial functions to sets of seven points of measurement using the method of least squares. The consumption rate at the substrate concentration of the middle one of the seven data pairs could then easily be calculated from the derivative of the obtained polynomial. In Figures 7–10 the experimental rates thus derived are compared to the diffusion-model calculations in dimensionless consumption rate ( $v_r/V_m$ ) graphs plotted as a function

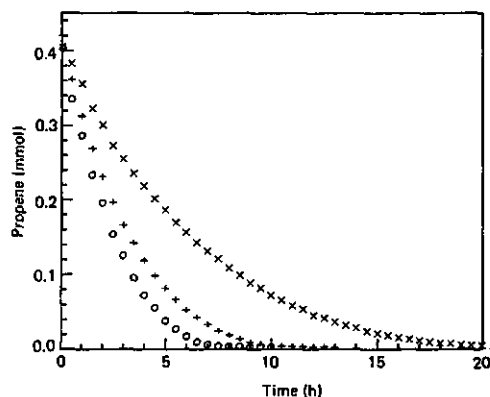


Figure 3 Amount of unconverted propene in the experimental system versus time showing the effect of immobilized cell density,  $X$  [1 mmol propene corresponds to  $S_1^* = 192 \mu\text{M}$ ,  $V_{m,1} = 3.7 \mu\text{mol min}^{-1}$  (g dry weight) $^{-1}$ ,  $d_p = 2.0$  mm];  $X$  [ $\times 10^4$  g dry weight ( $\text{m}^3$  particle) $^{-1}$ ]: 3.2 (o), 6.5 (+), 13.0 (x)

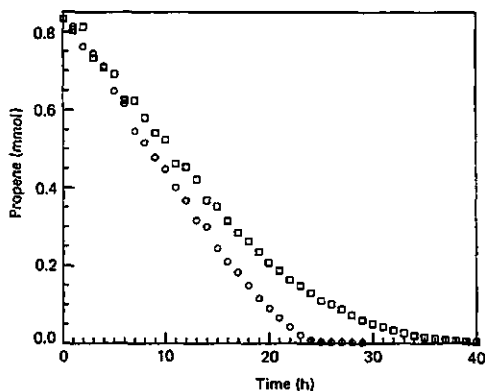


Figure 4 Amount of unconverted propene in the experimental system versus time showing the effect of particle diameter,  $d_p$ , at low biocatalytic activity [1 mmol propene corresponds to  $S_1^* = 192 \mu\text{M}$ ,  $V_{m,1} = 0.79 \mu\text{mol min}^{-1}$  (g dry weight) $^{-1}$ ,  $X = 5.8 \times 10^4$  g dry weight ( $\text{m}^3$  particle) $^{-1}$ ];  $d_p$  (mm): 0.7 (o), 2.5 (□)

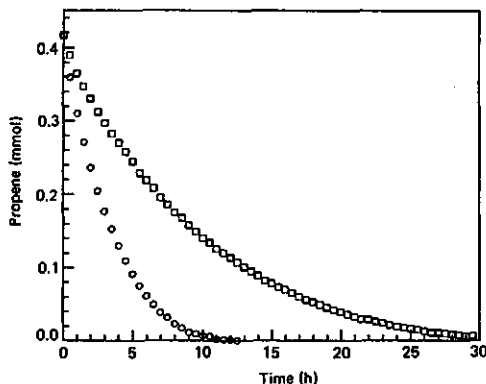


Figure 5 Amount of unconverted propene in the experimental system versus time showing the effect of particle diameter,  $d_p$ , at high biocatalytic activity [1 mmol propene corresponds to  $S_1^* = 82.2 \mu\text{M}$ ,  $V_{m,1} = 2.6 \mu\text{mol min}^{-1} (\text{g dry weight})^{-1}$ ,  $X = 7.3 \times 10^4 \text{ g dry weight } (\text{m}^3 \text{ particle})^{-1}$ ];  $d_p$  (mm): 0.7 ( $\circ$ ), 2.3 ( $\square$ )

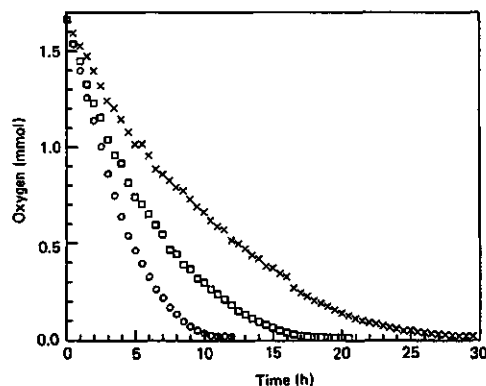


Figure 6 Amount of unconverted oxygen in the experimental system versus time showing the effects of immobilized cell density,  $X$ , and particle diameter,  $d_p$  [1 mmol oxygen corresponds to  $S_2^* = 48.1 \mu\text{M}$ ,  $V_{m,2} = 12.6 \mu\text{mol min}^{-1} (\text{g dry weight})^{-1}$ ]; ( $\circ$ )  $X = 1.2 \times 10^4 \text{ g dry weight } (\text{m}^3 \text{ particle})^{-1}$ ,  $d_p = 0.8 \text{ mm}$ ; ( $\square$ )  $X = 1.2 \times 10^4 \text{ g dry weight } (\text{m}^3 \text{ particle})^{-1}$ ,  $d_p = 2.3 \text{ mm}$ ; ( $\times$ )  $X = 3.6 \times 10^4 \text{ g dry weight } (\text{m}^3 \text{ particle})^{-1}$ ,  $d_p = 2.5 \text{ mm}$

of the propene or oxygen concentration,  $S^*$ . Good agreement is observed between the experimental and predicted overall reaction rates (or overall effectiveness factors, equation 3) at all levels of propene and oxygen. The absolute consumption rates as well as the effect of varying cell density and/or bead diameter are satisfactorily predicted. It may be concluded that the several assumptions made in the diffusion model (for instance the approximate solution to the diffusion equation and the pseudo-one-substrate conditions) all seem to be reasonable.

To test the accuracy of the theoretical effectiveness factors used, an alternative procedure to approximate equation (4), developed by Moo-Young and Kobayashi<sup>50</sup> and Kobayashi and Laidler<sup>51</sup> for immobilized enzyme systems, was also applied. The differences between the two methods were only a few percent of the predicted

external and internal effectiveness factors, which is within the experimental error of the measured reaction rates.

The observation that the experimental rates are generally somewhat smaller than the theoretical rates (Figures 7–10) might be connected to the high value of the effective diffusivity ( $2.4 \times 10^{-9} \text{ m}^2 \text{ s}^{-1}$ ) used in the predictions. On the whole, however, one could conclude that the diffusivity of a low molecular weight substrate (like oxygen or propene) in water is a reasonably accurate measure for the diffusivity of the pertinent compound in ( $\approx 4\%$ , w/v) calcium alginate gel. This seems to disagree with the previously found low value for the effective diffusion coefficient of oxygen in ( $\approx 4\%$ , w/v) barium alginate ( $\approx 0.7 \times 10^{-9} \text{ m}^2 \text{ s}^{-1}$ ),<sup>19</sup> but agrees well with the work of Tanaka *et al.*<sup>39</sup> and Adlercreutz.<sup>40</sup> The influence of polymer concentration and cell density on diffusion rates can be estimated from relationships proposed by Klein and coworkers.<sup>37,38</sup>

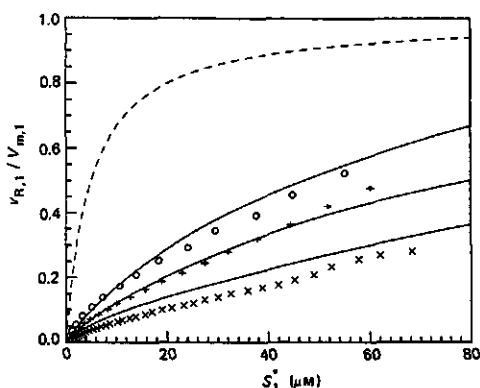


Figure 7 Dimensionless propene consumption rate,  $v_{R,1}/V_{m,1}$ , versus the propene concentration at the gas-liquid interface,  $S_1^*$  [ $V_{m,1} = 3.7 \mu\text{mol min}^{-1} (\text{g dry weight})^{-1}$ ,  $d_p = 2.0 \text{ mm}$ ]; experimental reaction rates (from Figure 3),  $X$  ( $\times 10^4 \text{ g dry weight } (\text{m}^3 \text{ particle})^{-1}$ ): 3.2 ( $\circ$ ), 6.5 ( $+$ ), 13.0 ( $\times$ ); diffusion model predictions (—); negligible diffusion resistance (---)

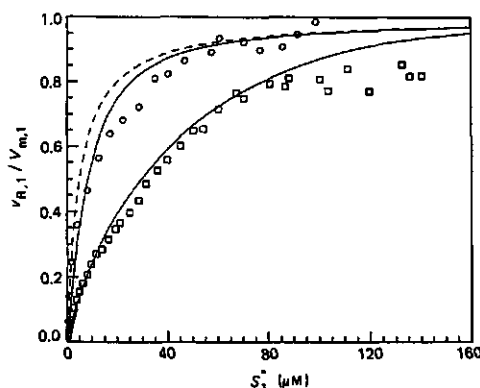


Figure 8 Dimensionless propene consumption rate,  $v_{R,1}/V_{m,1}$ , versus the propene concentration at the gas-liquid interface,  $S_1^*$  [ $V_{m,1} = 0.79 \mu\text{mol min}^{-1} (\text{g dry weight})^{-1}$ ,  $X = 5.8 \times 10^4 \text{ g dry weight } (\text{m}^3 \text{ particle})^{-1}$ ]; experimental reaction rates (from Figure 4),  $d_p$  (mm): 0.7 ( $\circ$ ), 2.5 ( $\square$ ); diffusion model predictions (—); negligible diffusion resistance (---)



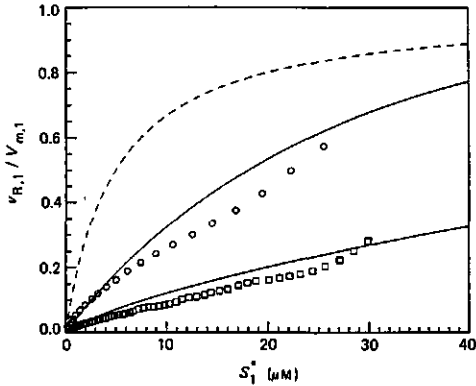


Figure 9 Dimensionless propene consumption rate,  $v_{R,1}/V_{m,1}$ , versus the propene concentration at the gas-liquid interface,  $S_1^*$  [ $V_{m,1} = 2.6 \mu\text{mol min}^{-1} (\text{g dry weight})^{-1}$ ,  $X = 7.3 \times 10^4 \text{ g dry weight } (\text{m}^3 \text{ particle})^{-1}$ ]; experimental reaction rates (from Figure 5),  $d_p$  (mm): 0.7 ( $\circ$ ), 2.3 ( $\square$ ); diffusion model predictions (—); negligible diffusion resistance (---)

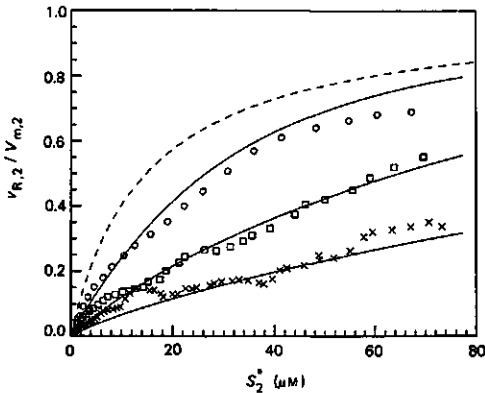


Figure 10 Dimensionless oxygen consumption rate,  $v_{R,2}/V_{m,2}$ , versus the oxygen concentration at the gas-liquid interface,  $S_2^*$  [ $V_{m,2} = 126 \mu\text{mol min}^{-1} (\text{g dry weight})^{-1}$ ]; experimental reaction rates (from Figure 6), ( $\circ$ )  $X = 1.2 \text{ g dry weight } (\text{m}^3 \text{ particle})^{-1}$ ,  $d_p = 0.8 \text{ mm}$ , ( $\square$ )  $X = 1.2 \text{ g dry weight } (\text{m}^3 \text{ particle})^{-1}$ ,  $d_p = 2.3 \text{ mm}$ , ( $\times$ )  $X = 3.6 \text{ g dry weight } (\text{m}^3 \text{ particle})^{-1}$ ,  $d_p = 2.5 \text{ mm}$ ; diffusion model predictions (—); negligible diffusion resistance (---)

When the effective diffusion coefficients thus obtained were used in our model, the predicted rates were in some cases considerably smaller than the measured rates.

In the experiments discussed above the predicted external effectiveness factors are mostly higher than 0.85, even at low concentrations of the limiting substrate ( $S^* \approx 20 \mu\text{M}$ ). Thus, the sometimes low overall (experimental and calculated) effectiveness factors of the immobilized biocatalyst preparations are mainly caused by severe pore diffusion limitation. This also implies that the accuracy of the equations and parameters in the modelling of the external diffusion resistances (like  $k_{1,a}$  values, Sh relation, slip velocity and  $\Delta\rho$ ) is not very critical. Furthermore, the correct description of coupled diffusion and reaction in the biocatalyst particles becomes more important. Therefore,

the results presented can essentially be regarded as a positive verification of the predictive capacity of the pore-diffusion model used.

### Acknowledgements

The authors are grateful to Prof. K. Ch. A. M. Luyben and Prof. Dr K. van't Riet for helpful discussions. These investigations were supported (in part) by the Netherlands Technology Foundation (STW).

### Nomenclature

$a$	gas-liquid specific surface area ( $\text{m}^{-1}$ )
$a_S$	liquid-solid specific surface area ( $\text{m}^{-1}$ )
$C$	drag coefficient
$D$	diffusion coefficient in water ( $\text{m}^2 \text{ s}^{-1}$ )
$D_e$	effective diffusion coefficient in calcium alginate ( $\text{m}^2 \text{ s}^{-1}$ )
$d_p$	particle diameter (m)
$g$	gravitational acceleration constant ( $\text{m s}^{-2}$ )
$k_{L1}$	mass-transfer coefficient in the liquid film adjacent to the gas-liquid interface ( $\text{m s}^{-1}$ )
$k_{S1}$	mass-transfer coefficient in the liquid film adjacent to the liquid-solid interface ( $\text{m s}^{-1}$ )
$K_m$	Michaelis-Menten constant ( $\text{mol m}^{-3}$ )
$r$	radial distance from the centre of the particle (m)
$Re$	Reynolds number
$S$	substrate concentration ( $\text{mol m}^{-3}$ )
$S^*$	substrate concentration at the gas-liquid interface ( $\text{mol m}^{-3}$ )
$S_S$	substrate concentration at the gel surface ( $\text{mol m}^{-3}$ )
$Sc$	Schmidt number
$Sh$	Sherwood number
$SL_1 L_2 G$	four phases: solid, water, organic solvent and gas
$t$	time (s)
$U$	velocity of the liquid relative to the particle ( $\text{m s}^{-1}$ )
$U_T$	terminal velocity ( $\text{m s}^{-1}$ )
$v_R$	overall substrate consumption rate [ $\mu\text{mol min}^{-1} (\text{g dry weight})^{-1}$ ]
$V_m$	maximum reaction rate ( $\mu\text{mol min}^{-1} (\text{g dry weight})^{-1}$ )
$X$	cell density [ $\text{g dry weight } (\text{m}^3 \text{ particle})^{-1}$ ]
$X_V$	reactor-volume-based cell density [ $\text{g dry weight } (\text{m}^3 \text{ reactor})^{-1}$ ]
$\beta$	overall external mass-transfer coefficient ( $\text{m s}^{-1}$ )
$\Delta\rho$	density difference between alginate beads and aqueous phase ( $\text{kg m}^{-3}$ )
$\eta$	overall effectiveness factor
$\eta_e$	external effectiveness factor
$\eta_i$	internal effectiveness factor
$\mu_L$	dynamic viscosity of the fluid ( $\text{N s m}^{-2}$ )
$\rho_L$	density of the fluid ( $\text{kg m}^{-3}$ )

### Subscripts

1	propene
2	oxygen

### References

- Goldstein, L. *Methods Enzymol.* 1976, 44, 397-443
- Engasser, J. M. and Horvath, C. in *Applied Biochemistry and Bioengineering* (Wingard, L. B., Katchalski-Katzir, E. and

Papers

- Goldstein, L., eds), Academic Press, New York, 1976, vol. 1, pp. 127-220
- 3 Pitcher, W. H. *Adv. Biochem. Eng.* 1978, 10, 1-26
- 4 Moo-Young, M. and Blanch, H. W. *Adv. Biochem. Eng.* 1981, 19, 1-69
- 5 Buchholz, K. *Adv. Biochem. Eng.* 1982, 24, 39-71
- 6 Kasche, V. *Enzyme Microb. Technol.* 1983, 5, 2-13
- 7a Radovich, J. M. *Enzyme Microb. Technol.* 1985, 7, 2-10
- 7b Karel, S. F., Libicki, S. B. and Robertson, C. R. *Chem. Eng. Sci.* 1985, 40, 1321-1354
- 8 Bischoff, K. B. *AIChE J.* 1965, 11, 351-355
- 9 Weisz, P. B. *Science* 1973, 179, 433-440
- 10 Marsh, D. R., Lee, Y. Y. and Tsao, G. T. *Biotechnol. Bioeng.* 1973, 15, 483-492
- 11 Rovito, B. J. and Kittrell, J. R. *Biotechnol. Bioeng.* 1973, 15, 143-161
- 12 Bunting, P. S. and Laidler, K. J. *Biochemistry* 1972, 11, 4477-4483
- 13 Kobayashi, T. and Moo-Young, M. *Biotechnol. Bioeng.* 1973, 15, 47-67
- 14 Korus, R. and O'Driscoll, K. F. *Can. J. Chem. Eng.* 1974, 52, 775-780
- 15 Dahodwala, S. K., Humphrey, A. E. and Weibel, M. K. *Biotechnol. Bioeng.* 1976, 18, 987-1000
- 16 Kasche, V., Kapune, A. and Schwegler, H. *Enzyme Microb. Technol.* 1979, 1, 41-46
- 17 Kasche, V. in *Characterization of Immobilized Biocatalysts* (Buchholz, K., ed.), Dechema Monograph No. 1724-1731, Verlag Chemie, Weinheim, 1979, vol. 84, pp. 224-243
- 18 Boersma, J. G., Vellenga, K., de Wilt, H. G. J. and Joosten, G. E. H. *Biotechnol. Bioeng.* 1979, 21, 1711-1724
- 19 Hiemstra, H., Dijkhuizen, L. and Harder, W. *Eur. J. Appl. Microbiol. Biotechnol.* 1983, 18, 189-196
- 20 Klein, J. and Vorlop, K.-D. *Am. Chem. Soc. Symp. Ser.* 1983, 207, 376-392
- 21 Klein, J., Hackel, U. and Wagner, F. *Am. Chem. Soc. Symp. Ser.* 1979, 106, 101-118
- 22 Klein, J. and Wagner, F. in *Biotechnology*, Dechema Monograph No. 1693-1703, Verlag Chemie, Weinheim, 1978, vol. 82, pp. 142-164
- 23 Klein, J. in *Characterization of Immobilized Biocatalysts* (Buchholz, K., ed.), Dechema Monograph No. 1724-1731, Verlag Chemie, Weinheim, 1979, vol. 84, pp. 303-314
- 24 Jain, D. and Ghose, T. K. *Biotechnol. Bioeng.* 1984, 26, 340-346
- 25 Brink, L. E. S., Tramper, J., van't Riet, K. and Luyben, K. Ch. A. M. *Anal. Chim. Acta* 1984, 163, 207-217
- 26 Habets-Crützen, A. Q. H., Brink, L. E. S., van Ginkel, C. G., de Bont, J. A. M. and Tramper, J. *Appl. Microbiol. Biotechnol.* 1984, 20, 245-250
- 27 Habets-Crützen, A. Q. H., Carlier, S. J. N., de Bont, J. A. M., Wistuba, D., Schurig, V., Hartmans, S. and Tramper, J. *Enzyme Microb. Technol.* 1985, 7, 17-21
- 28 Tramper, J., Brink, L. E. S., Hamstra, R. S., de Bont, J. A. M., Habets-Crützen, A. Q. H. and van Ginkel, C. G. *Proceedings of the 3rd Eur. Congress on Biotechnol.* Verlag Chemie, Weinheim, 1984, vol. 2, pp. 269-276
- 29 Brink, L. E. S. and Tramper, J. *Biotechnol. Bioeng.* 1985, 27, 1258-1269
- 30 Brink, L. E. S. and Tramper, J. *Proceedings of the 1st IFAC Symposium on Modelling and Control of Biotechnological Processes*, Noordwijkerhout, 1985, pp. 111-117
- 31 Reuss, M. *Fortschr. Verf.* 1976, 14, 551-563
- 32 Villadsen, J. V. and Stewart, W. E. *Chem. Eng. Sci.* 1967, 22, 1483-1501
- 33 Ramachandran, P. A. *Biotechnol. Bioeng.* 1975, 17, 211-226
- 34 Brink, L. E. S. and Tramper, J. *Enzyme Microb. Technol.* 1986, 8, in the press
- 35 Buchholz, K. in *Characterization of Immobilized Biocatalysts* (Buchholz, K., ed.), Dechema Monograph No. 1724-1731, Verlag Chemie, Weinheim, 1979, vol. 84, pp. 111-117
- 36 Satterfield, C. N. and Sherwood, T. K. in *The Role of Diffusion in Catalysis*, Addison-Wesley, Reading, MA, 1963, pp. 20-26
- 37 Klein, J. and Washausen, P. in *Characterization of Immobilized Biocatalysts* (Buchholz, K., ed.), Dechema Monograph No. 1724-1731, Verlag Chemie, Weinheim, 1979, vol. 84, pp. 300-302
- 38 Klein, J. and Manecke, G. in *Enzyme Engineering* (Chibata, I., Fukui, S. and Wingard, L. B., eds), Plenum Press, New York, 1982, vol. 6, pp. 181-189
- 39 Tanaka, H., Matsumura, M. and Veliky, I. A. *Biotechnol. Bioeng.* 1984, 26, 53-58
- 40 Adlercreutz, P. *Oxygen Supply to Immobilized Cells*, PhD Thesis, University of Lund, Lund, Sweden, 1985
- 41 Klein, J., Stock, J. and Vorlop, K.-D. *Eur. J. Appl. Microbiol. Biotechnol.* 1983, 18, 86-91
- 42 Vivian, J. E. and King, C. J. *AIChE J.* 1964, 10, 220-221
- 43 Duda, J. L. and Vrentas, J. S. *AIChE J.* 1968, 14, 286-294
- 44 Ichikawa, Y., Sato, S. and Takahashi, J. J. *Ferment. Technol.* 1981, 59, 269-273
- 45 Brian, P. L. T. and Hales, H. B. *AIChE J.* 1969, 15, 419-425
- 46 Ranz, W. E. and Marshall, W. R. *Chem. Eng. Progr.* 1952, 48, 141-146, 173-180
- 47 Sherwood, T. K., Pigford, R. L. and Wilke, C. R. in *Mass Transfer*, McGraw-Hill, Inc., New York, 1975, 220-224
- 48 Boucher, D. F. and Alves, G. E. in *Chemical Engineers' Handbook* (Perry, R. H. and Chilton, C. H., eds), McGraw-Hill, Inc., New York, 1974, 5th edn, section 5, 61-62
- 49 Habets-Crützen, A. Q. H. and de Bont, J. A. M. *Appl. Microbiol. Biotechnol.* 1985, 22, 428-433
- 50 Moo-Young, M. and Kobayashi, T. *Can. J. Chem. Eng.* 1972, 50, 162-167
- 51 Kobayashi, T. and Laidler, K. J. *Biochim. Biophys. Acta* 1973, 302, 1-12

## 5. MODELLING THE EFFECTS OF MASS TRANSFER ON KINETICS OF PROPENE EPOXIDATION OF IMMOBILIZED *MYCOBACTERIUM* CELLS: PRODUCT INHIBITION

L. E. S. Brink and J. Tramper

*Department of Food Science, Food and Bioengineering Group, Agricultural University Wageningen, De Dreyen 12, 6703 BC Wageningen, The Netherlands*

(Received 9 September 1985; revised 12 December 1985)

*An existing model for the external and internal mass transfer effects on the kinetics of propene epoxidation of calcium alginate-entrapped cells was extended to account for inhibition of the produced propene oxide. The intrinsic kinetics of the product-inhibited epoxidation reaction were derived and its applicability was demonstrated using independent time course experiments in a circulation batch-reactor system. The problem of coupled product-inhibited epoxidation and oxygen diffusion to and in the spherical gel beads was solved applying the collocation method. The predicted and experimental propene and oxygen-consumption rates were found to be in agreement for various degrees of oxygen-diffusion limitation and propene oxide inhibition.*

**Keywords:** Immobilized cells; mass transfer modelling; propene oxide inhibition; propene epoxidation kinetics

### Introduction

In paper 1<sup>1</sup> it was shown that the propene epoxidation rate of calcium alginate-entrapped *Mycobacterium* cells could be severely limited due to internal and, to a smaller extent, external mass transfer resistances of the two substrates, propene and oxygen. The pore diffusion model was successfully applied to quantify these diffusion effects, assuming pseudo-one-substrate conditions (with propene or oxygen as the limiting substrate) and negligible product inhibition. The latter two simplifications, though justifiable in a fundamental study, could restrict, however, the application of the diffusion model in many cases of practical importance.

A possible process scheme for the production of chiral propene oxide in an organic liquid phase/immobilized cell system<sup>2-5</sup> is the two-phase fixed-bed bioreactor. In this reactor configuration the organic solvent is pumped through a stagnant, aqueous phase consisting of the calcium alginate beads, thereby continuously supplying the two dissolved substrates and extracting the formed epoxide. After separation of the epoxide from the product stream, for instance by distillation, and replenishment of the substrates, the solvent is recycled. As the solubility of propene in a suitable organic solvent (for instance n-hexadecane) is much higher than that of oxygen,<sup>4</sup> it is likely that the assumption of pseudo-one-substrate conditions (with oxygen as the limiting substrate) will hold. In this respect the above-mentioned one-substrate microkinetic model can be

used to form the basis of a macrokinetic model describing the performance of the fixed-bed bioreactor. However, application of the second assumption, negligible product inhibition, might lead to erroneous model predictions in view of the very toxic nature of propene oxide,<sup>6</sup> the relatively high solubility of the epoxide in water (or calcium alginate gel)<sup>4</sup> and, finally, the desirability of high product concentrations for ease of product recovery. Therefore, modelling of the product-inhibited epoxidation kinetics of immobilized cells in conjunction with (oxygen) mass transfer resistances will be dealt with in this paper.

A simple, kinetic model is derived, using time-course experiments, which relates the propene and oxygen consumption rate and epoxide production rate of the immobilized cells to the oxygen and propene oxide concentrations (excess level of propene). The three-point collocation method<sup>7,8</sup> was used to solve the problem of coupled product-inhibited epoxidation and pore diffusion in the calcium alginate beads in series with external film diffusion. This made it possible to estimate the influences of changing bead size, cell density and oxygen and epoxide concentration on the observed propene and oxygen consumption rates.

### Materials and methods

#### *Chemicals and microorganism*

Liquid propene oxide was purchased from Merck.

Alginate Industries, London, UK provided the support material, sodium alginate (Manucol DM). Microbial aspects of the *Mycobacterium* strain E3 used for the epoxidation reaction have been described elsewhere.<sup>2</sup>

### Immobilization

The technique of immobilization in calcium alginate has been reported earlier.<sup>2</sup> The mean diameter of the spherical gel particles was determined by microscopic measurement of about 40 bead diameters.

### Measurement of product-inhibited kinetics and mass transfer effects

The propene, oxygen and propene oxide concentrations were measured in a laboratory-scale batch-reactor system with gas circuit. Full details concerning method of measurement of kinetic rate have been published before.<sup>5,9</sup> A small bubble-column bioreactor (250 cm<sup>3</sup>) was used for contacting the calcium alginate beads and an aqueous 0.05 M calcium chloride solution with the circulating gas. In the case of large biocatalyst particles and a large amount of calcium alginate gel, a bubble-column bioreactor with an increased volume (500 cm<sup>3</sup>) was used to assure suspension of the gel particles by the circulating gas. The total amount of biocatalyst used in one experiment was always about 1 g dry weight of cells. The excess liquid concentrations of propene and oxygen in experiments with pseudo-one-substrate reaction conditions were 160 μM and 240 μM, respectively.

## Results and discussion

### Product-inhibited epoxidation kinetics

An accurate, kinetic model should be available to make meaningful predictions of the coupled diffusion and product-inhibited reaction rate in the biocatalyst bead. In the absence of propene oxide the experimental propene consumption rate,  $v_1$ , of the gel-entrapped, non-growing cells can be described by the ping-pong mechanism.<sup>5</sup> This kinetic model is mostly used for bisubstrate enzyme-catalysed reactions.<sup>10</sup> However, a more accurate prediction of  $v_1$  as a function of the oxygen concentration,  $S_2$ , is obtained when an allosteric effect<sup>10</sup> of oxygen is incorporated in the rate equation (see results below):

$$v_1 = -\frac{dS_1}{dt} = \frac{V S_1 S_2^2}{K_A S_1 + K_1 S_2^2 + S_1 S_2^2} \approx \frac{V S_2^2}{K_A + S_2^2} \quad (1)$$

where  $V$  is the maximal epoxidation rate;  $S_1$  and  $S_2$  the propene and oxygen concentration, respectively;  $K_1$  and  $K_A$  are kinetic parameters. The approximation in the right hand side of equation (1) is valid at high levels of propene ( $S_1 \gg K_1$ ).

The immobilized cells also appeared to consume oxygen in the absence of propene (and propene oxide). This cell respiration was found to obey irreversible Michaelis-Menten kinetics with a maximum respiration rate of  $\alpha V$ ,<sup>5</sup>  $\alpha$  being a parameter. As it was also found experimentally that about one mole of oxygen is needed for the epoxidation of one mole of propene in addition to respiration, the total oxygen consumption rate,  $v_2$ , is given by:

$$v_2 = -\frac{dS_2}{dt} = -\frac{dS_1}{dt} + \frac{\alpha V S_2}{K_R + S_2} \quad (2)$$

where  $K_R$  is the Michaelis-Menten constant of the cell respiration.

The propene consumption rate of free<sup>6</sup> and immobilized cells is inhibited strongly by the product, propene oxide ( $P$ ). This inhibition can be described by the following general rate equation (excess propene):<sup>11</sup>

$$v_1 = -\frac{dS_1}{dt} = \frac{V S_2^2}{K_A (1 + P/K_P') + S_2^2 (1 + P/K_P'')} \quad (3)$$

where  $K_P'$  and  $K_P''$  are the epoxide inhibition parameters. The inhibitory effect of the epoxide on the oxygen consumption rate of free<sup>6</sup> and immobilized cells (see below) is much less severe, indicating no significant dependence of the cell respiration on the propene oxide level. In the case of immobilized cells the latter was substantiated by measurements in a biological oxygen monitor ( $P < 15$  mm). Thus, equation (2) (combined with equation 3) can still be used to predict the oxygen consumption rate in the case of product inhibition.

A part of the propene oxide formed is consumed by the bacteria.<sup>2,4</sup> Therefore, the production rate of the epoxide,  $v_P$ , will be lower than the propene consumption rate:

$$v_P = \frac{dP}{dt} = -\frac{dS_1}{dt} - v_C(P, S_2) \quad (4)$$

where  $v_C(P, S_2)$  is the  $P$  and  $S_2$  dependent epoxide consumption rate.

### Estimation of kinetic parameters

The parameters in the above kinetic model  $V$ ,  $\alpha$ ,  $K_1$ ,  $K_A$ ,  $K_R$ ,  $K_P'$  and  $K_P''$  were estimated by fitting the kinetic model, as predicted by equations (1–3), to different types of experimental time-course data. The influences of the propene oxide formed and the small inactivation of the immobilized cells were not significant in these experiments, as has already been discussed.<sup>1</sup> Furthermore, despite the very low solubilities of the gaseous substrates in water, diffusional effects were eliminated by proper selection of particle size ( $\approx 0.7$  mm) and biocatalytic activity [ $\approx 5 \times 10^4$  μmol min<sup>-1</sup> (m<sup>3</sup> particle)<sup>-1</sup>]. Under these conditions the calculated effectiveness factors (see paper 1 for method of calculation)<sup>1</sup> are between unity and 0.9 when propene is the limiting substrate and between unity and 0.8 in case of oxygen limitation, dependent on the substrate concentration ( $10 < S_1 < 160$  μM,  $10 < S_2 < 80$  μM). The effects of these small diffusion resistances on the derived kinetic parameters, and consequently on the model predictions, are only limited.

At an excess level of oxygen ( $S_2 \gg K_A$ ) equation (1) can be rearranged as:

$$v_1 = -\frac{dS_1}{dt} = \frac{V S_1}{K_1 + S_1} \quad (5)$$

Fitting the integrated form of equation (5) to experimental  $S_1(t)$  data, using a non-linear regression technique, then gives values for  $V$  and  $K_1$  (Figure 1). In the absence of propene, equation (2) becomes:

$$v_2 = -\frac{dS_2}{dt} = \frac{\alpha V S_2}{K_R + S_2} \quad (6)$$

Values for  $\alpha$  and  $K_R$  are then determined from experimental  $S_2(t)$  by applying the same fitting technique as above. The described procedure was performed with five different cell batches. Low values were found for the (pseudo)equilibrium constants ( $K_1 = 6 (\pm 3)$  μM,  $K_R = 20 (\pm 8)$  μM). The relatively high variation in these values does not give rise to inaccurate model predictions in view of the small effect of the two parameters on the calculated reaction

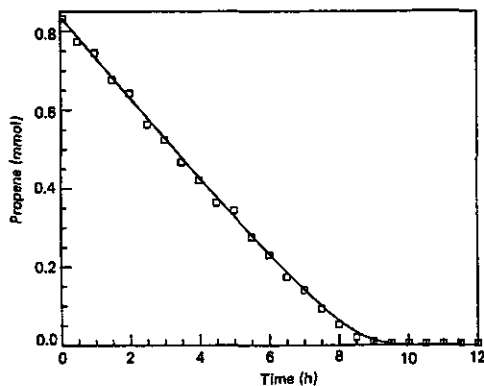


Figure 1 Amount of unconverted propene in the experimental system versus time at an excess level of oxygen (1 mmol propene corresponds to  $S_1 = 192 \mu\text{M}$ ); model fit; equation (5) with  $V = 3.4 \mu\text{mol min}^{-1} (\text{g dry weight})^{-1}$  and  $K_1 = 7.4 \mu\text{M}$

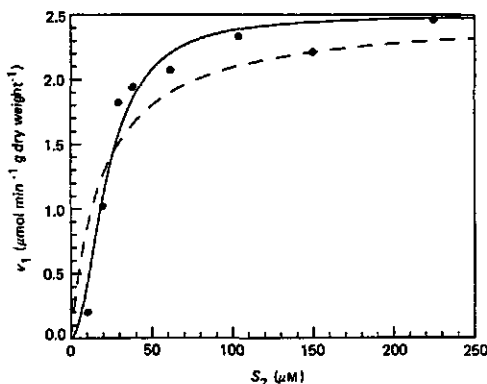


Figure 2 Propene consumption rate,  $v_1$ , versus the oxygen concentration,  $S_2$ , at an excess level of propene [ $V = 2.5 \mu\text{mol min}^{-1} (\text{g dry weight})^{-1}$ ]; —, model fit; equation (7) with  $K_A = 5.1 \times 10^2 \mu\text{M}^2$ ; ---, Michaelis-Menten fit; Michaelis-Menten constant =  $20 \mu\text{M}$

rates. This is not the case for the kinetic rate parameters,  $V$  and  $\alpha$ . Specific estimates for these parameters are necessary for each cell batch, as considerable differences were found between the activities of the five cell batches used [ $1 < V < 3.5 \mu\text{mol min}^{-1} (\text{g dry weight})^{-1}$ ;  $1.5 < \alpha < 5$ ].

At an excess concentration of propene ( $S_1 \gg K_1$ ) the propene consumption rate is described by (equation 1):

$$v_1 = -\frac{dS_1}{dt} = \frac{V S_2^2}{K_A + S_2^2} \quad (7)$$

The parameter  $K_A$  can be estimated from experimentally determined  $v_1$  values at various constant oxygen concentrations using the appropriate known value for  $V$  and a non-linear regression technique ( $K_A = 5.1 \times 10^2$  and  $4.4 \times 10^2 \mu\text{M}^2$ ; two different cell batches). Equation (7) proved to be superior over a Michaelis-Menten-type relation between  $v_1$  and  $S_2$  in describing the experimental data (Figure 2).

In contrast to the consumption rate of propene, the influence of propene oxide ( $P < 10 \text{ mM}$ ) on the oxygen

consumption is limited (Figure 3). Apparently, the cell respiration, the dominant term in equation (2), is not affected by low concentrations of the epoxide. As in these experiments an excess amount of propene was continuously present, the propene consumption rate,  $v_1$ , is only a function of  $S_2$  and  $P$  (equation 3). Experimental  $v_1(S_2, P)$  can be extracted from the data in Figure 3, employing a fitting technique described in paper 1<sup>1</sup> to obtain experimental  $v_1$  values from the  $S_1(t)$  data (fitting second-order polynomial functions to sets of seven or nine points of measurement). The following, optimal parameter set was found to give a sufficiently accurate description of the observed  $v_1(S_2, P)$ :  $K_A = 4.6 \times 10^2 \mu\text{M}^2$ ,  $K_P' = 1.3 \text{ mM}$ ,  $K_P'' = 9.6 \text{ mM}$ ,  $V = 1.2 \mu\text{mol min}^{-1} (\text{g dry weight})^{-1}$  (Figure 4). The value obtained for  $K_A$  agrees well with the above-mentioned values. Both the inhibition parameters,  $K_P'$  and  $K_P''$ , appear necessary to model the decreasing maximal rate and the increasing, apparent  $K_A$  [i.e.  $K_A(1 + P/K_P')/(1 + P/K_P'')$ ].

The propene oxide consumption rate,  $v_C$ , of the different cell batches was always  $\approx 10$ –15% of the maximum propene consumption rate,  $V$ . A similar result was reported earlier for free *Mycobacterium* cells (strain E3).<sup>2</sup>

To examine the predictive capacity of the derived kinetic model (excess propene, equations 2–4) two different tests were performed. Model predictions were obtained by

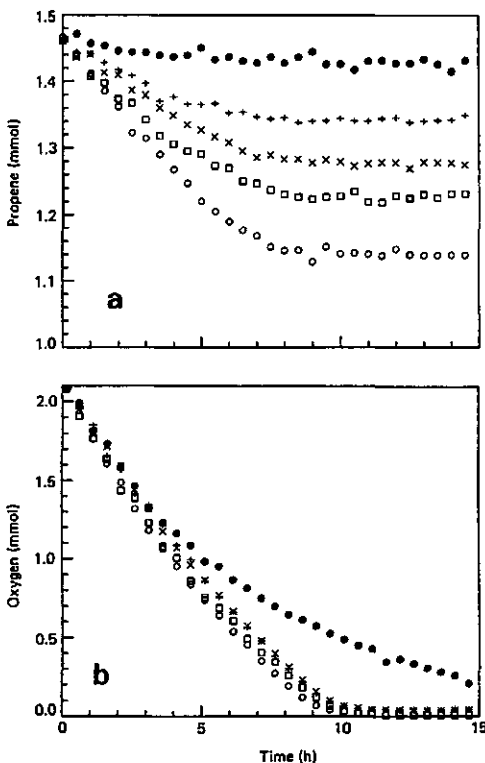


Figure 3 Amount of unconverted substrate in the experimental system (a: propene, b: oxygen; measured simultaneously) versus time at various propene oxide levels (1 mmol propene corresponds to  $S_1 = 233 \mu\text{M}$ , 1 mmol oxygen corresponds to  $S_2 = 58.3 \mu\text{M}$ ;  $P$  (mM): 0 (○), 3.0 (□), 5.3 (×), 10.6 (+), 116 (●)

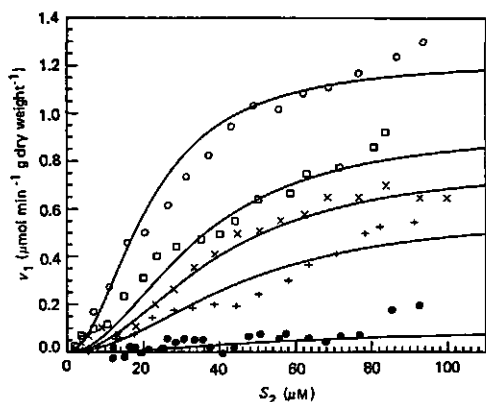


Figure 4 Propene consumption rate,  $v_1$ , versus the oxygen concentration,  $S_2$ , at various propene oxide levels;  $P$  (mM): 0 ( $\circ$ ), 3.0 ( $\square$ ), 5.3 ( $\times$ ), 10.6 ( $\triangle$ ), 116 ( $\diamond$ ); model fit: equation (3) with  $K_A = 4.6 \times 10^2 \mu\text{M}^2$ ,  $K_P = 1.3 \text{ mM}$ ,  $K_P'' = 9.8 \text{ mM}$  and  $V = 1.2 \mu\text{mol min}^{-1} (\text{g dry weight})^{-1}$

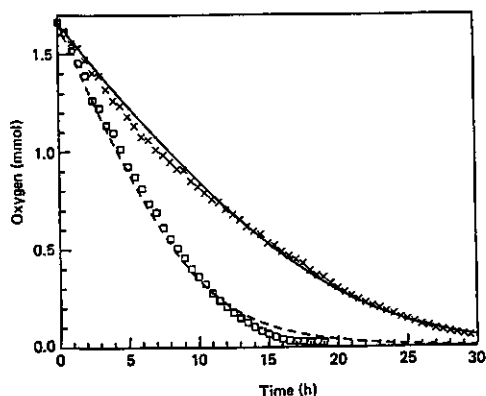


Figure 5 Amount of unconverted oxygen in the experimental system versus time in the absence of propene ( $\times$ ) and at an excess level of propene ( $\square$ ) (1 mmol oxygen corresponds to  $S_2 = 48.1 \mu\text{M}$ ); —, model fit: equation (6) with  $\alpha V = 2.2 \mu\text{mol min}^{-1} (\text{g dry weight})^{-1}$  and  $K_R = 29 \mu\text{M}$ ; ----, kinetic model predictions: equation (8) with  $V = 1.4 \mu\text{mol min}^{-1} (\text{g dry weight})^{-1}$ ,  $K_A = 4.4 \times 10^2 \mu\text{M}^2$  and  $\alpha V$  and  $K_R$  as stated above

numerically solving the relevant differential equations, using the Runge-Kutta procedure.

Firstly, calculated oxygen consumption rates at a high, constant concentration of propene ( $S_1 \gg K_1$ ) and in the absence of propene oxide ( $P \approx 0 \text{ mM}$ ):

$$v_2 = -\frac{dS_2}{dt} = \frac{V S_2^2}{K_A + S_2^2} + \frac{\alpha V S_2}{K_R + S_2} \quad (8)$$

compared favourably with independently determined experimental rates of the immobilized cells in a concentration versus time plot (Figure 5). At excess levels of propene the dependence of the oxygen consumption rate on  $S_2$  can also be successfully described by the Michaelis-Menten equation  $V_{m,2} S_2 / (K_{m,2} + S_2)$ , when optimum values for

$V_{m,2}$  and  $K_{m,2}$  are chosen. This approach has been used in paper 1.<sup>1</sup>

Secondly, independently determined propene, oxygen and epoxide time-course data were compared to the calculated  $S_1(t)$ ,  $S_2(t)$  and  $P(t)$  (excess propene, equations 2-4). See Figure 6. The epoxide consumption rate,  $v_C$ , was assumed to equal  $0.3 \mu\text{mol min}^{-1} (\text{g dry weight})^{-1}$  ( $\approx 12\%$  of  $V$ ) and, furthermore, to be independent of the oxygen and epoxide concentrations. Again, a good agreement is found between model predictions and experimental values. Though the influence of the produced epoxide ( $P < 2 \text{ mM}$ ) is relatively small in this experiment, the accuracy of the predicted propene concentrations becomes significantly better by taking the product inhibition into account. The observed epoxide levels at the end of the experiment are somewhat higher than the predicted ones. This may be a result of neglecting the dependence of the epoxide consumption rate on the decreasing oxygen level.

#### Product inhibition and oxygen diffusion limitation

At an excess level of propene the apparent kinetics of the gel-entrapped cells may be limited due to diffusion of oxygen and propene oxide to, in and from the biocatalyst particles. The differential equation describing coupled oxygen diffusion and consumption in the catalyst bead is (equations 2 and 3; see also paper 1):<sup>1</sup>

$$D_{e,2} \left( \frac{d^2 S_2}{dr^2} + \frac{2dS_2}{rdr} \right) = X \left( \frac{V S_2^2}{K_A (1 + P/K_P) + S_2^2 (1 + P/K_P'')} + \frac{\alpha V S_2}{K_R + S_2} \right) \quad (9)$$

with the boundary conditions:

$$D_{e,2} dS_2/dr = \beta (S^* - S_S) \quad \text{at } r = 0.5 d_p \quad (10)$$

$$dS_2/dr = 0 \quad \text{at } r = 0 \quad (11)$$

and with the overall external mass transfer coefficient:<sup>1</sup>

$$\beta = \{ a_S [1/(k_L a) + 1/(k_S a_S)] \}^{-1} \quad (12)$$

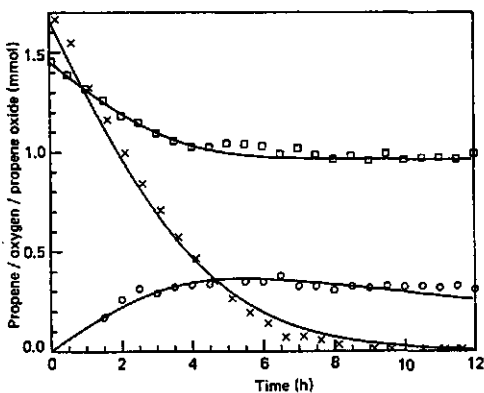


Figure 6 Amount of unconverted propene ( $\circ$ ) and oxygen ( $\times$ ) and accumulated propene oxide ( $\square$ ) in the experimental system versus time (1 mmol propene corresponds to  $S_1 = 192 \mu\text{M}$ , 1 mmol oxygen corresponds to  $S_2 = 48.1 \mu\text{M}$ , 1 mmol propene oxide corresponds to  $P = 4.0 \text{ mM}$ ); kinetic model predictions: equations (2-4) with  $V = 2.5 \mu\text{mol min}^{-1} (\text{g dry weight})^{-1}$ ,  $K_A = 5.1 \times 10^2 \mu\text{M}^2$ ,  $K_P = 1.3 \text{ mM}$ ,  $K_P'' = 9.6 \text{ mM}$ ,  $\alpha = 1.9$ ,  $K_R = 27 \mu\text{M}$  and  $v_C = 0.3 \mu\text{mol min}^{-1} (\text{g dry weight})^{-1}$

Likewise, coupled propene oxide diffusion (out of the bead) and formation is modelled by:

$$D_{e,p} \left( \frac{d^2 P}{dr^2} + \frac{2dP}{rdr} \right) = -X \left( \frac{V S_2^2}{K_A (1 + P/K_P) + S_2^2 (1 + P/K_P')} - \nu_C (P, S_2) \right) \quad (13)$$

with the boundary conditions:

$$D_{e,p} \frac{dP}{dr} = -\beta_P (P_s - P_b) \quad \text{at } r = 0.5 d_p \quad (14)$$

$$dP/dr = 0 \quad \text{at } r = 0 \quad (15)$$

Equation (9) has to be solved simultaneously with equation (13) to obtain the oxygen and epoxide profiles in the catalyst bead, and from these the theoretical reaction rates. The diverse kinetic-rate terms in these two equations prevents the derivation of a simple relation between  $P(r)$  and  $S_2(r)$ , as has been done by Ramachandran,<sup>8</sup> Jain and Ghose<sup>12</sup> and Karel *et al.*<sup>13</sup> However, for estimating the epoxide profile in the gel bead, the dependence of  $\nu_2$  on the epoxide concentration can be neglected (Figure 3b) and a Michaelis-Menten equation was used to describe  $\nu_2(S_2)$ . The oxygen profile can now be calculated by solving equation (9),<sup>1</sup> and, inserting  $S_2(r)$  in equation (13), the epoxide concentration profile was estimated using the three-point collocation method.<sup>7,8</sup> In the absence of external epoxide diffusion limitation ( $P_s \approx P_b$  in equation (14); see also the comparable cases for oxygen and propene)<sup>1</sup> and under oxygen diffusion limited conditions the epoxide profiles thus calculated were not found significant ( $P_b = 3 \text{ mM}$ ,  $P \approx 3 \text{ mM}$  at  $r = 0$ ), even with a very low estimate for  $D_{e,p}$  [ $D_{e,p}/10 \approx 1.5 \times 10^{-10} (\text{m}^2 \text{ s}^{-1})$ ]<sup>1</sup> and with a negligible epoxide consumption rate,  $\nu_C$ . The relatively high propene oxide concentrations in the water and calcium alginate phase (millimolar range), in contrast with the low solubilities of the gaseous substrates in an aqueous phase (micromolar range), is the main cause for this observation. Therefore, the propene oxide concentrations in the alginate bead can be assumed to equal the epoxide concentration in the bulk liquid.

The influence of external and internal diffusion limitations on the substrate consumption rate of the immobilized cells has been quantified.<sup>1</sup> These effects were described by the Thiele effectiveness factor,  $\eta$ , which relates the reaction rate if no diffusion resistance existed to the observed rate. Accordingly, assuming uniform propene and epoxide concentration profiles in the alginate bead, the oxygen consumption rate under diffusion-limited conditions can be calculated as (equations 2 and 3):

$$\nu_2(S_2, P_b) = \eta \left( \frac{V S_2^2}{K_A (1 + P_b/K_P) + S_2^2 (1 + P_b/K_P')} + \frac{\alpha V S_2}{K_R + S_2} \right) \quad (16)$$

The effectiveness factor is obtained by solving equations (9–11) ( $P = P_b$ ) using the three-point collocation method<sup>7,8</sup> with the mass-transfer parameters derived in paper 1<sup>1</sup> ( $D_{e,2}$ ,  $\beta$ ). As the effectiveness of the biocatalyst is entirely determined by oxygen diffusion, the propene consumption rate can also be described with the above calculated effectiveness factor:

$$\nu_1(S_2, P_b) = \eta \left( \frac{V S_2^2}{K_A (1 + P_b/K_P) + S_2^2 (1 + P_b/K_P')} \right) \quad (17)$$

To test the accuracy of the predicted oxygen and

propene consumption rates (equations 16 and 17) for various degrees of oxygen diffusion resistance and epoxide inhibition, the experiments of Table 1 were performed. One of these tests [ $d_p = 0.7 \text{ mm}$ ,  $X = 7.6 \times 10^3 \text{ g dry weight } (\text{m}^3 \text{ particle})^{-1}$ ,  $P_b = 0 \text{ mM}$ ] has been used (together with the experiments of Figure 4) to derive the kinetic parameters  $V$ ,  $\alpha$ ,  $K_A$ ,  $K_R$ ,  $K_P$  and  $K_P'$ . These parameters were then combined with equations (16) and (17) to obtain model predictions for the other three experiments in Table 1. Experimental reaction rates,  $\nu_1(S_2, P_b)$  and  $\nu_2(S_2, P_b)$ , were again derived from graphs of substrate concentration versus time using the fitting technique described in paper 1.<sup>1</sup> In Figures 7 and 8 these experimental rates are compared to the corresponding, theoretical values of equations (16) and (17). The various assumptions made in the model calculations (kinetic model, uniform propene and epoxide profiles, collocation method) do not seem to affect the reliability of the model predictions to an unacceptable degree. The discrepancies in Figures 7 and 8 are considerable (error in overall effectiveness mostly  $\approx 30\%$ ,  $20 < S_2 < 100 \text{ } \mu\text{M}$ ) but not unanticipated. Kasche<sup>14</sup> has already indicated that the prediction of overall effectiveness factors of immobilized biocatalysts cannot be better than  $\approx 20\text{--}30\%$  (when  $\eta < 1$ ) as a result of a cumulation of experimental errors in system properties (e.g. kinetic parameters, particle size, effective diffusivity), which are used to determine the Thiele modulus and Sherwood number and thus the effec-

Table 1 Reaction conditions (particle diameter, immobilized cell density and propene oxide concentration in the bulk liquid) of the experiments with coupled oxygen diffusion and epoxide inhibition

Expt no.	$d_p$ (mm)	$X$ [ $\times 10^3 \text{ g dry weight } (\text{m}^3 \text{ particle})^{-1}$ ]	$P_b$ (mM)
1	0.7	7.6	0
2	2.6	7.7	0
3	2.7	7.7	1.6
4	2.9	46	2.7

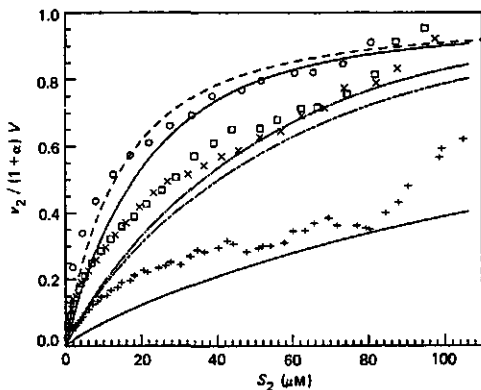


Figure 7 Dimensionless oxygen consumption rate,  $\nu_2/(1 + \alpha)V$ , versus the oxygen concentration at the gas-liquid interface,  $S_2 = S^*$ ; experimental reaction rates (see Table 1):  $\circ$ , no. 1;  $\square$ , no. 2;  $\times$ , no. 3;  $+$ , no. 4; model predictions (—, nos. 1 and 4; ---, no. 2; ····, no. 3); equations (9–11) and (16) with  $V = 1.2 \text{ } \mu\text{mol min}^{-1} \text{ g dry weight}^{-1}$ ,  $K_A = 4.6 \times 10^2 \text{ } \mu\text{M}^2$ ,  $K_P = 1.3 \text{ mM}$ ,  $K_P' = 9.6 \text{ mM}$ ,  $\alpha = 4.8$  and  $K_R = 11 \text{ } \mu\text{M}$ ; ····, negligible diffusion resistance and  $P_b = 0 \text{ mM}$

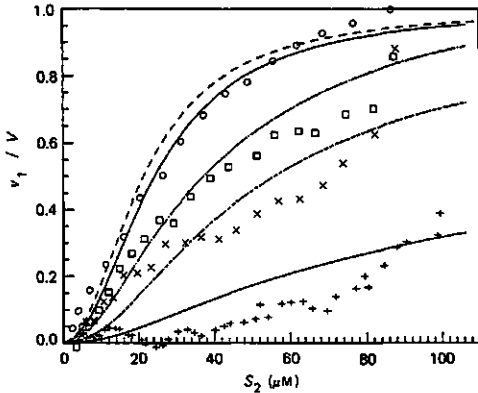


Figure 8 Dimensionless propene consumption rate,  $v_1/V$ , versus the oxygen concentration at the gas-liquid interface,  $S_2 = S^*$ ; experimental reaction rates (see Table 1):  $\circ$ , no. 1;  $\square$ , no. 2;  $\times$ , no. 3;  $+$ , no. 4; model predictions (—, nos 1 and 4; ---, no. 2; ----, no. 3): equations (9–11) and (17) with  $V = 1.2 \mu\text{mol min}^{-1}$  (g dry weight) $^{-1}$ ,  $K_A = 4.6 \times 10^2 \mu\text{M}^2$ ,  $K_p = 1.3 \text{ mM}$ ,  $K_p' = 9.6 \text{ mM}$ ,  $\alpha = 4.8$  and  $K_R = 11 \mu\text{M}$ ; ----, negligible diffusion resistance and  $P_b = 0 \text{ mM}$

tiveness factor. However, theoretical calculations, such as these in Figures 7 and 8, are still useful to estimate the effectiveness of the immobilized biocatalyst under influence of changing process parameters in practical applications (e.g. an organic liquid phase/immobilized cell bioreactor).<sup>15</sup>

As in paper 1, the calculated, external oxygen diffusion limitation is much less severe than the internal diffusion limitation. Experimental oxygen consumption rates are mostly somewhat higher than the theoretical values, but the effects of the changing reaction conditions (Table 1) and oxygen concentration are correctly predicted. The calculated and experimentally observed effects of propene oxide on the propene consumption rate are of more importance than the effects on the oxygen consumption (experiments 2 and 3, Table 1). At the highest epoxide inhibition level and with severe oxygen diffusion limitation (experiment 4) it becomes difficult to measure accurately the decrease in the excess propene concentration. This may explain the substantial difference between the observed and calculated propene consumption rates found in this experiment.

### Conclusions

The inhibitory effect of propene oxide on the propene epoxidation kinetics of gel-entrapped cells was successfully incorporated in an existing external film and internal pore diffusion model. In view of the high solubility of propene in a non-polar organic solvent, the reaction medium for the epoxidation reaction in future applications, oxygen was considered the limiting substrate in this diffusion model. The microkinetic model will play a central role in the design of an organic liquid phase/immobilized cell bioreactor.

### Acknowledgements

The authors are grateful to Prof. K. Ch. A. M. Luyben and Prof. Dr. K. van't Riet for helpful discussions. These

investigations were supported (in part) by the Netherlands Technology Foundation (STW).

### Nomenclature

$a$	gas-liquid specific surface area ( $\text{m}^{-1}$ )
$a_S$	liquid-solid specific surface area ( $\text{m}^{-1}$ )
$D_{e,1}$	effective propene diffusion coefficient in calcium alginate ( $\text{m}^2 \text{s}^{-1}$ )
$D_{e,2}$	effective oxygen diffusion coefficient in calcium alginate ( $\text{m}^2 \text{s}^{-1}$ )
$D_{e,P}$	effective propene oxide diffusion coefficient in calcium alginate ( $\text{m}^2 \text{s}^{-1}$ )
$d_P$	particle diameter (m)
$k_L$	oxygen mass transfer coefficient in the liquid film adjacent to the gas-liquid interface ( $\text{m s}^{-1}$ )
$k_S$	oxygen mass transfer coefficient in the liquid film adjacent to the liquid-solid interface ( $\text{m s}^{-1}$ )
$K_1$	kinetic parameter in equation (1) ( $\text{mol m}^{-3}$ )
$K_A$	kinetic parameter in equation (1) ( $\text{mol}^2 \text{m}^{-6}$ )
$K_{m,2}$	Michaelis-Menten constant of the overall oxygen consumption ( $\text{mol m}^{-3}$ )
$K_R$	Michaelis-Menten constant of the cell respiration ( $\text{mol m}^{-3}$ )
$K_p'$	propene oxide inhibition parameter ( $\text{mol m}^{-3}$ )
$K_p$	propene oxide inhibition parameter ( $\text{mol m}^{-3}$ )
$P$	propene oxide concentration ( $\text{mol m}^{-3}$ )
$P_b$	propene oxide concentration in the bulk liquid ( $\text{mol m}^{-3}$ )
$P_s$	propene oxide concentration at the gel surface ( $\text{mol m}^{-3}$ )
$r$	radial distance from the centre of the particle (m)
$S_1$	propene concentration ( $\text{mol m}^{-3}$ )
$S_2$	oxygen concentration ( $\text{mol m}^{-3}$ )
$S^*$	oxygen concentration at the gas-liquid interface ( $\text{mol m}^{-3}$ )
$S_S$	oxygen concentration at the gel surface ( $\text{mol m}^{-3}$ )
$t$	time (s)
$v_1$	propene consumption rate [ $\mu\text{mol min}^{-1}$ (g dry weight) $^{-1}$ ]
$v_2$	oxygen consumption rate [ $\mu\text{mol min}^{-1}$ (g dry weight) $^{-1}$ ]
$v_C$	propene oxide consumption rate [ $\mu\text{mol min}^{-1}$ (g dry weight) $^{-1}$ ]
$v_P$	propene oxide production rate [ $\mu\text{mol min}^{-1}$ (g dry weight) $^{-1}$ ]
$V$	maximum propene epoxidation rate [ $\mu\text{mol min}^{-1}$ (g dry weight) $^{-1}$ ]
$V_{m,2}$	maximum overall oxygen consumption rate [ $\mu\text{mol min}^{-1}$ (g dry weight) $^{-1}$ ]
$X$	cell density [g dry weight ( $\text{m}^3 \text{ particle}$ ) $^{-1}$ ]
$\alpha$	cell respiration parameter in equation (2)
$\beta$	overall external oxygen mass transfer coefficient ( $\text{m s}^{-1}$ )
$\beta_P$	external propene oxide mass transfer coefficient ( $\text{m s}^{-1}$ )
$\eta$	overall oxygen effectiveness factor

### References

- 1 Brink, L. E. S. and Tramper, J. *Enzyme Microb. Technol.* 1986, 8, 281–288
- 2 Habets-Criutzen, A. Q. H., Brink, L. E. S., van Ginkel, C. G., de Bont, J. A. M. and Tramper, J. *Appl. Microbiol. Biotechnol.* 1984, 20, 245–250
- 3 Tramper, J., Brink, L. E. S., Hamstra, R. S., de Bont, J. A. M.,



## Papers

- Habets-Crützen, A. Q. H. and van Ginkel, C. G. *Proceedings of the 3rd Eur. Congress on Biotechnol.* Munich, FRG, 1984, vol. 2, pp. 269-276
- 4 Brink, L. E. S. and Tramper, J. *Biotechnol. Bioeng.* 1985, 27, 1258-1269
- 5 Brink, L. E. S. and Tramper, J. *Proceedings of the 1st IFAC Symposium on Modelling and Control of Biotechnological Processes*, Noordwijkerhout, The Netherlands, 1985, pp. 111-117
- 6 Habets-Crützen, A. Q. H. and de Bont, J. A. M. *Appl. Microbiol. Biotechnol.* 1985, 22, 428-433
- 7 Villadsen, J. V. and Stewart, W. E. *Chem. Eng. Sci.* 1967, 22, 1483-1501
- 8 Ramachandran, P. A. *Biotechnol. Bioeng.* 1975, 17, 211-226
- 9 Brink, L. E. S., Tramper, J., van't Riet, K. and Luyben, K. Ch. A. M. *Anal. Chim. Acta* 1984, 163, 207-217
- 10 Mahler, H. R. and Cordes, E. H. in *Biological Chemistry*, Harper and Row, New York, 1966, pp. 237-263
- 11 Beltrame, P. L., Carniti, P., Focher, B., Marzetti, A. and Sarto, V. *Biotechnol. Bioeng.* 1984, 26, 1233-1238
- 12 Jain, D. and Ghose, T. K. *Biotechnol. Bioeng.* 1984, 26, 340-346
- 13 Karel, S. F., Libicki, S. B. and Robertson, C. R. *Chem. Eng. Sci.* 1985, 40, 1321-1354
- 14 Kasche, V. *Enzyme Microb. Technol.* 1983, 5, 2-13
- 15 Brink, L. E. S. and Tramper, J. submitted

# 6. FACILITATED MASS TRANSFER IN A PACKED-BED IMMOBILIZED-CELL REACTOR BY USING AN ORGANIC SOLVENT AS SUBSTRATE RESERVOIR

## Summary

The production of propene oxide from propene and oxygen by non-growing *Mycobacterium* cells entrapped in calcium alginate was used to study the behaviour of a packed-bed immobilized-cell reactor operated with an organic solvent as the substrate reservoir. As a result of the high solubility of propene in the solvent used, *n*-hexadecane, oxygen was considered the limiting substrate. Dilution of the biocatalyst bed with small glass particles appeared necessary to attain a high liquid/solid contacting efficiency between the hydrophilic gel particles and the hydrophobic solvent. The bed dilution also avoided bed compaction and reduced pressure drops. The use of an organic solvent as the transport medium prevented oxygen depletion along the length of the packed-bed reactor. This eliminated the need for a separate gas phase in the bioreactor. A mathematical reactor model was developed to describe the combined effects of contacting pattern and external and internal diffusion limitations on the intrinsic kinetics of the immobilized cells. Experiments with the packed-bed immobilized-cell reactor were performed using an aqueous solution or *n*-hexadecane as the reaction medium. Predicted oxygen conversions compared favourably to the observed values without the need for fitting factors.

*Keywords:* packed-bed bioreactor, mass-transfer modelling, reactor design equation, immobilized cells, organic substrate reservoir, alginate, propene epoxidation.

## Introduction

The design of reactors containing immobilized enzymes or (non)viable cells is a research field of growing importance in the biochemical-engineering discipline [1-5]. The usually-employed, aqueous reaction medium in immobilized-biocatalyst reactors, with its inherent, low capacity for apolar and gaseous substrates/products, has restricted severely the number of practical applications. The recent trend to use a water-immiscible organic solvent as substrate and/or product reservoir in bioconversions, however, may offer certain substantial advantages [6-11]. The high concentrations of poorly water-soluble substrates (e.g. oxygen) and/or products, which are possible in suitable organic solvents, could lead to enhanced mass-transfer rates, decreased levels of substrate or product inhibition and facilitated product recovery. Entrapment of the enzymes or cells in hydrophilic gels like agar(ose), alginate,  $\kappa$ -carrageenan and gelatin is one of the most widely used immobilization techniques due to its convenience, mildness, reproducibility and versatility [12, 13]. In addition, the technique of gel entrapment permits a high cell loading and is suited for scale-up [13, 14], an important consideration in case of pilot plant or industrial applications. Consequently, the combined use of hydrophilic-gel entrapment as

technique of immobilization and a water-immiscible organic solvent as a main constituent of the reaction medium should have great potential. The fixed-bed reactor, rather than the slurry reactor, would be a suitable configuration for this organic-liquid-phase/immobilized-biocatalyst system. A well-defined suspension of the hydrophilic particles in the hydrophobic solvent cannot be obtained. In a fixed bed, however, the hydrophobic organic phase can be forced to flow through a stationary bed of hydrophilic-gel particles, thereby continuously supplying the substrate(s) and extracting the product(s). The feasibility of this process has been demonstrated by Ter Meulen and Annokkee [15]. Similar approaches, though with different immobilization techniques, were followed by Bell et al. [16] and Macrae [17, 18], who used solid-phase lipolytic enzymes of *Rhizopus arrhizus* and inorganic support materials coated with lipases, respectively, as the stationary biocatalyst phases.

Dependent on the presence of a gas phase, and omitting gas-solid reactor configurations, fixed-bed reactors can be divided into two categories: two-phase fixed bed or packed bed (liquid-solid) and three-phase fixed bed or trickle bed (gas-liquid-solid). It is generally believed, that trickle-bed bioreactors are required if supply and/or removal of gaseous substrates (especially oxygen) and/or products are important features of the immobilized-biocatalyst process [2, 4]. However, when using as the transport medium a suitable organic solvent with a high capacity for gases, it should be possible to eliminate the gas phase in the bioreactor. This would simplify the design and scale-up of the immobilized-biocatalyst reactor considerably.

The chemical-engineering analysis of immobilized-enzyme and immobilized-cell reactors has been reviewed by Vieth et al. [1] and Venkatasubramanian et al. [2], respectively. The bioreactor performance was described by reactor design equations incorporating the reaction kinetics, combined internal and external mass-transfer limitations and reactor hydrodynamics (fluid-flow rate and contacting patterns). From these reactor design equations the substrate conversion, reactor size, space time and, finally, amount of immobilized biocatalyst can be optimized to give a maximal reactor productivity. Vieth et al. [1] pointed out that experimental validation of theoretical immobilized-enzyme reactor models is lacking. Since then several studies have appeared in which theoretical design equations of fixed-bed immobilized-biocatalyst reactors were verified with experimental reactor-performance data. In many of these investigations, however, simplifying assumptions were made or model parameters were estimated from the experimental results. The mass-transfer limitations were assumed to be negligible by O'Neill et al. [19], Saini and Vieth [20], Choi and Perlmutter [21], Cho et al. [22], Ching and Ho [23] and Furui [24]. Only interparticle mass transfer was considered by Toda [25] and Lee et al. [26]. Park et al. [27] also assumed no internal-diffusion limitation and derived a Colburn-type mass-transfer correlation from the experimental substrate conversions to describe the external-diffusion rate in a packed-bed immobilized-cell reactor. Model parameters were also obtained from observed conversions in packed-bed immobilized-enzyme reactors by Marrazzo et al. [28], Cabral et al. [29] and Lortie and Thomas [30]. Interparticle and intraparticle-diffusion effects were quantified separately by Kobayashi and Moo-Young [31] and also by Rovito and Kittrell [32]. In two studies on ethanol fermentation in packed-bed immobilized-viable-cell reactors, experimental performance data were used to evaluate model parameters like specific growth rate, specific productivity and ethanol-inhibition level [33, 34]. A true, experimental validation of fixed-bed

immobilized-enzyme reactor models, including the combined effects of external and internal-diffusion limitations and a flow pattern model (e.g. plug flow), has been given by Mercer and O'Driscoll [35], Tsukamoto et al. [36], Ooshima and Harano [37] and Bihari [38]. However, to our knowledge, experimentally verified design equations of fixed-bed immobilized-biocatalyst reactors operating with an organic solvent as substrate/product reservoir have not been presented yet. The introduction of an additional liquid phase in an immobilized-biocatalyst reactor system could in theory complicate the design of these reactors [10].

In order to investigate the potential of an organic-liquid-phase/immobilized-biocatalyst packed-bed reactor, the production of chiral propene oxide from propene and oxygen by non-growing *Mycobacterium* cells entrapped in calcium alginate [39, 40] has been used as the model. Several aspects concerning the use of an organic solvent in this reaction system, particularly retention of immobilized-cell activity, have already been examined in detail [11]. Moreover, it has been experimentally verified that reliable predictions of the external and internal-diffusion effects on the epoxidation kinetics of the immobilized cells can be made [41, 42]. Furthermore, quantitative gas analysis [43] and the prediction of thermodynamic and physical properties are facilitated as a result of the relatively simple molecules involved in the epoxidation (propene, oxygen, propene oxide). The selection of a packed-bed reactor has been favoured by the following considerations [2]. As a result of the large difference in surface tension between the hydrophobic solvent and the hydrophilic calcium alginate gel, it will be difficult to suspend the particles evenly in the organic solvent. Therefore, a sufficient organic-liquid/gel contacting efficiency will be easier obtained in a fixed-bed reactor than in a slurry reactor. A large fraction of the reactor volume is occupied by the biocatalyst in a fixed-bed reactor, thus high reactor productivities can be reached. The epoxidation rate is severely inhibited even at low concentrations of the product [42, 44], therefore a fixed bed (with limited backmixing) is kinetically favourable. The reactor feed (solvent and dissolved substrates) is a clean liquid without any particulate matter, thus clogging problems are not expected. Control of temperature and pH are not critical, and there are no gaseous products. A major drawback of employing a liquid/solid fixed-bed reactor could be depletion of the two gaseous substrates along the length of the column. As mentioned, this may be overcome by using an organic solvent, having a high solubility for the pertinent substrates, as the reaction medium.

Epoxidation experiments were carried out in an organic-liquid-phase/immobilized-cell tubular reactor with recycle of the solvent. Due to the high solubility of propene in an organic solvent, oxygen was considered the limiting substrate. The use of an organic phase as substrate reservoir prevented axial depletion of oxygen and the need for an additional gas phase in the reactor. Theoretical design equations for the packed-bed reactor, including combined external and internal mass-transfer effects, with water or organic solvent as the transport medium, were experimentally validated.

## Experimental

### *Chemicals and microorganism*

The organic solvent used in the experiments, n-hexadecane, was of analytical grade (> 99%) and purchased from Baker Chemicals. Propene and oxygen were of

commercial purity and obtained from the Matheson company, East Rutherford, NY. Alginate Industries, London, U.K. provided the support material, sodium alginate (Manucol DM). A *Mycobacterium* strain E3 was used for the epoxidation reaction. Microbial aspects of this strain have been described elsewhere [39].

### Immobilization

Details of the procedure of immobilization in calcium alginate have been given earlier [39]. The average diameter of the spherical gel particles was determined by microscopic measurement of about 50 bead diameters.

### Packed-bed reactor system

A schematic representation of the experimental set-up is depicted in figure 1. The

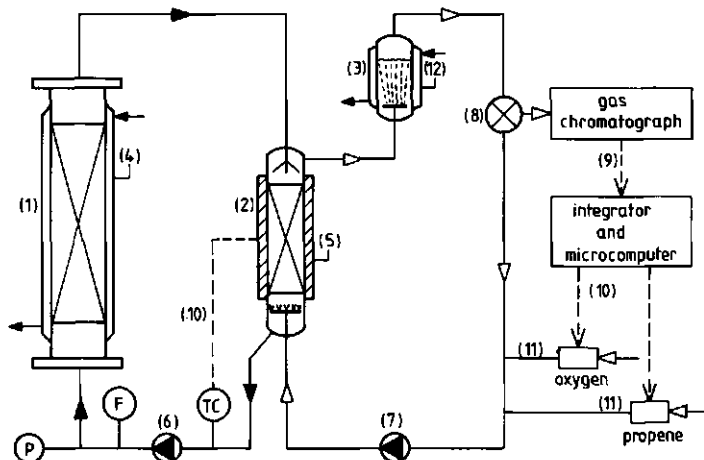


Fig. 1. Schematic diagram of the packed-bed reactor use (closed arrows: liquid flow, open arrows: gas flow); (1) packed-bed bioreactor; (2) trickle-bed countercurrent-flow contactor packed with 6 mm glass beads; (3) bubble-column with sulphuric-acid solution pH~1 to absorb and hydrolyse propene oxide; (4) jacket for circulation of water of constant temperature (~30°C); (5) heat tape; (6) magnet drive gear pump; (7) diaphragm pump; (8) two-position gas-sampling valve; (9) g.c. signal; (10) control signals; (11) mass-flow controllers; P: pressure gauge; F: rotameter; TC: temperature measurement and control.

biocatalyst particles (average sizes:  $0.7 \pm 0.1$ ,  $1.0 \pm 0.1$ ,  $2.8 \pm 0.1$  and  $3.3 \pm 0.1$  mm) were packed in a plexiglass column (internal diameter 2.9 cm, bed height ~36 cm). The column was surrounded by a jacket to circulate water of constant temperature (~30°C). The biocatalyst bed was diluted with small glass beads ( $1.0 \pm 0.2$  mm) to reduce axial dispersion and to attain a high liquid/solid contacting efficiency. Typical values for the volume fractions of calcium alginate and glass are 0.05 and 0.6, respectively (void fraction ~0.35). The total amount of gel-entrapped biocatalyst used in one experiment was mostly  $0.80 \pm 0.02$  g dry weight of cells ( $1.58 \pm 0.02$  g dry weight in case of the stagnant water film experiments). A circulating gas stream, containing the two gaseous substrates, oxygen and propene, was equilibrated with the liquid reaction medium (~350 cm<sup>3</sup> aqueous 0.05 M calcium chloride solution or n-hexadecane) in a trickle-bed countercurrent-flow contactor. The transport medium (aqueous or organic) with the dissolved substrates was then passed upwards through the bioreactor column. The

reactor-exit stream was completely recycled to the gas/liquid contactor, where the substrates were replenished. The concentration of produced propene oxide in the different phases (gas, reaction medium, calcium alginate) was kept insignificantly low by continuous hydrolysis of the epoxide in a sulphuric-acid solution pH~1 (removal from the circulating gas). It was experimentally verified that diffusion and/or leakage of oxygen and propene into or out of the experimental system did not interfere with the measurements. Propene and oxygen-consumption rates of the gel-entrapped cells in the packed-bed reactor were measured by on-line gas chromatographic analysis of the gaseous substrates in the circulating gas stream. The details of the analysis have been described previously [43]. The concentrations of the substrates in the organic or aqueous reactor-inlet stream, in equilibrium with the gas phase, could then be calculated using Henry's law [43]. The on-line gas chromatograph is coupled to an integrator and a microcomputer. This enabled automatic operation of the gas-sampling valve in conjunction with a column-switching valve [43, 45]. Besides data acquisition and reduction, the coupling to the computer has also made it possible to control the concentrations of the two substrates in the gas phase and, consequently, in the reactor-inlet stream by computer-controlled addition of the gaseous substrates. Controlling both substrate concentrations at a high, constant level is suited for measurement of e.g. the operational stability of the biocatalyst (propene and oxygen concentrations in the biocatalyst phase in equilibrium with the reactor-inlet stream: 160 and 245  $\mu\text{M}$ , respectively). Level control of propene only (propene concentration in the biocatalyst phase in equilibrium with the reactor-inlet stream: 160  $\mu\text{M}$ ), and thus allowing the oxygen level to drop, is used for examination of the effects of various oxygen reactor-inlet concentrations on the volumetric oxygen-consumption rate and on the degree of oxygen conversion under pseudo-one-substrate conditions (initial total amount of oxygen 0.8 to 2.5 mmol, dependent on the volume of the gas phase).

## Theoretical

The classical approach of chemical reaction engineering to formulate the reactor design equations is the combination of microkinetics and macrokinetics. Microkinetics involve the (bio)chemical and physical kinetics at the scale of the particles, while macrokinetics concern the transport of e.g. mass at the scale of the (bio)reactor. This procedure will be followed below. Furthermore, it will be assumed that oxygen is the limiting substrate due to the high solubility of propene in an organic solvent (relative to oxygen) [11] and due to the high concentrations of propene employed in the measurements. The epoxidation rate of propene is dependent on oxygen concentrations [42], thus a main design criteria is the prevention of axial depletion of oxygen. The total oxygen consumption of the immobilized cells is the sum of oxygen consumption due to epoxidation and endogenous respiration [42]. The cell respiration was found to obey Michaelis-Menten kinetics and, furthermore, to be the main constituent of the overall consumption of oxygen. Even in the presence of propene, Michaelis-Menten kinetics could be used to describe the overall oxygen-consumption rate [41, 42]. Therefore, the immobilized-cell reactor was treated essentially as an immobilized-enzyme reactor [2].

### Microkinetics

The main, microkinetic transport processes that could restrict the intrinsic oxygen-consumption of the gel-entrapped cells in the packed-bed reactor are transfer of oxygen through organic and/or aqueous films around the biocatalyst particles and, subsequently, coupled diffusion and reaction in the solid gel [45]. Transport of the formed propene oxide out of the biocatalyst and into the bulk liquid will not be considered here in view of the low, experimental epoxide concentrations applied. The theoretical oxygen-concentration profiles are dependent on the type of bulk liquid: aqueous or organic (figure 2). In case of an organic solvent as the continuous phase, an additional mass-transfer limitation in an aqueous film (between the hydrophobic solvent film and the hydrophilic gel particle) may arise (figure 2b). As this water film is not in contact with a (turbulent) aqueous bulk phase, it will be referred to as 'stagnant' in this work. The aqueous and organic film associated with the aqueous and organic bulk phase, figure 2a and 2b respectively, will be referred to as 'laminar'. The possibility of aqueous films around free cells or insoluble biocatalysts in organic media has already been suggested (without experimental prove) by Yamané et al. [46] and by Lilly and Woodley [10], respectively. It is assumed in figure 2, that no partitioning between the uncharged substrate in the aqueous film and in the gel phase occurs.

The above mentioned external and internal mass-transfer limitations are usually expressed in terms of an overall effectiveness of the biocatalyst,  $\eta$ . Thus, in case of Michaelis-Menten kinetics with intrinsic parameters  $V_M$  and  $K_M$ , the observed oxygen-consumption rate,  $v_o$ , can be written as:

$$v_o = \eta (S^*) \cdot V_M \cdot (S^*/P) / (K_M + S^*/P) \quad (1)$$

with  $S^*$  the oxygen concentration in the bulk liquid (aqueous or organic) and  $P$  the partition coefficient of oxygen between the organic solvent and water ( $P = S_{\text{SOLVENT}}/S_{\text{WATER}}$ ;  $P$  mostly  $> 1$  [11]; if the bulk liquid is an aqueous solution, the value of  $P$  must be set equal to unity). The substrate-dependent overall effectiveness factor,  $\eta (S^*)$ , can be obtained from the solution of the following, steady-state, differential mass balance, describing coupled pore diffusion and reaction within the spherical biocatalyst particle:

$$D_e \left( \frac{d^2S}{dr^2} + \frac{2dS}{r dr} \right) = \frac{X V_M S}{K_M + S} \quad (2)$$

with the boundary conditions:

$$D_e dS/dr = k_o (S^*/P - S_s) \quad \text{at } r = 0.5 dr \quad (3)$$

$$dS/dr = 0 \quad \text{at } r = 0 \quad (4)$$

and the overall external mass-transfer coefficient  $k_o$ :

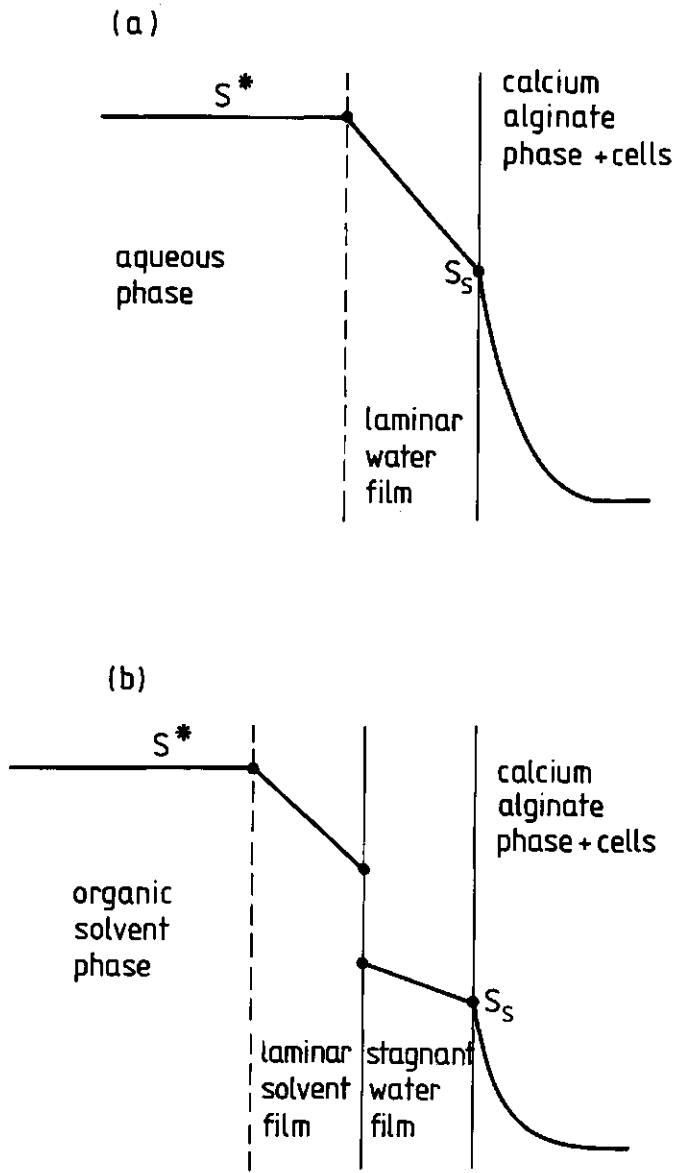


Fig. 2. Theoretical oxygen-concentration profiles in the packed-bed immobilized-cell reactor; a: aqueous bulk liquid, b: organic bulk liquid.



$$k_o = k_{L, w} \quad (\text{aqueous bulk liquid}) \quad (5)$$

$$k_o = (1/(P_{kL, s}) + 1/k_w)^{-1} \quad (\text{organic bulk liquid}) \quad (6)$$

( $D_e$  is the concentration-independent, effective diffusion coefficient of oxygen in calcium alginate;  $r$  the radial distance from the centre of the particle;  $X$  the homogeneous cell density;  $S_s$  the oxygen concentration at the gel surface;  $d_p$  the particle diameter;  $k_{L, w}$  and  $k_{L, s}$  the liquid/solid mass-transfer coefficients in the laminar water and solvent film, respectively;  $k_w$  the mass-transfer coefficient in the stagnant water film)

In previous studies [41, 42] the diffusivity at 30°C of oxygen in water ( $\sim 2.4 \times 10^{-9} \text{ m}^2 \text{ s}^{-1}$  [47]) was successfully used as the effective diffusion coefficient of oxygen,  $D_e$ , in the calcium alginate beads. The mass-transfer coefficients,  $k_{L, w}$  and  $k_{L, s}$ , can be estimated from the Chilton-Colburn mass-transfer factor,  $J_D$  [48]. Rovito and Kittrell [32] and Traher and Kittrell [50] demonstrated that the McCune-Wilhelm  $J_D$ -correlation is a reliable prediction method for film diffusion in tubular immobilized-enzyme reactors. The experimental data of McCune and Wilhelm [51] have also been considered in an extensive review of experimental data on particle-fluid mass transfer in fixed and fluidized beds [49], in which the following equation for  $J_D$  was recommended:

$$\epsilon J_D = 0.765/Re^{0.82} + 0.365/Re^{0.386} \quad (7)$$

with:

$$J_D = (k_L/U) Sc^{2/3} \quad (8)$$

$$Re = \rho U d_p / \mu \quad (9)$$

$$Sc = \mu / (\rho D) \quad (10)$$

( $\epsilon$  is the void fraction of the biocatalyst bed;  $U$  the superficial fluid velocity;  $k_L$  the liquid/solid mass-transfer coefficient in the laminar film;  $\rho$  and  $\mu$  the density and dynamic viscosity of the fluid, respectively;  $D$  the oxygen diffusion coefficient in the laminar fluid film)

Equation 7 can be applied to estimate  $k_L$  in case of an aqueous as well as an organic bulk liquid. This relation was utilized successfully by Tsukamoto et al. [36] to predict external mass-transfer rates in a two-phase fixed-bed immobilized-enzyme reactor.

The mass-transfer resistance in the stagnant water film (figure 2b) is not a laminar-film type resistance, thus equation 7 cannot be applied. However, it is likely that molecular diffusion is the main mechanism of mass transfer in this stagnant water film, hence  $k_w$  can be related to the oxygen diffusion coefficient in water,  $D$ , and the diffusion layer thickness,  $\delta$ , as follows:

$$k_w \sim D / \delta \quad (11)$$

or in dimensionless form:

$$Sh_w = k_w d_p / D \sim d_p / \delta \quad (12)$$

with  $Sh_w$  the Sherwood number relevant to the stagnant water film. As it is difficult to quantify the water-film thickness, experiments have been performed to determine whether this mass-transfer resistance has a significant effect on the overall oxygen-consumption rate (i.e.:  $Sh_w < \sim 20$  [52]).

Solution of the differential mass balance (equation 2) with the boundary conditions of equations 3 and 4 would yield the oxygen-concentration profile in the biocatalyst bead, and from this the overall, stationary effectiveness factor,  $\eta$  [41]. As equation 2 cannot be solved analytically, the three-point collocation method [53–55] has been successfully employed to obtain approximative solutions. The effectiveness of the biocatalyst,  $\eta$ , can then be predicted as a function of the bulk concentration,  $S^*$ , if values for  $V_M$ ,  $K_M$ ,  $X$ ,  $d_p$ ,  $D_e$ ,  $P$  (aqueous bulk liquid:  $P = 1$ ),  $\epsilon$ ,  $Re$  (aqueous or organic bulk liquid),  $Sc$  (aqueous or organic bulk liquid) and  $Sh_w$  (organic bulk liquid) are available.

#### *Macrokinetics and integral bioreactor model*

Plug flow (PF) is an obvious postulation for the hydrodynamics of a packed-bed bioreactor. This assumption was made in various experimental studies on immobilized enzymes or cells in tubular reactors [20–22, 25–32, 34–38]. Recently, Ching and Ho [23] concluded that the axial-dispersed plug-flow model was superior to the two extreme models in contacting patterns, complete back-mix and plug flow, in predicting the performance of the investigated packed and fluidized-bed immobilized-enzyme reactors. This observation can be explained by the use of the additional model parameter (the dispersion number). However, the differences between the plug-flow model and the dispersion model (with the experimentally determined dispersion number) were found only limited in case of the packed-bed reactor due to the small degree of liquid dispersion in this reactor configuration.

A criterion for negligible axial dispersion in a packed-bed reactor was given by Mears [56]:

$$L / d_p > (20 n / Bo_p) \ln (S_i^* / S_o^*) \quad (13)$$

( $L$  is the bed length;  $n$  the order of the reaction (power-law kinetics);  $Bo_p$  the Bodenstein number based on particle diameter ( $Bo_p = Ud_p/D_A$  with  $D_A$  the axial-dispersion coefficient);  $S_i^*$  and  $S_o^*$  the substrate concentrations in the inlet and outlet of the reactor, respectively)

When this criterion is applied to the present system of investigation (merely glass beads:  $d_p \sim 1$  mm, Michaelis-Menten kinetics:  $0 < n < 1$ ), and using a very low value for  $Bo_p$  ( $\sim 0.3$  [57, 58]) and a high conversion (99%), it follows that the length of the diluted biocatalyst bed,  $L$ , should be larger than  $\sim 0.3$  m to avoid significant dispersion effects (actual length 0.36 m).

In view of the above stated, the plug-flow model is applied to predict the performance of the packed-bed immobilized-cell reactor used in this study. Hence, assuming steady-state conditions, the oxygen concentration in the bulk liquid,  $S^*$ , is given by the following material balance:

$$UdS^*/dz + \epsilon_a \cdot \eta_c \cdot \eta(S^*) \cdot X \cdot V_M \cdot (S^*/P)/(K_M + S^*/P) = 0 \quad (14)$$

with the boundary condition:

$$S^* = S_i^* \quad \text{at } z = 0 \quad (15)$$

and with  $z$  the axial distance from the bottom of the biocatalyst bed,  $\epsilon_a$  the volume fraction of calcium alginate beads and  $\eta_c$  the liquid/solid contacting efficiency. Radial dispersion effects can usually be neglected in case of a reaction with low heat generation carried out in an isothermal plug-flow reactor [2]. Wall effects are also not expected in view of the high reactor diameter/particle diameter ratio ( $\sim 30$ ) [56]. Furthermore, the contacting efficiency,  $\eta_c$ , is assumed to approach unity considering the low alginate volume fraction,  $\epsilon_a$  ( $\sim 0.05$ ). As mentioned earlier, the biocatalyst effectiveness factor,  $\eta$ , can be calculated at any given bulk concentration,  $S^*$ . To facilitate the computational efforts, a third-order polynomial function was used to express  $\eta$  explicitly as a function of  $S^*$  [1]:

$$\eta(S^*) = b_0 + b_1 S^* + b_2 S^{*2} + b_3 S^{*3} \quad (16)$$

The parameters in this function,  $b_0$ ,  $b_1$ ,  $b_2$  and  $b_3$ , are obtained by fitting equation 16 to about 20 calculated  $\eta$ ,  $S^*$ -data pairs ( $0 < S^*/P < 245 \mu\text{M}$ ). The third-order polynomial gave a satisfactory fit of the calculated data. The resulting values are valid for only one set of the following parameters:  $V_M$ ,  $K_M$ ,  $X$ ,  $d_P$ ,  $D_e$ ,  $P$ ,  $\epsilon$ ,  $Re$ ,  $Sc$  and  $Sh_w$ . Equations 14 and 16 can now be integrated numerically (Runge-Kutta) for different values of the oxygen concentration in the reactor inlet,  $S_i^*$ , and reactor space time,  $\tau = \epsilon L/U$ . This gives the concentration profile in the bulk liquid,  $S^*(z)$  ( $S_o^* = S^*(z = L)$ ), the oxygen conversion,  $\xi = (S_i^* - S_o^*)/S_i^*$ , and the volumetric oxygen-consumption rate  $v_R = S_i^* \xi \epsilon / \tau$ .

For comparison, the continuous stirred-tank reactor (CSTR) model would yield the following oxygen balance:

$$(S_i^* - S_o^*)/\tau - (\epsilon_a/\epsilon) \cdot \eta(S_o^*) \cdot X \cdot V_M \cdot (S_o^*/P)/(K_M + S_o^*/P) = 0 \quad (17)$$

The oxygen concentration in the outlet of this bioreactor can be predicted by solving equations 16 and 17 for  $S_o^*$ .

## Results and discussion

### *Organic solvent*

The organic reaction medium should meet many requirements. In this work *n*-hexadecane is used as the substrate reservoir. This solvent does not give rise to a significant decrease in immobilized-cell activity [11], and has a high selectivity for propene oxide, a high normal boiling point (287°C), a limited flammability and a low toxicity. In addition, its viscosity is not very high ( $\mu \sim 3.1 \times 10^{-3} \text{ N s m}^{-2}$  [59, 60], 30°C), and it has a large capacity (as most organic solvents have) for propene compared to that of water. The capacity for oxygen is relatively small [11] ( $P \sim 5$ ; estimated from the solubilities of oxygen in water and in *n*-hexadecane [61, 62]). It was experimentally observed, that *n*-hexadecane did not alter the intrinsic Michaelis-Menten constant,  $K_M$ , of the overall oxygen consumption by the immobilized cells ( $K_M \sim 15 \mu\text{M}$  [41]). Other relevant properties of *n*-hexadecane, necessary for modelling the bioreactor performance, are the density (773.3  $\text{kg m}^{-3}$ ) and the diffusivity of oxygen in this solvent ( $\sim 1.6 \times 10^{-9} \text{ m}^2 \text{ s}^{-1}$  [63], 30°C).

### *Bed dilution*

When dilution of the immobilized-biocatalyst bed with small glass beads was not employed, the use of an organic solvent as substrate reservoir resulted in considerably lower volumetric oxygen and propene-consumption rates as compared to those of packed beds operated with an aqueous reaction medium (in the latter case:  $\eta \sim 1$  and  $\xi \sim 0$ , thus diffusion effects and substrate depletion do not affect the reaction rate). Furthermore, substantial bed compression and increasing pressure drops were observed. The differences in consumption rates did not occur (also with  $\eta \sim 1$  and  $\xi \sim 0$ ), and less flow resistance was produced, when the bed was highly diluted with glass beads ( $\epsilon_a \sim 0.05$ ,  $\epsilon_g \sim 0.6$ ). Thus, the above mentioned, decreased consumption rates were most probably caused by a low contacting efficiency (e.g. channeling) between the hydrophilic calcium alginate particles and the hydrophobic solvent. The bed dilution will also reduce any disadvantageous axial-dispersion effects [64]. Comparable observations were made by Furui and Yamashita [65], who equipped a packed-bed immobilized-cell reactor with horizontal baffles. This avoided bed compression, reduced pressure drops and decreased liquid mixing. In the present, fundamental study these low alginate fractions ( $\sim 0.05$ ) are used to facilitate the modelling of the experiments. It was observed, however, that higher volume fractions (e.g.  $\epsilon_a \sim 0.3$ ) can be employed without significant problems.

### *Stagnant water film*

The only, unknown parameter in the above described, theoretical bioreactor model is the mass-transfer coefficient in the stagnant water film,  $k_w$  or  $Sh_w$ . This external-diffusion resistance might play a role of importance, if an organic solvent is used as the reaction medium and the biocatalyst effectiveness factor is markedly below unity. Packed-bed experiments were performed with *n*-hexadecane as the oxygen and propene reservoir to determine the magnitude of  $Sh_w$ . The propene and oxygen concentrations were held constant (in *n*-hexadecane;  $\sim 12$  and  $1.2 \text{ mM}$ , respectively; in the biocatalyst (water):  $160$  and  $245 \mu\text{M}$ , respectively). Under these conditions, oxygen can be considered the limiting substrate, as a result of the lower immobilized-cell activity for propene compared to that for oxygen (oxygen consumption is for a main part endogeneous respiration [42]). Also, the substrate conversions were kept insignificant by employing a low space time ( $\tau \sim 40 \text{ s}$ ). Thus,

only microkinetic effects were measured.

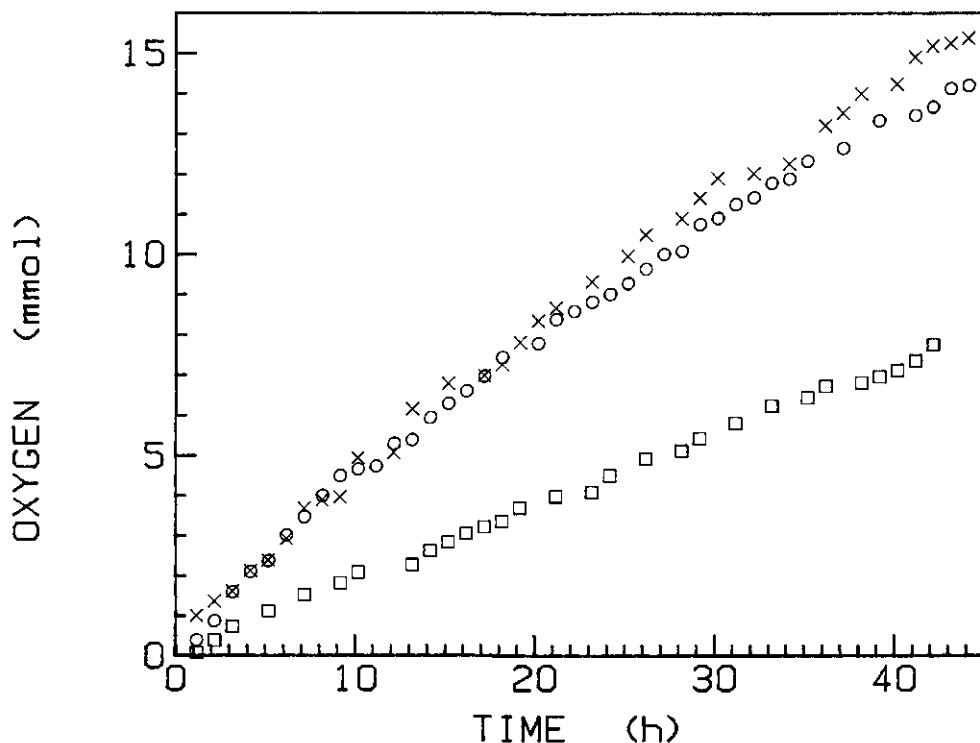


Fig. 3. Cumulative amount of oxygen consumed in a time-course packed-bed experiment with n-hexadecane as the continuous phase showing the microkinetic effect of particle diameter (X ~  $130 \times 10^3$  g dry weight ( $m^3$  particle) $^{-1}$ ,  $\tau \sim 40$  s);  $d_p$  (mm): 0.7 (o,  $S^* = 1.2$  mM), 0.7 (x,  $S^* = 2.1$  mM), 3.3 (□,  $S^* = 1.2$  mM).

As observed before [41], increasing the diameter of the biocatalyst particles from 0.7 to 3.3 mm reduced the (oxygen) effectiveness factor of the catalyst in the packed-bed reactor considerably (figure 3). The effectiveness factor appeared to be about unity when the smaller particles were used, as an increase in the oxygen level did not enhance the oxygen-consumption rate (nor, though not shown in figure 3, the propene-consumption rate). Hence the intrinsic, maximal rate of the immobilized cells,  $V_M$ , as well as the decay of immobilized-cell activity could be derived by fitting a suitable polynomial function to the data in figure 3 ( $d_p \sim 0.7$  mm; 1.2 mM oxygen) and, subsequently, by derivation of the thus calculated polynomial. A fourth-order polynomial gave a sufficiently good fit of the time-course data of figure 3. Assuming values for  $Sh_w$  (10, 20, 100, 1000), the theoretical biocatalyst effectiveness of the larger particles ( $d_p \sim 3.3$  mm) could then be computed using the found range of  $V_M$ -values. These predictions were compared to the corresponding, experimental effectiveness factors, obtained by dividing the oxygen-consumption rates of the large particles (extracted from figure 3 by fitting second-order polynomials to sets of eleven points of measurement) by the diffusion-free rates of

the small particles (figure 4). It follows that  $Sh_w \sim 1000$  (i.e.: negligible resistance in the stagnant water film) gives satisfactory results. Therefore, diffusion limitation in this water film was ignored in the modelling of the combined effects of microkinetics and macrokinetics in the following section.

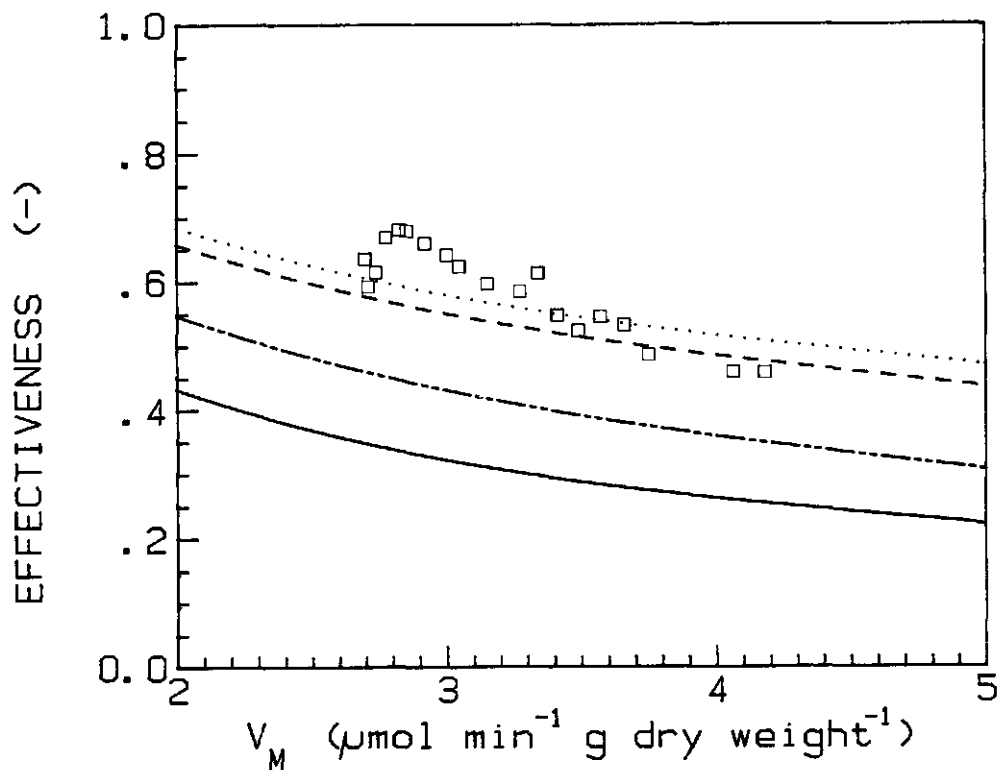


Fig. 4. Comparison between experimental ( $\square$ ) and predicted ( $Sh_w = 10$ : —,  $Sh_w = 20$ : ---,  $Sh_w = 100$ : - · -,  $Sh_w = 1000$ : · · ·) effectiveness factors of the immobilized cells using the time-course data of figure 3.

#### Reactor performance and model validation

The microkinetic and macrokinetic models were combined to predict the performance of the packed-bed immobilized-cell reactor. These theoretical predictions were tested by comparing with experimental, volumetric oxygen-consumption rates and degrees of oxygen conversion using water (0.05 M  $CaCl_2$  solution) or n-hexadecane as the reaction medium. Again, pseudo-one-substrate conditions were applicable (with oxygen as the limiting substrate), since the propene concentration was controlled at a high, constant level. The total amount of unconverted oxygen in the experimental system (mainly present in the gas phase) was allowed to drop with time. This gave the possibility to determine experimentally both the volumetric oxygen-consumption rate,  $v_{R}^{EXP}$ , and the degree of conversion,  $\xi^{EXP}$ , as a function of the oxygen concentration in the reactor-inlet,  $S_i^*$  (in equilibrium with the measured oxygen concentration in the

circulating gas phase; in case of *n*-hexadecane the reactor-inlet concentrations are higher as a result of the higher solubility of oxygen in this solvent). The volumetric consumption rate was extracted from the measured time-course data (mmol oxygen as a function of time) employing a fitting technique described before [41] (fitting second-order polynomial functions to sets of five or seven points of measurement). The experimental oxygen conversion is then computed as follows:

$$\xi^{\text{EXP}} = v_{\text{R}}^{\text{EXP}} \tau / (\varepsilon S_{\text{i}}^*) \quad (18)$$

The relative error in the oxygen conversion,  $\Delta\xi/\xi$ , is the sum of the estimated, relative errors in  $v_{\text{R}}^{\text{EXP}}$ ,  $\tau$  and  $S_{\text{i}}^*$  ( $\Delta v_{\text{R}}^{\text{EXP}} \sim 2.8 \times 10^{-6} \text{ mol s}^{-1} (\text{m}^3 \text{ reactor})^{-1}$ ,  $\Delta\tau \sim 1.3 \times 10^{-5} \text{ s}$  and  $\Delta S_{\text{i}}^* \sim 1.5 \times P \text{ } \mu\text{M}$ ).

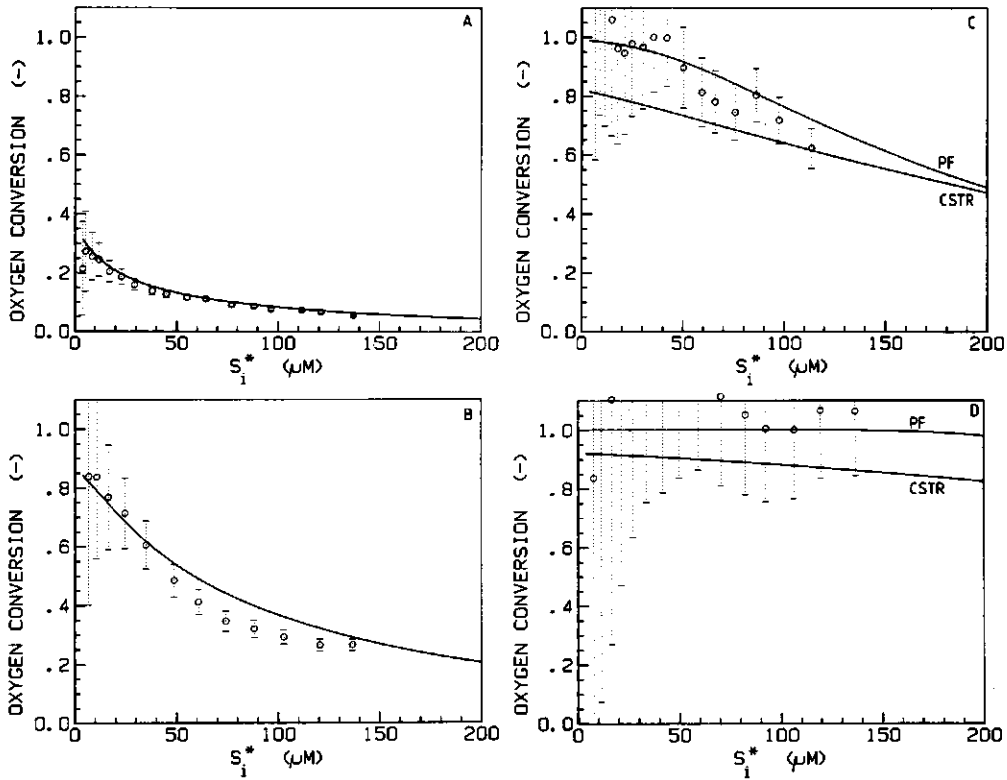
The packed-bed experiments (aqueous or organic substrate reservoir) were carried out with two different values for the diameter of the biocatalyst particles (1.0 and 2.8 mm, both with a standard deviation of 0.1 mm) and three or four different reactor space times (table 1).

Table 1. Reaction conditions (reaction medium, particle diameter, reactor space time) of the packed-bed experiments.

reaction medium	$d_{\text{p}}$ (mm)	$\tau$ (s)	figure number
water	1.0	40	5a
		200	5b
		460	5c
		1290	5d
	2.8	40	6a, 7a
		220	6b, 7b
		510	6c, 7c
		1440	6d, 7d
organic solvent	1.0	40	8a
		200	8b
		430	8c
	2.8	40	9a
		220	9b
		960	9c

Microkinetic effects are not pronounced in case of the smaller particles, while both microkinetics and macrokinetics play a role when the cells are immobilized in the larger particles. The immobilized-cell density,  $X$ , was always  $\sim 70 \times 10^3 \text{ g dry weight } (\text{m}^3 \text{ particle})^{-1}$ . The intrinsic, maximal rates,  $V_{\text{M}}$ , of the immobilized cells used in the experiments of table 1 vary between  $1.4$  and  $2.6 \text{ } \mu\text{mol min}^{-1} (\text{g dry weight})^{-1}$  as a

result of a decay in immobilized-cell activity. Therefore, some care must be taken when comparing the experiments mutually. The decrease in  $V_M$  during one experiment, however, does not significantly influence the results (error in estimated  $V_M < 4\%$ ).



**Fig. 5.** Experimental (o) and predicted (solid lines) oxygen conversions,  $\xi$ , in the packed-bed immobilized-cell reactor versus the oxygen concentration in the reactor inlet,  $S_i^*$ , using an aqueous solution as the substrate reservoir ( $d_p = 1.0$  mm);  $\tau$  (s): 40 (A), 200 (B), 460 (C), 1290 (D); dotted lines: estimated errors in experimental oxygen conversions.

With water as the reaction medium, axial depletion of oxygen, i.e. oxygen conversions approaching unity, is a serious problem, especially if long space times and low oxygen concentrations in the reactor-inlet stream are employed (figure 5). This is somewhat less critical when the apparent biocatalyst activity is reduced by using larger particles ( $d_p \sim 2.8$  mm; figure 6). A good agreement is seen between theory (equations 14 to 16) and experiment at all values of particle diameter, space time and reactor-inlet concentration. The theoretically predicted oxygen conversions are mostly within the experimental errors of the observed oxygen conversions.

The calculated and experimental results can also be presented as the dimensionless, volumetric oxygen-consumption rate,  $v_R/V_{M,R}$ , plotted as a function of the reactor-inlet concentration to show the relative influence of microkinetics and



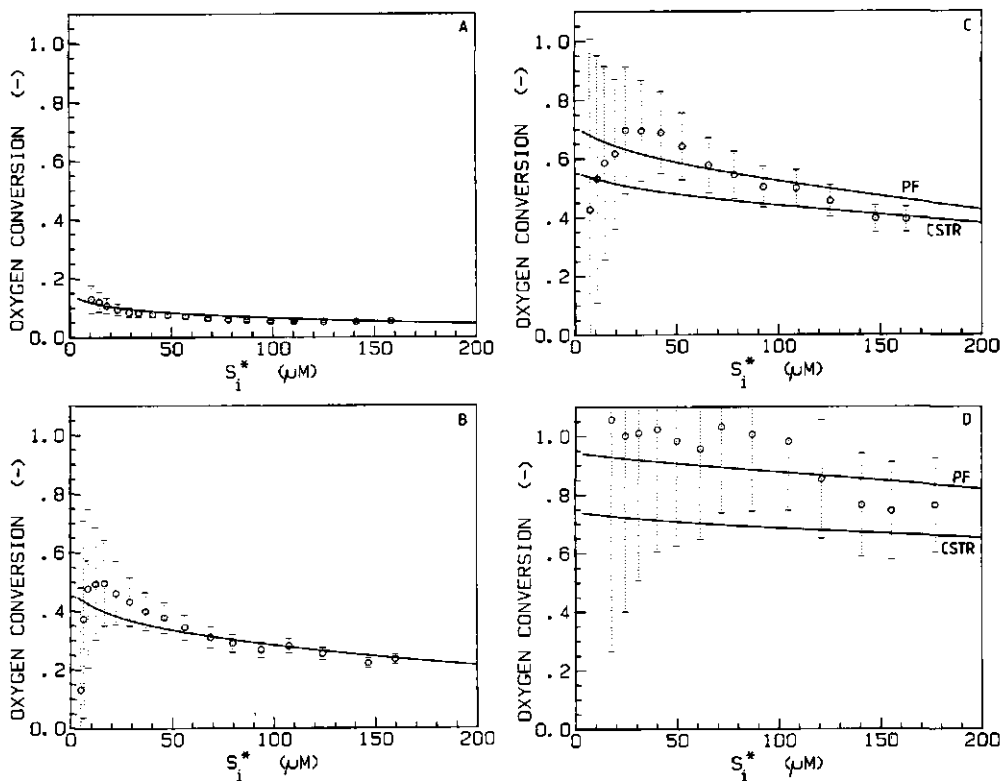


**Fig. 6.** Experimental (o) and predicted (solid lines) oxygen conversions,  $\xi$ , in the packed-bed immobilized-cell reactor versus the oxygen concentration in the reactor inlet,  $S_1^*$ , using an aqueous solution as the substrate reservoir ( $d_p = 2.8$  mm);  $\tau$  (s): 40 (A), 220 (B), 510 (C), 1440 (D); dotted lines: estimated errors in experimental oxygen conversions.

macrokinetics in case of large particles (figure 7). External and, especially, internal-diffusion limitation restricts the consumption rate at all oxygen levels in the reactor-inlet stream (external effectiveness factor mostly larger than 0.7). As demonstrated before [41], the various assumptions in the microkinetic model (mass transfer in laminar (water) film (equation 7), effective diffusion coefficient, Michaelis-Menten kinetics and  $K_M$ -value) seem to be reasonable. Macrokinetics become significant when the longer reactor space times are used (figure 7c and 7d). As was to be expected [23, 28], the plug-flow model (PF) gives a more adequate description of the hydrodynamics of the packed-bed immobilized-cell reactor than the CSTR model (figures 5c, 5d, 6c and 6d). However, the differences between these two models are small at low conversions, see for instance figure 5c and 6c.

The use of *n*-hexadecane as substrate carrier prevents depletion of oxygen along the length of the column even at the longer reactor space times and the lower reactor-inlet concentrations (figure 8 and 9;  $d_p \sim 1.0$  and 2.8 mm, respectively). Even though the absolute amount converted is higher, the observed degrees of oxygen conversion are all markedly lower than the corresponding oxygen

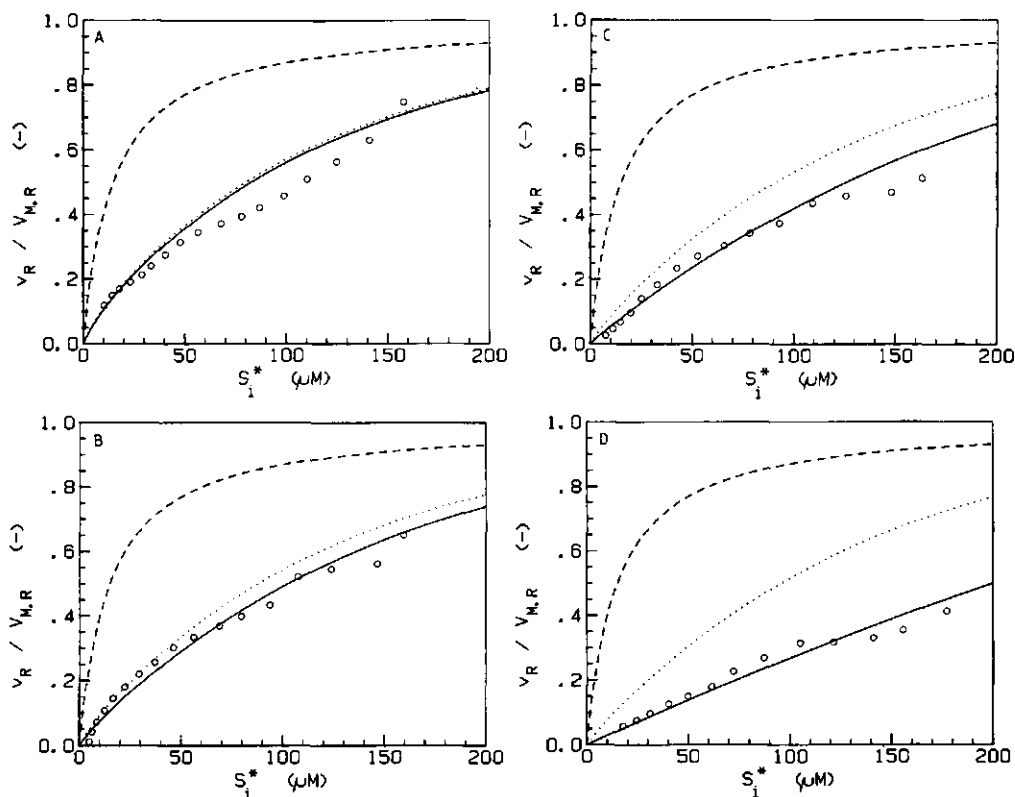


**Fig. 7.** Experimental (o) and predicted (solid lines), dimensionless, volumetric oxygen-consumption rates,  $v_R/V_{M,R}$ , in the packed-bed immobilized-cell reactor versus the oxygen concentration in the reactor inlet,  $S_1^*$ , using an aqueous solution as the substrate reservoir ( $d_p = 2.8$  mm);  $\tau$  (s): 40 (A), 220 (B), 510 (C), 1440 (D); (—): intrinsic kinetics, (....): intrinsic kinetics and microkinetics.

conversions obtained with water as the reaction medium (figure 5 and 6), which is the result of the higher inlet concentrations. For example, with a space time of 200 s, the conversions are between  $\sim 0.3$  and  $\sim 0.8$  in case of an aqueous oxygen reservoir (figure 5b), whereas values between  $\sim 0.1$  and  $\sim 0.4$  are measured when *n*-hexadecane is used to supply the oxygen to the biocatalyst particles (figure 8b). Also, with large particles and a space time of  $\sim 220$  s, the conversion ranges in case of water and *n*-hexadecane are  $\sim 0.25 < \xi < \sim 0.45$  (figure 6b) and  $\sim 0.05 < \xi < \sim 0.1$  (figure 9b), respectively. The lower oxygen conversions in case of an organic solvent as the transport medium are very beneficial. Higher oxygen concentrations will increase the propene-consumption rate and the epoxide-production rate markedly [42]. The agreement between predicted and measured conversions is satisfactory if a small particle size is used and diffusion limitation is not important (figure 8). However, the theoretical conversions are always somewhat higher than the observations in case of the experiments with effectiveness factors much lower than unity (figure 9). This might be explained by irregularities in the contact between the hydrophobic solvent and the hydrophilic gel. These effects would

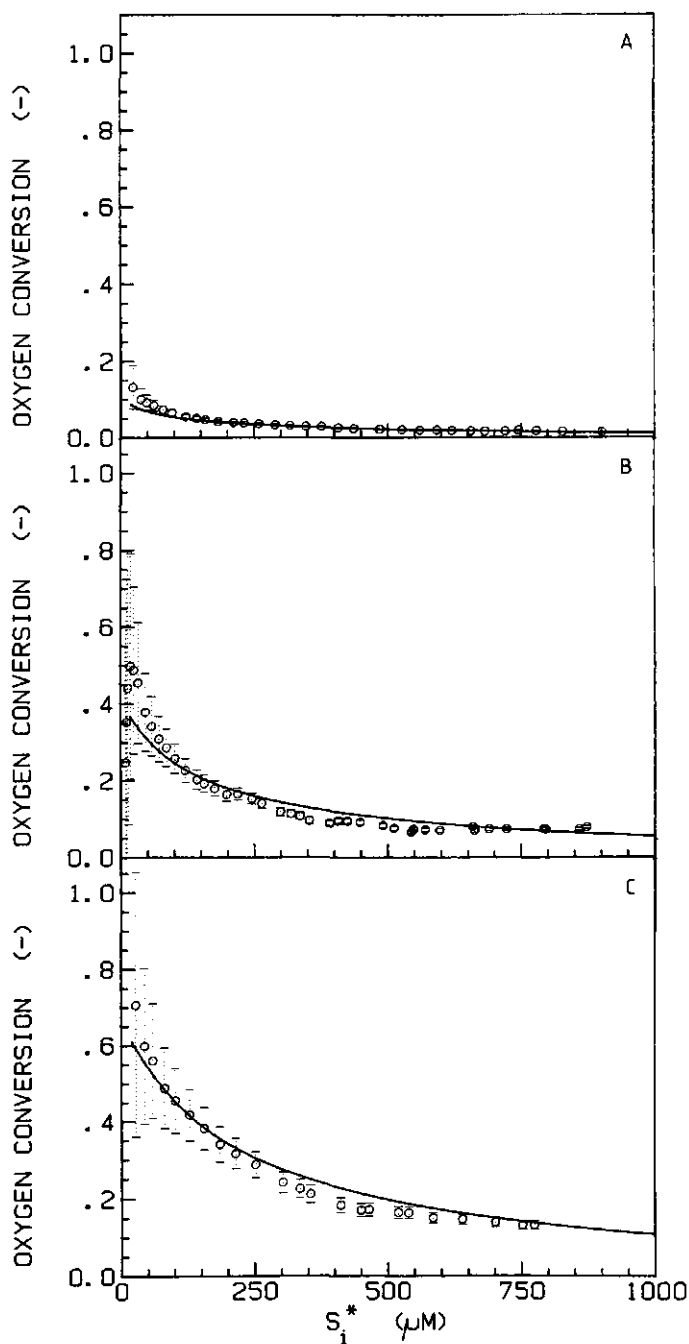


**Fig. 8.** Experimental (o) and predicted (solid lines) oxygen conversions,  $\xi$ , in the packed-bed immobilized-cell reactor versus the oxygen concentration in the reactor inlet,  $S_i^*$ , using n-hexadecane as the substrate reservoir ( $d_r = 1.0$  mm);  $\tau$  (s): 40 (A), 200 (B), 430 (C); dotted lines; estimated errors in experimental oxygen conversions.

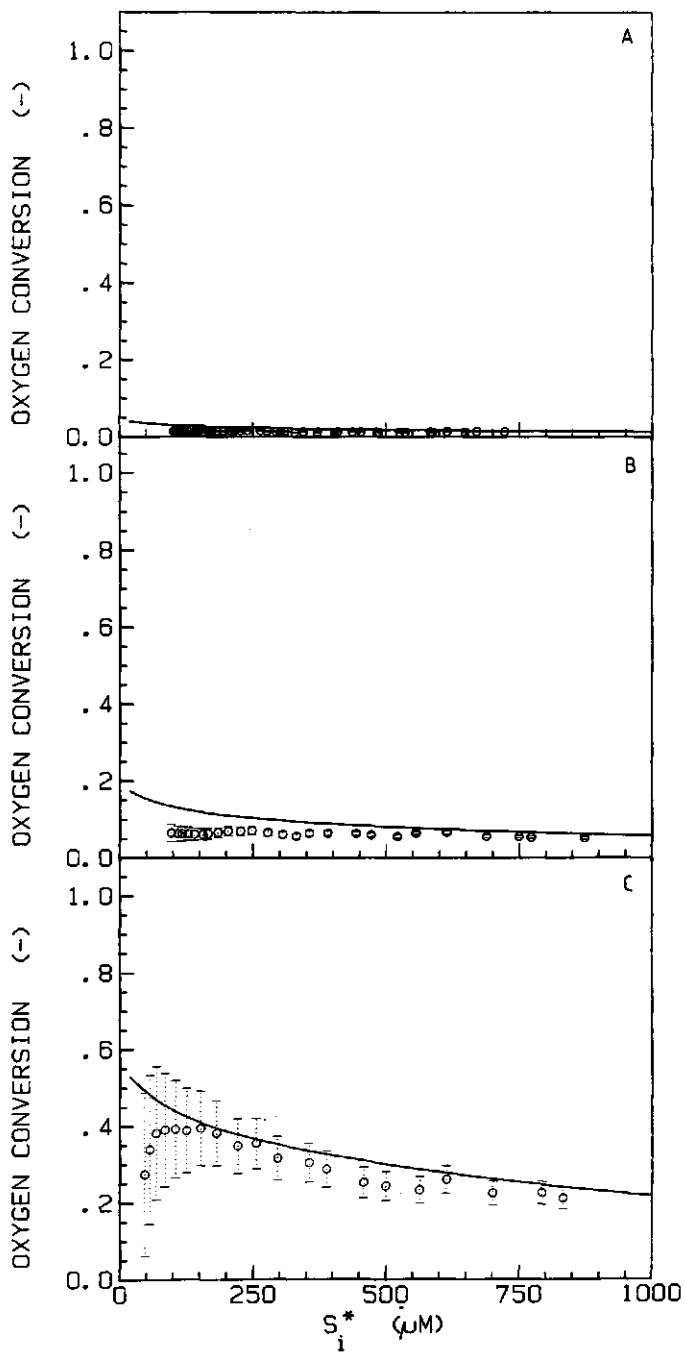


Fig. 9. Experimental (o) and predicted (solid lines) oxygen conversions,  $\xi$ , in the packed-bed immobilized-cell reactor versus the oxygen concentration in the reactor inlet,  $S_i^*$ , using n-hexadecane as the substrate reservoir ( $d_F = 2.8$  mm);  $\tau$  (s): 40 (A), 220 (B), 960 (C); dotted lines: estimated errors in experimental oxygen conversions.

decrease the organic liquid/gel contacting efficiency,  $\eta_c$ , and/or the biocatalyst effectiveness factor,  $\eta$ . A similar, disadvantageous effect in a packed-bed immobilized-enzyme reactor (aqueous reaction medium) was reported by O'Neill et al. [19]. The observed differences between theory and experiment could also be explained by a significant influence of the stagnant water film on the biocatalyst effectiveness. As mentioned above, the diffusion limitation in this water film was neglected ( $Sh_w \gg 20$ ) in the modelling of the microkinetics. Low flow rates of the solvent (high space times), however, might have induced thick, stagnant water films around the biocatalyst particles and, thus, caused increased diffusion resistances.

The advantages of employing an organic substrate reservoir in the present system of investigation might be even more pronounced when axial depletion of propene would also occur. Further, higher volumetric oxygen-consumption rates could be attained by using an organic solvent with an increased capacity for oxygen. However, the choice of a solvent is limited, as many solvents were found to inactivate the gel-entrapped cells [11]. Completely fluorinated hydrocarbons, with their inert properties and their high capacity for oxygen, would provide an attractive but expensive alternative for n-hexadecane.

## Conclusions

The epoxidation of propene by *Mycobacterium* cells entrapped in calcium alginate was used to investigate the potential of an organic-liquid-phase/immobilized-cell reactor. The two-phase fixed-bed reactor, rather than the slurry reactor, proved to be convenient for contacting the hydrophilic alginate particles with the hydrophobic solvent, though dilution of the packed bed with inert particles turned out to be necessary to achieve a high liquid/solid contacting efficiency. Microkinetic and macrokinetic mass-transfer effects on the overall oxygen-consumption rate in the packed-bed bioreactor could be reliably predicted using common chemical-engineering principles. External diffusion of oxygen through a 'stagnant' water film (between the hydrophobic solvent and the hydrophilic gel particle) appeared not to be a rate-limiting step. The high solubility of the two gaseous substrates, oxygen and propene, in the organic solvent used, n-hexadecane, prevented axial depletion of the substrates and eliminated the need for a separate gas phase in the reactor. The latter will simplify the design and scale-up of the organic-liquid-phase/immobilized-cell packed-bed reactor considerably.

## Acknowledgements

The authors wish to thank Prof. Ir. K.Ch.A.M. Luyben and Prof. Dr. Ir. K. van 't Riet for helpful discussions. These investigations were supported (in part) by the Netherlands Technology Foundation (STW).

## Nomenclature

$b_0, b_1, b_2, b_3$	kinetic parameters in equation 16
$Bo_p$	Bodenstein number based on particle diameter (-)
$D$	oxygen diffusion coefficient in the laminar fluid film ( $m^2 s^{-1}$ )
$DA$	axial-dispersion coefficient ( $m^2 s^{-1}$ )
$D_e$	effective diffusion coefficient of oxygen in calcium alginate ( $m^2 s^{-1}$ )
$d_p$	particle diameter (m)
$J_D$	Chilton-Colburn mass-transfer factor (-)
$k_L$	liquid/solid mass-transfer coefficient in the laminar fluid film ( $m s^{-1}$ )
$k_{L,S}$	liquid/solid mass-transfer coefficient in the laminar solvent film ( $m s^{-1}$ )
$k_{L,W}$	liquid/solid mass-transfer coefficient in the laminar water film ( $m s^{-1}$ )
$k_w$	mass-transfer coefficient in the stagnant water film ( $m s^{-1}$ )
$ko$	overall external mass-transfer coefficient ( $m s^{-1}$ )
$K_M$	Michaelis-Menten constant of the overall oxygen consumption ( $mol m^{-3}$ )
$L$	length of the diluted biocatalyst bed (m)
$n$	reaction order (-)
$P$	partition coefficient of oxygen between the organic solvent and water (-)
$r$	radial distance from the centre of the particle (m)
$Re$	Reynolds number (-)
$S$	oxygen concentration ( $mol m^{-3}$ )
$S_s$	oxygen concentration at the gel surface ( $mol m^{-3}$ )
$S^*$	oxygen concentration in the bulk liquid ( $mol m^{-3}$ )
$S_i^*$	oxygen concentration in the inlet of the reactor ( $mol m^{-3}$ )
$S_o^*$	oxygen concentration in the outlet of the reactor ( $mol m^{-3}$ )
$Sc$	Schmidt number (-)
$Sh_w$	Sherwood number relevant to the stagnant water film (-)
$U$	superficial fluid velocity ( $m s^{-1}$ )
$VO$	observed oxygen-consumption rate ( $\mu mol min^{-1} (g \text{ dry weight})^{-1}$ )
$V_M$	maximal oxygen-consumption rate ( $\mu mol min^{-1} (g \text{ dry weight})^{-1}$ )
$V_{M,R}$	volumetric, maximal oxygen-consumption rate ( $mol s^{-1} (m^3 \text{ reactor})^{-1}$ )
$VR$	volumetric oxygen-consumption rate ( $mol s^{-1} (m^3 \text{ reactor})^{-1}$ )
$VR^{EXP}$	experimental, volumetric oxygen-consumption rate ( $mol s^{-1} (m^3 \text{ reactor})^{-1}$ )
$X$	cell density ( $g \text{ dry weight} (m^3 \text{ particle})^{-1}$ )
$z$	axial distance from the bottom of the biocatalyst bed (m)
$\delta$	thickness of the stagnant water film (m)
$\Delta$	error sign
$\epsilon$	void fraction of the biocatalyst bed or volume fraction of liquid in CSTR (-)
$\epsilon_a$	volume fraction of calcium alginate beads (-)
$\epsilon_g$	volume fraction of glass beads (-)
$\eta$	overall effectiveness factor of the biocatalyst (-)
$\eta_c$	liquid/solid contacting efficiency (-)
$\mu$	dynamic viscosity of the fluid ( $N s m^{-2}$ )
$\xi$	oxygen conversion (-)
$\xi^{EXP}$	experimental oxygen conversion (-)
$\rho$	density of the fluid ( $kg m^{-3}$ )
$\tau$	reactor space time (s)

## References

1. Vieth, W.R.; Venkatasubramanian, K.; Constantinides, A.; Davidson, B. In: *Applied Biochemistry and Bioengineering* Vol. 1 (Wingard, L.B.; Katchalski-Katzir, E.; Goldstein, L., Eds), Academic Press, New York, 1976, p. 211.
2. Venkatasubramanian, K.; Karkare, S.B.; Vieth, W.R. In: *Applied Biochemistry and Bioengineering* Vol. 4 (Wingard, L.B.; Katchalski-Katzir, E.; Goldstein, L., Eds), Academic Press, New York, 1983, p. 311.
3. Radovich, J.M. *Enzyme Microb. Technol.* 1985, **7**, 2.
4. Karel, S.F.; Libicki, S.B.; Robertson, C.R. *Chem. Eng. Sci.* 1985, **40**, 1321.
5. Kleinstreuer, C.; Poweigha, T. *Adv. Biochem. Eng.* 1984, **30**, 91.
6. Antonini, E.; Carrea, G.; Cremonesi, P. *Enzyme. Microb. Technol.* 1981, **3**, 291
7. Carrea, G. *Trends in Biotechnol.* 1984, **2**, 102.
8. Lilly, M.D. *J. Chem. Tech. Biotechnol.* 1982, **32**, 162.
9. Lilly, M.D. *Phil. Trans. R. Soc. Lond.* 1983, **B300**, 391.
10. Lilly, M.D.; Woodley, J.M. In: *Biocatalysts in Organic Syntheses* (Tramper, J.; van der Plas, H.C.; Linko, P., Eds), Elsevier, Amsterdam, 1985, p. 179.
11. Brink, L.E.S.; Tramper, J. *Biotechnol. Bioeng.* 1985, **27**, 1258.
12. Klein, J.; Wagner, F. In: *Applied Biochemistry and Bioengineering* Vol. 4 (Wingard, L.B.; Katchalski-Katzir, E.; Goldstein, L., Eds), Academic Press, New York, 1983, p. 11.
13. Tramper, J. *Trends in Biotechnol.* 1985, **3**, 45.
14. Hulst, A.C.; Tramper, J.; van 't Riet, K.; Westerbeek, J.M.M. *Biotechnol. Bioeng.* 1985, **27**, 870.
15. Ter Meulen, B.P.; Annokke, G.J. *Eur. Patent* No. 68594 (1983).
16. Bell, G.; Todd, J.R.; Blain, J.A.; Patterson, J.D.E.; Shaw, C.E.L. *Biotechnol. Bioeng.* 1981, **23**, 1703.
17. Macrae, A.R. *J. Amer. Oil Chem. Soc.* 1983, **60**, 291.
18. Macrae, A.R. In: *Biocatalysts in Organic Syntheses* (Tramper, J.; van der Plas, H.C.; Linko, P., Eds), Elsevier, Amsterdam, 1985, p. 195.
19. O'Neill, S.P.; Dunnill, P.; Lilly, M.D. *Biotechnol. Bioeng.* 1971, **13**, 337.
20. Saini, R.; Vieth, W.R. *J. Appl. Chem. Biotechnol.* 1975, **25**, 115.
21. Choi, C.Y.; Perlmutter, D.D. *AIChE J.* 1977, **23**, 319.
22. Cho, G.H.; Choi, C.Y.; Choi, Y.D.; Han, M.H. *J. Chem. Techn. Biotechnol.* 1982, **32**, 959.
23. Ching, C.B.; Ho, Y.Y. *Appl. Microbiol. Biotechnol.* 1984, **20**, 303.
24. Furui, M. *J. Ferment. Technol.* 1985, **63**, 371.
25. Toda, K. *Biotechnol. Bioeng.* 1975, **17**, 1729.
26. Lee, S.B.; Kim, S.M.; Ryu, D.D.Y. *Biotechnol. Bioeng.* 1979, **21**, 2023.
27. Park, Y.H.; Han, M.H.; Rhee, H.-K. *J. Chem. Techn. Biotechnol.* 1984, **34B**, 57.
28. Marrazzo, W.N.; Merson, R.L.; McCoy, B.J. *Biotechnol. Bioeng.* 1975, **17**, 1515.
29. Cabral, J.M.S.; Cardoso, J.P.; Novais, J.M. *Enzyme Microb. Technol.* 1984, **6**, 365.
30. Lortie, R.; Thomas, D. *Biotechnol. Bioeng.* (in press).
31. Kobayashi, T.; Moo-Young, M. *Biotechnol. Bioeng.* 1973, **15**, 47.
32. Rovito, B.J.; Kittrell, J.R. *Biotechnol. Bioeng.* 1973, **15**, 143.
33. Tyagi, R.D.; Ghose, T.K. *Biotechnol. Bioeng.* 1982, **24**, 781.
34. Gencer, M.A.; Mutharasan, R. *Biotechnol. Bioeng.* 1983, **25**, 2243.
35. Mercer, D.G.; O'Driscoll, K.F. *Biotechnol. Bioeng.* 1981, **23**, 2447.
36. Tsukamoto, T.; Morita, S.; Okada, J. *Chem. Pharm. Bull.* 1982, **30**, 1539.
37. Ooshima, H.; Harano, Y. *Biotechnol. Bioeng.* 1983, **25**, 143.
38. Bihari, V. *J. Chem. Tech. Biotechnol.* 1985, **35B**, 83.
39. Habets-Crützen, A.Q.H.; Brink, L.E.S.; van Ginkel, C.G.; de Bont, J.A.M.; Tramper, J. *Appl. Microbiol. Biotechnol.* 1984, **20**, 245.
40. Tramper, J.; Brink, L.E.S.; Hamstra, R.S.; de Bont, J.A.M.; Habets-Crützen, A.Q.H.; van Ginkel, C.G. In: *Third European Congress on Biotechnology* Vol. 2, Verlag Chemie, Weinheim, 1984, p. 269.
41. Brink, L.E.S.; Tramper, J. *Enzyme Microb. Technol.* 1986, **8**, 281.
42. Brink, L.E.S.; Tramper, J. *Enzyme Microb. Technol.* 1986, **8**, 334.
43. Brink, L.E.S.; Tramper, J.; van 't Riet, K.; Luyben, K.Ch.A.M. *Anal. Chim. Acta* 1984, **163**, 207.

44. Habets-Crützen, A.Q.H.; de Bont, J.A.M. *Appl. Microbiol. Biotechnol.* 1985, **22**, 428.
45. Brink, L.E.S.; Tramper, J. In: *Modelling and Control of Biotechnological Processes* (Johnson, A., Ed.), Pergamon Press, Oxford, 1986, (in press).
46. Yamané, T.; Nakatani, H.; Sada, E.; Omata, T.; Tanaka, A.; Fukui, S. *Biotechnol. Bioeng.* 1979, **21**, 2133.
47. Duda, J.L.; Vrentas, J.S. *AIChE J.* 1968, **14**, 286.
48. Chilton, T.H.; Colburn, A.P. *Ind. Eng. Chem.* 1934, **26**, 1183.
49. Dwivedi, P.N.; Upadhyay, S.N. *Ind. Eng. Chem. Proc. Des. Dev.* 1977, **16**, 157.
50. Traher, A.D.; Kittrell, J.R. *Biotechnol. Bioeng.* 1974, **16**, 419.
51. McCune, L.K.; Wilhelm, R.H. *Ind. Eng. Chem.* 1949, **41**, 1124.
52. Buchholz, K. *Adv. Biochem. Eng.* 1982, **24**, 39.
53. Villadsen, J.V.; Stewart, W.E. *Chem. Eng. Sci.* 1967, **22**, 1483.
54. Ramachandran, P.A. *Biotechnol. Bioeng.* 1975, **17**, 211.
55. Kasche, V.; Kapune, A.; Schwegler, H. *Enzyme Microb. Technol.* 1979, **1**, 41.
56. Mears, D.E. *Ind. Eng. Chem. Proc. Des. Dev.* 1971, **10**, 541.
57. Charpentier, J.C.; Bakos, M.; Le Goff, P. *Proceedings of 2nd Conference on Applied Physical Chemistry* Vol. 2, Veszpremt, Hungary, 1971, p. 31.
58. Wicke, E. *Adv. Chem. Series* 1975, **148**, 75.
59. *Handbook of Chemistry and Physics* (Weast, R.C., Ed.), CRC Press, Cleveland, OH, 1976, 57th edn, p. F-55.
60. Liley, P.E.; Gambill, W.R. In: *Chemical Engineers' Handbook* (Perry, R.H.; Chilton, C.H., Eds), McGraw-Hill, New York, 1974, 5th ed., section 3, p. 247.
61. Landolt-Börnstein, *Gleichgewicht der Absorption von Gasen in Flüssigkeiten IV*. Band, 4. Teil, Bandteil c, Springer-Verlag, Berlin, 1976, p. 33.
62. Makranczy, J.; Megyery-Balog, K.; Ruzs, L.; Patyi, L. *Hungarian J. Ind. Chem.* 1976, **4**, 269.
63. Wilke, C.R.; Chang, P. *AIChE J.* 1955, **1**, 264.
64. van Klinken, J. *Proceedings of International Symposium on Chemical Engineering of Gas-Liquid-Solid Catalyst Reactions* (L'Homme, G.A., Ed.), Liège, Belgium, 1978, p. 172.
65. Furui, M.; Yamashita, K. *J. Ferment. Technol.* 1985, **63**, 73.



# 7. PRODUCTION OF PROPENE OXIDE IN AN ORGANIC-LIQUID-PHASE/IMMOBILIZED-CELL REACTOR

## Summary

Some major restrictions of the production of propene oxide in an organic-liquid-phase/immobilized-cell packed-bed reactor were quantified, and techniques were investigated to enhance the epoxide production rates. Propene-epoxidizing *Mycobacterium* cells were entrapped in calcium alginate gel and contacted with the substrates, propene and oxygen, which were dissolved in a continuous organic phase, n-hexadecane. The effects of product inhibition by the toxic epoxide, microbial consumption of propene oxide and immobilized-cell deactivation restricted severely the accumulation of the epoxide in the recirculation reactor system and could be predicted using a simple, mathematical model. Epoxide inhibition was reduced by absorbing the product in the gas phase in cold di-n-octyl phthalate. The resulting increase in propene oxide production was in agreement with model calculations. An alternating supply of propene and a co-substrate (ethene) prolonged the half-life of the immobilized cells. Using 50 g dry weight of cells, 1.5 g stereospecific propene oxide was produced in two days, of which 1.0 g was absorbed in the di-n-octyl phthalate phase.

## Introduction

The application of immobilized biocatalysts is all too often hampered by fundamental restrictions such as kinetic limitations (e.g. substrate or product inhibition), external and internal mass-transfer resistances, an insufficient stability of the immobilized biocatalyst, low solubility of substrate(s) and/or product(s) in water or in hydrophilic support materials and an arduous product recovery from dilute, aqueous solutions. Some of these problems, especially those associated with the use of an aqueous reaction environment, can be averted by employing water-immiscible organic media [1-4]. Some, like the mass-transfer limitations and the biocatalyst deactivation, are, however, always likely to occur, independent whether the aqueous medium is replaced by an organic one, or not.

An example that illustrates the above well is the production of propene oxide from propene and oxygen by *Mycobacterium* cells entrapped in calcium alginate [5, 6]. The use of a suitable organic solvent [7] as the continuous phase in this reaction system will lead to an enhanced capacity of the reaction medium for the two gaseous substrates and to a corresponding, smaller chance of substrate depletion in a packed-bed immobilized-cell reactor [8]. The situation that one can choose an optimal reaction medium, e.g. a medium with a high boiling point to facilitate the epoxide recovery, can also be considered as an advantage. No influence of the type of reaction medium is, however, to be expected on the main mass-transfer limitation, i.e. internal pore diffusion in the gel beads [9], as the low solubility of the substrates in the hydrophilic calcium alginate will not change much. Immobilization in hydrophobic, synthetic supports, as proposed by Fukui and Tanaka [10], is not applicable for the present system of investigation, as this resulted in very low

epoxidation activities [11]. Also, in view of the necessary, non-polar nature of the organic solvent and the relatively high solubility of the epoxide in water [7], replacement of (part of) the aqueous phase by an equal volume of water-immiscible organic solvent will have only limited influence on the partitioning of the epoxide between the various phases and, thus, on the inhibition by the polar propene oxide [12]. Finally, the half-life of the immobilized biocatalyst, in contact with a suitable (i.e. non-polar) solvent, is as low as that of the immobilized cells in an aqueous environment (1 to 3 days).

In this study some major restrictions, not related to the type of reaction medium, of the epoxide production in an organic-liquid-phase/immobilized-cell reactor are quantified and techniques are investigated to avoid these problems. These restrictions are kinetic limitations and operational stability. *N*-hexadecane is used as the continuous organic phase. By comparing measured amounts of consumed propene and accumulated propene oxide to the corresponding, theoretical values, it is shown that the combined influences of product inhibition, microbial epoxide consumption and biocatalyst deactivation can be predicted with the use of a simple model. Propene oxide levels were held low by absorption of the epoxide in a di-*n*-octyl phthalate phase. This diminished the effect of product inhibition and thus increased the production rate of the epoxide. The operational stability could be improved by supplying the immobilized cells alternately with propene and a co-substrate (ethene). By extracting the product into di-*n*-octyl phthalate, it appeared possible to produce ~1.5 g chiral propene oxide in two days using ~50 g dry weight of cells in a 1.7 dm<sup>3</sup> organic-liquid-phase/immobilized-cell packed-bed reactor.

## Experimental

### *Chemicals*

Di-*n*-octyl phthalate was purchased from Lamers and Indemans, Den Bosch, The Netherlands, and was of analytical grade (99%). Baker Chemicals provided *n*-hexadecane (analytical grade, > 99%). Ethene and propene were of commercial purity and obtained from the Matheson company, East Rutherford, NY. The support material, sodium alginate (Manucol DM), was purchased from Alginate Industries, London, U.K.

### *Microorganism*

The *Mycobacterium* strain E3 used for the epoxidation reaction was grown fed-batch on ethene in mineral medium in a 2 dm<sup>3</sup> fermentor at 30°C and pH 7.0. Microbial aspects of this strain have been described before [5].

### *Immobilization*

The procedure of immobilization in calcium alginate has been published earlier [5]. It was determined microscopically that the average diameter of the spherical gel beads was 0.7 (± 0.1) mm.

### *Measurement of Kinetic Limitations and Deactivation Rate*

The consumption rates of propene (or ethene) and oxygen and the accumulation rates of propene oxide were measured in an organic-liquid-phase/immobilized-cell packed-bed reactor (internal diameter 3.2 cm, bed height ~45 cm). Full details of

this automated experimental set-up have been given previously [8, 13]. The reaction medium ( $\sim 350 \text{ cm}^3$  n-hexadecane and dissolved (co-)substrates) was forced to flow upwards through the packed bed of immobilized-cell particles, and, subsequently, equilibrated with a circulating gas phase in a trickle-bed contactor and recycled completely. All temperatures were maintained at  $30^\circ\text{C}$ . The catalyst bed was diluted with small glass beads ( $\sim 1 \text{ mm}$ ) to achieve a high solvent/gel contacting efficiency (alginate fraction  $\sim 0.3$ , glass bead fraction  $\sim 0.4$ ) [8]. Varying amounts of immobilized cells (1 to 10 g dry weight of cells) were used in the different experiment types. If needed, the propene oxide concentration in the different phases (calcium alginate, n-hexadecane, gas) was held negligible by continuous hydrolysis in a sulphuric-acid solution. For that, the epoxide was removed from the circulating gas phase by absorption in acid ( $\text{pH} \sim 1$ ,  $30^\circ\text{C}$ ). The gas stream was led through a di-n-octyl phthalate phase at  $0^\circ\text{C}$  instead if the influence of epoxide absorption in this solvent on the epoxidation rate was to be examined. High circulation rates of solvent and gas ( $\sim 300 \text{ cm}^3$  hexadecane  $\text{min}^{-1}$ ,  $\sim 1500 \text{ cm}^3$  gas  $\text{min}^{-1}$ ) were applied to simulate the characteristics of a well-stirred batch reactor. Furthermore, the mass-transfer rates of the various gas/liquid and liquid/solid contacting processes (gas/n-hexadecane, gas/sulphuric-acid solution, gas/di-n-octyl phthalate, n-hexadecane/alginate) were sufficiently high to assure unretarded supply and removal of reactants and products. For example, even trace amounts of propene oxide could not be detected in case of epoxide hydrolysis in the sulphuric-acid solution. Ethene, propene and oxygen-consumption rates and epoxide-production rates of the gel-entrapped cells in the packed-bed were measured by on-line gas chromatographic analysis of the gaseous (co-)substrates and the volatile product in the circulating gas stream. To maintain high, constant levels of propene and oxygen in the experimental system the gas chromatograph was coupled to an integrator and a microcomputer. This enabled computer-controlled addition of these two substrates (propene and oxygen concentrations in the biocatalyst phase:  $\sim 160$  and  $\sim 245 \mu\text{M}$ , respectively). Ethene (co-substrate) levels were allowed to drop with reaction time (initial concentration in the gel phase  $\sim 150 \mu\text{M}$ ). It was attempted to improve the operational stability of the gel-entrapped cells by supplying alternately ethene and propene (ethene on the first day, propene on the second, ethene again on the third, etc.).

#### *Propene Oxide Production*

Experimental conditions deviating from the above mentioned were used in case of the production of a practical amount of propene oxide (a few grammes). A larger bioreactor was employed (internal diameter 6.2 cm, bed height  $\sim 55 \text{ cm}$ ), and  $\sim 50 \text{ g}$  dry weight of cells were immobilized in  $\sim 600 \text{ cm}^3$  calcium alginate (4%, w/v). About  $1000 \text{ cm}^3$  n-hexadecane was used to supply the substrates to and extract the product from the immobilized cells. A large part of the formed epoxide was absorbed in  $\sim 1100 \text{ cm}^3$  di-n-octyl phthalate. The cells were supplied with propene during two periods of two days with one ethene-regeneration interval of one day between these periods. The optical activity of the absorbed propene oxide was determined by complexation g.l.c. as described before [14].

## **Results and discussion**

### *Modelling Epoxidation Kinetics and Deactivation Kinetics*

Supply of the two substrates (oxygen and alkene) to the gel-entrapped cells was accomplished by forcing the organic solvent, *n*-hexadecane [8], with the dissolved substrates to flow through a stagnant bed of calcium alginate gel particles. The packed bed was mixed with glass particles to enhance the flow characteristics of the packed bed. In a separate step the circulating solvent was contacted with a gas phase, also circulating, containing high, controlled levels of the two gaseous substrates. In the work described here the circulation rates of solvent and gas were sufficiently high to prevent macroscopic, spatial dependencies of the substrate and product concentrations in the packed bed [8] and in the gas/liquid contactor. The entire set-up can thus be considered to behave like a (recirculation) batch reactor system with continuous feed of the two substrates.

Several limitations are likely to restrict the propene-consumption rate,  $dm_1/dt$ , and the epoxide-production rate,  $dm_P/dt$ , of the immobilized cells in the above described reactor system. They can be related to the following phenomena: mass transfer, epoxidation kinetics and deactivation kinetics. The main mass-transfer effects are external diffusion of the two substrates from the organic bulk phase to the gel surface and, more important, internal diffusion of the substrates in the biocatalyst particles [9, 12]. As mentioned above, substrate depletion along the length of the packed-bed reactor can be assumed not to occur [8]. The external and internal diffusion limitations can be expressed by the Thiele effectiveness factor,  $\eta$ , of the biocatalyst, which is defined as the ratio of observed reaction rate to the diffusion-free rate [9]. At zero-order reaction conditions the principal, kinetic limitations are product inhibition and consumption of the formed propene oxide [12]. Deactivation of the immobilized cells may be ascribed to an inability of the cells to maintain a constant level of NADH, which is a necessary co-factor for the mono-oxygenase-catalyzed epoxidation of propene [15].

Assuming first-order deactivation kinetics and zero-order reaction kinetics, the mentioned limitations can be described by a simple, mathematical model as follows:

$$dm_1(t)/dt = \eta(t) X V_0 \exp(-k_D t) / (1 + P(t)/K_P'') \quad (1)$$

$$dm_P(t)/dt = dm_1(t)/dt - v_C \quad (2)$$

$$P(t) = f(m_P(t), \gamma_{ALG}, \gamma_{HEX}) \quad (3)$$

with  $m_1$  and  $m_P$  the total amount of propene consumed and propene oxide accumulated, respectively,  $X$  the amount of immobilized biocatalyst,  $V_0$  the initial propene-consumption rate,  $k_D$  the first-order deactivation parameter,  $P$  the propene oxide concentration in the calcium alginate phase,  $K_P''$  the propene oxide-inhibition parameter [12],  $v_C$  the propene oxide-consumption rate [12] and  $\gamma$  the activity coefficient of propene oxide. Equation 3 relates the propene oxide concentration in the biocatalyst phase, which determines the degree of product inhibition, to the total amount of produced epoxide,  $m_P$ , and to the relevant activity coefficients ( $\gamma_{ALG}$ ,  $\gamma_{HEX}$ ). The full expression is derived in the appendix. The propene-consumption activity will decrease with reaction time due to biocatalyst deactivation and product inhibition (equation 1). Therefore, the effectiveness factor will also vary with time:  $\eta(t=0) \leq \eta(t) \leq 1$ . For simplification the reaction conditions (particle diameter  $< 0.9$  mm, cell density  $< 80$  kg dry weight  $(m^3 \text{particle})^{-1}$ , oxygen and propene concentrations (in alginate phase)  $\sim 245$  and  $160$   $\mu\text{M}$ , respectively, superficial velocity of solvent  $\sim 6 \times 10^{-3}$  m  $s^{-1}$ ) were chosen such

that external and internal diffusion effects can be assumed to be negligible ( $\eta(t=0) \sim 1$ ) [8, 9].

The combined influence of epoxidation kinetics (product inhibition and epoxide consumption) and deactivation kinetics on the amount of consumed propene and accumulated propene oxide can now be predicted by using equations 1 to 3 (Runge-Kutta integration,  $\eta \sim 1$ ). These predictions were compared with the corresponding, experimental values, measured in the packed-bed reactor, of immobilized cells with an initial activity,  $V_0$ , of  $2.9 \mu\text{mol min}^{-1} (\text{g dry weight})^{-1}$  and a deactivation parameter,  $k_D$ , of  $1.6 \times 10^{-4} \text{ min}^{-1}$  (half-life 3.0 days). The four remaining model parameters ( $K_P''$ ,  $v_C$ ,  $\gamma_{\text{ALG}} \sim \gamma_{\text{WAT}}$ ,  $\gamma_{\text{HEX}}$ ) were estimated from literature data (Table 1). A good agreement was found between the calculated and

**Table 1.** Estimated values and literature source of model parameters

parameter	value	unit	reference no.
$K_P''$	9.6	mM	12
$v_C$	$0.15 \times V_0$	$\mu\text{mol min}^{-1} (\text{g dry weight})^{-1}$	12
$\gamma_{\text{ALG}} (30^\circ\text{C})$	17.6	-	13
$\gamma_{\text{HEX}} (30^\circ\text{C})$	1.9	-	16
$\gamma_{\text{DNOP}} (0^\circ\text{C})$	0.95	-	this work

observed values (Figure 1). Furthermore, it can be seen that the produced amount of propene oxide (experimental and predicted) is considerably smaller than the

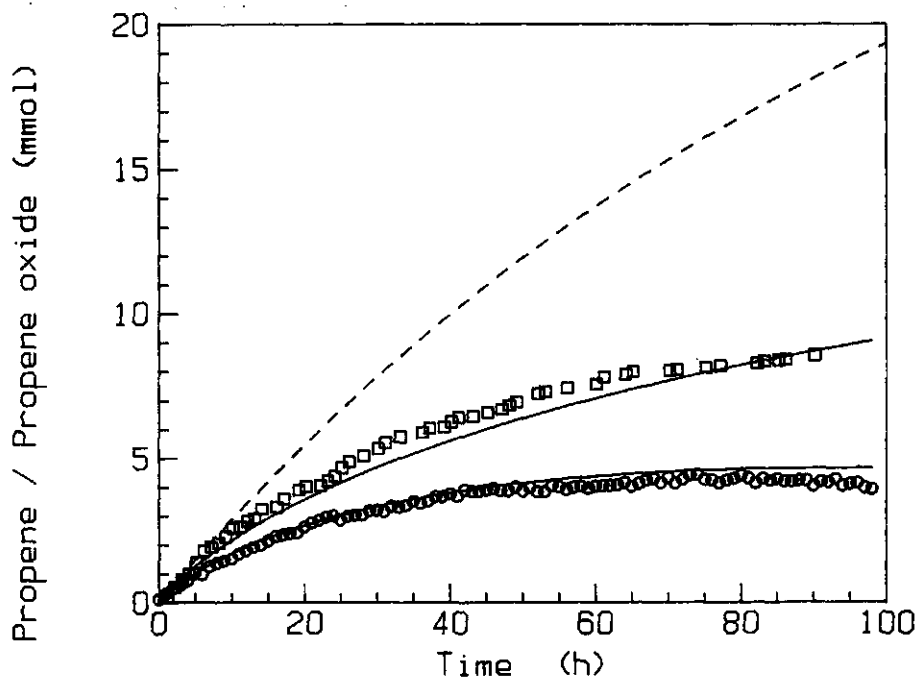


**Figure 1.** Total amount in mmol of consumed propene and accumulated propene oxide in the recirculation packed-bed reactor system versus time (no DnOP phase present);  $V_0 = 2.9 \mu\text{mol min}^{-1} (\text{g dry weight})^{-1}$ ;  $X = 1.7 \text{ g dry weight}$ ;  $k_D = 1.6 \times 10^{-4} \text{ min}^{-1}$ ; measured quantities ( $\square$ , propene;  $\circ$ , propene oxide); model predictions (—); calculated values when only the effect of deactivation is considered (---).

hypothetic maximum due to product inhibition and epoxide consumption. In the following two sections techniques are discussed to increase the production rate of the epoxide.

### *Product Inhibition*

The effect of inhibition by the formed propene oxide can be diminished by avoiding high epoxide concentrations in the biocatalyst phase. Distillation of the circulating *n*-hexadecane (boiling point 287°C) stream is, in principle, suited for recovery of the produced epoxide. However, continuous distillation in the present bench-scale set-up appeared burdensome, and, therefore, an alternative epoxide-recovery technique was chosen. In view of the very high volatility of propene oxide (boiling point ~34°C), it appeared also possible to remove the product from the circulating gas stream. In this work the propene oxide was absorbed in di-*n*-octyl phthalate (DnOP) at a low temperature (0°C). DnOP was used instead of *n*-hexadecane for the following reasons. DnOP is one of the few organic solvents that do not show any disadvantageous effects on the immobilized-cell activity [7] and, furthermore, has a very low vapour pressure, which will facilitate a final epoxide/DnOP separation. *N*-hexadecane cannot be applied for the epoxide absorption at 0°C, as this solvent possesses a melting point of ~18°C. Absorption in *n*-hexadecane at e.g. 25°C is less suited, as in that case no advantage can be taken of the relatively low vapour pressure of pure propene oxide at 0°C (see appendix). DnOP is not used as the reaction medium in the packed-bed bioreactor in view of its high viscosity, which could result in high pressure drops over the packed-bed and reduced mass-transfer rates. Furthermore, in contrast to DnOP, *n*-hexadecane appeared to stabilize the gel-entrapped cells to a small degree [11].

The presence of an additional DnOP phase will change the distribution of the epoxide between the various phases in the batch-reactor system markedly (see appendix):

$$P(t) = f(\text{mp}(t), \gamma_{\text{ALG}}, \gamma_{\text{HEX}}, \gamma_{\text{DnOP}}) \quad (4)$$

The activity coefficient of propene oxide in the DnOP phase was estimated from independent vapour/liquid equilibria data ( $\gamma_{\text{DnOP}}(0^\circ\text{C}) \sim 0.95$ ). The negative deviation from Raoult's law ( $\gamma < 1$ ) was also found in case of other, larger di-*n*-alkyl phthalates, and can be explained by the formation of (weak) complexes between the ester and the epoxide [17].

The effect of the absorption of the epoxide in a DnOP phase (300 cm<sup>3</sup>, 0°C) on the propene consumption and the propene oxide production of the immobilized cells of the previous section can be predicted using the above formulated model (equations 1, 2 and 4) and the parameters in Table 1. Again, these predictions correlated favourably to the corresponding, experimental values, albeit the observed amounts of propene and epoxide are in this case somewhat lower than the calculated quantities (Figure 2). From comparing Figure 1 and 2 it can be concluded that absorption of the formed epoxide in DnOP enhances the amount of propene consumed significantly as a result of the lower epoxide concentrations in the biocatalyst phase. Even though at the end of the experiment the epoxide levels in the alginate phase are now about twice as low (predicted levels in mM after 100 h: 16.8 without and 7.5 with absorption in DnOP), the total epoxide production is about twice as high (experimental amounts in mmol after 100 h: ~4 without and ~7 with absorption in DnOP). The main part (76%) of the produced propene oxide is

absorbed in 300 cm<sup>3</sup> DnOP (alginate gel 8%, n-hexadecane 15%, gas 1%). Larger quantities of DnOP would result in even higher 'extraction' capacities.

#### Deactivation

The operational stability of free *Mycobacterium* cells (strain E3) is rather low. The typical half-life of propene-epoxidizing, free cells is only 1 to 3 days. Immobilization in calcium alginate [13] or  $\kappa$ -carrageenan (unpublished results) did not result in a significant improvement of the stability. As mentioned above, energy shortage (NADH) is thought to be the main cause of the instability of the cells.

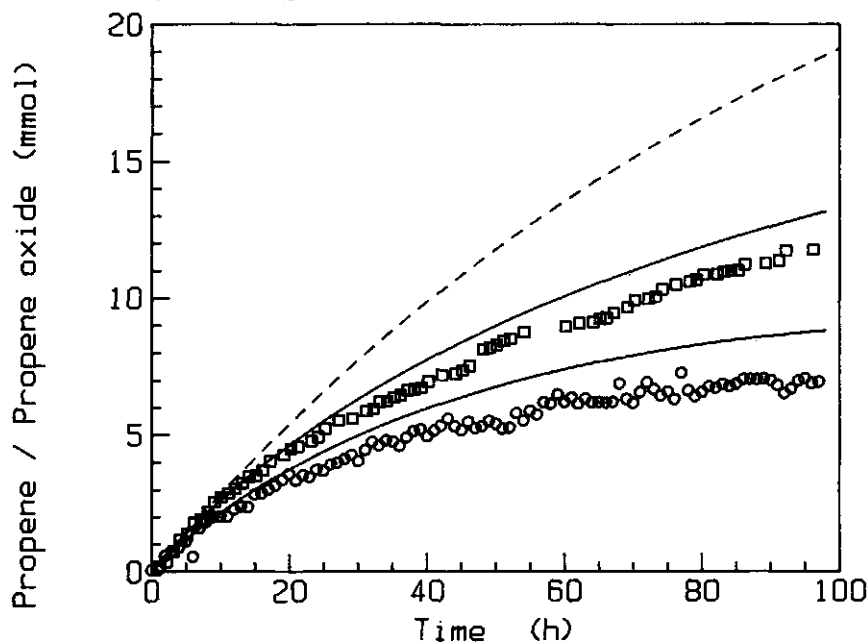
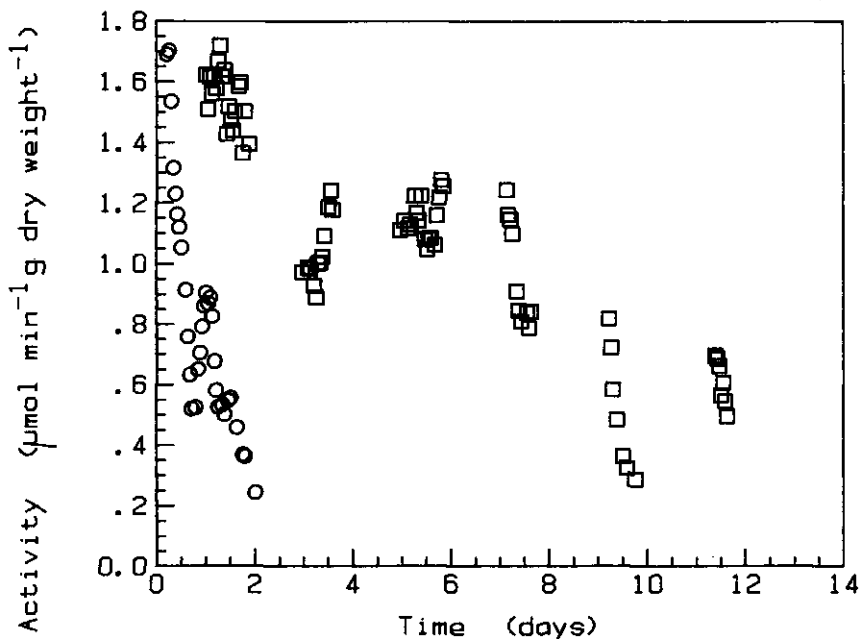


Figure 2. Total amount in mmol of consumed propene and accumulated propene oxide in the recirculation packed-bed reactor system versus time (300 cm<sup>3</sup> DnOP phase present);  $V_0 = 2.9 \mu\text{mol min}^{-1}$  (g dry weight)<sup>-1</sup>;  $X = 1.7$  g dry weight;  $k_D = 1.6 \times 10^{-4} \text{ min}^{-1}$ ; measured quantities ( $\square$ , propene;  $\circ$ , propene oxide); model predictions (—); calculated values when only the effect of deactivation is considered (---).

Therefore, several more or less energy-rich co-substrates (e.g. acetate, ethyl acetate, ethanol, ethene) have been tested on their usefulness as energy-suppliers to cells of various *Mycobacterium* strains by Habets-Crützen and de Bont [15]. It appeared that supplying alternately ethene and propene is a promising technique to maintain a high propene-epoxidation activity of free and immobilized cells. An illustration of this finding for calcium alginate gel-entrapped cells (strain E3) in the packed-bed reactor system is shown in Figure 3. The propene-epoxidation activities of Figure 3 were extracted from the measured time-course data (mmol propene consumed at various points of time) by fitting second-order polynomials to sets of 7 points of measurement and by taking the derivative of the thus derived polynomials. The rates of propene consumption in the regeneration intervals are unknown, as only ethene was supplied during these periods. Propene oxide levels were kept

insignificantly low by hydrolysis in a sulphuric-acid solution. The half-life of the immobilized cells is several times higher than that of cells without ethene as co-substrate. The increase in overall volumetric productivity will, however, be less remarkable, due to the necessary periods of cell regeneration with ethene as co-substrate. The rate of ethene consumption was found to be about three times higher than the propene-consumption rate.

A similar stability of the propene-consumption rate was observed when the produced epoxide was not removed completely by hydrolysis but absorbed in DnOP (800 cm<sup>3</sup>). See Figure 4. The activities of Figure 4 were obtained by using the above



**Figure 3.** Propene-consumption rates (□) of the immobilized cells in the recirculation reactor system versus time; the formed epoxide is hydrolyzed; the cells are supplied alternately with propene and a co-substrate (ethene); without regeneration of the cells with ethene (○).

mentioned fitting technique. The relative amount of epoxide consumed appears rather constant, which suggests that the deactivation rates of propene-epoxidation and epoxide-consumption activities are comparable.

#### *Propene Oxide Production*

To investigate the possibilities of the production of larger quantities propene oxide and also to obtain a practical amount of epoxide for determination of chemical and physical properties (e.g. the optical activity [14]), about 50 g dry weight of cells (initial activity 1.0 μmol min<sup>-1</sup> (g dry weight)<sup>-1</sup>) were immobilized and contacted with the dissolved substrates (oxygen and alkene) in a 1.7 dm<sup>3</sup> packed-bed reactor. The formed propene oxide was absorbed in DnOP (1100 cm<sup>3</sup>). Model predictions, using equations 1, 2 and 4, the parameters in Table 1 and an assumed value for  $k_D$  equal to that used above ( $1.6 \times 10^{-4}$  min<sup>-1</sup>), provided again an acceptably accurate description of the observed amount of consumed propene (Figure 5). However, a



remarkable discrepancy was found between theory and experiment in case of propene oxide production. A possible explanation might be given by the fact that the used biocatalyst was composed of 11 different cell batches (each about 4 to 5 g dry weight of cells), whereas the cells used in the experiments of Figure 1 and 2 both originated from one cell batch. Different points of time of cell harvesting [18] and/or

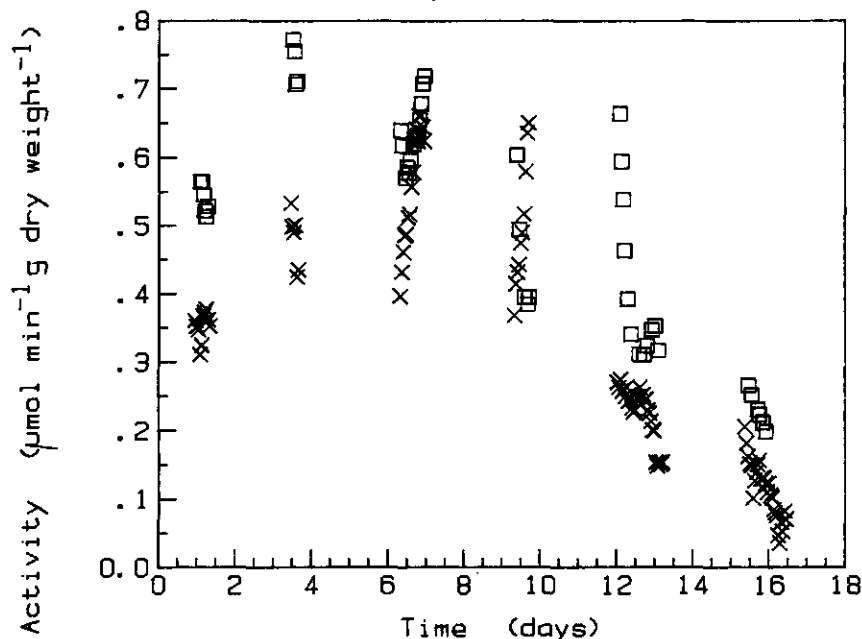


**Figure 4.** Propene-consumption rates (□) and propene oxide-accumulation rates (×) of the immobilized cells in the recirculation reactor system versus time; the formed epoxide is absorbed in DnOP; the cells are supplied alternately with propene and a co-substrate (ethene).

fluctuating cell-growth conditions can change the cell kinetics significantly. For example, the experimental results of Figure 5, both of propene and propene oxide, could be described well with a higher epoxide consumption rate ( $\sim 0.4 \times V_0$ ).

After two days about 1.5 g ( $\sim 24$  mmol) propene oxide was produced. It was calculated that 66% ( $\sim 1.0$  g,  $\sim 16$  mmol) was absorbed in 1100 cm<sup>3</sup> of DnOP (alginate gel 19%, n-hexadecane 12%, gas 3%). These production rates are comparable to that of 10 g dry weight of suspended cells of another strain (2W) in a 2.5 dm<sup>3</sup> fermentor (aqueous medium, acetate was used as a co-substrate) [14]. After one day the produced amount of epoxide was in this case 1.5 g (absorbed in 7.5 dm<sup>3</sup> tetrachloro methane, after distillation 0.65 g in 7 cm<sup>3</sup> tetrachloro methane). Ethene was supplied to the immobilized cells during one day, after which the epoxide production was repeated. The accumulated quantity of epoxide during two days ( $\sim 1.3$  g,  $\sim 22$  mmol) was only slightly smaller as compared to the first production period, but the consumed amount of propene was, however, 20 to 30% lower.

The stereospecificity of the absorbed propene oxide, produced during the first production period, was determined by complexation g.l.c. Mainly the R-form appeared to be formed (enantiomeric purity  $92 \pm 1\%$ ). In previous work a similar purity was observed ( $93 \pm 1\%$  R, strain E3) [14].

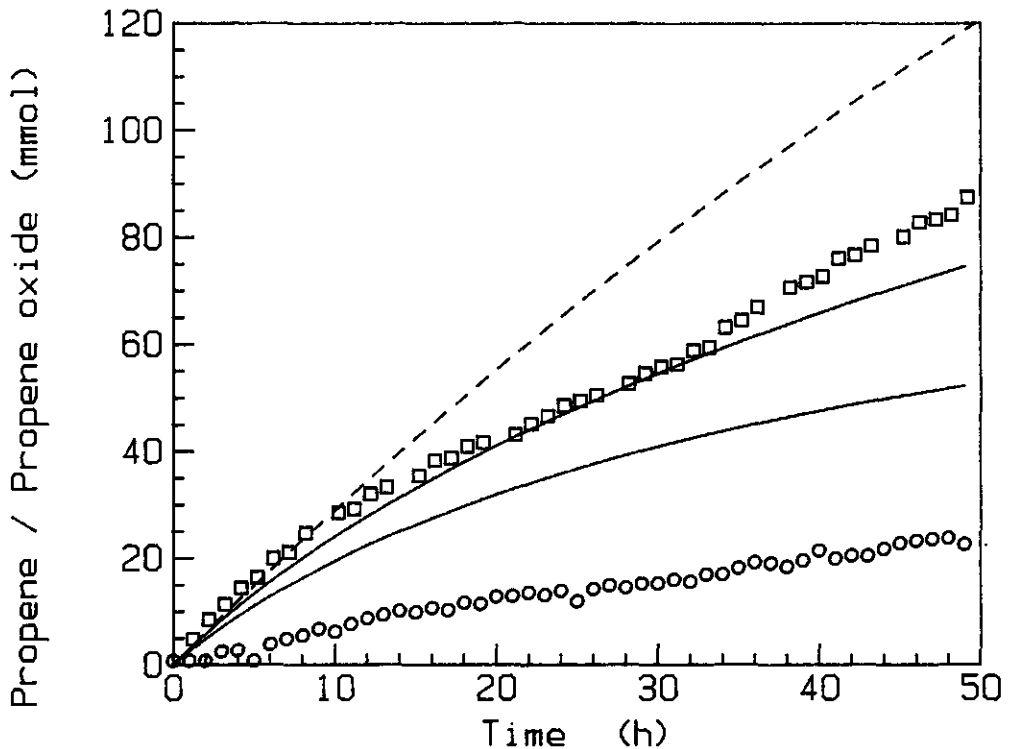


**Figure 5.** Total amount in mmol of consumed propene and accumulated propene oxide in the recirculation packed-bed reactor system versus time (1100 cm<sup>3</sup> DnOP phase present);  $V_o = 1.0 \mu\text{mol min}^{-1} (\text{g dry weight})^{-1}$ ;  $X = 50 \text{ g dry weight}$ ;  $k_D = 1.6 \times 10^{-4} \text{ min}^{-1}$ ; measured quantities ( $\square$ , propene;  $\circ$ , propene oxide); model predictions (—); calculated values when only the effect of deactivation is considered (---).

## Conclusions

Propene oxide has a relatively high solubility in the used aqueous support material, calcium alginate. Thus, rapid extraction of the inhibitory product into an organic reaction medium, as a result of a high partition coefficient of the epoxide between solvent and gel, will not occur. However, in this work it was shown that the production of propene-epoxidizing, gel-entrapped cells in a recirculation packed-bed reactor system could be enhanced by absorbing the toxic product in an additional, cold DnOP phase. The operational stability of the immobilized cells could be increased by supplying the cells with ethene as a co-substrate, but is still insufficient by industrial standard. Due to the low epoxidation activity ( $1 \text{ to } 3 \mu\text{mol min}^{-1} (\text{g dry weight})^{-1}$ ), product inhibition, epoxide consumption and cell deactivation, 50 g dry weight of cells in a 1.7 dm<sup>3</sup> packed-bed organic-liquid-phase/immobilized-cell reactor were required to produce  $\sim 1.5 \text{ g}$  stereospecific propene oxide, of which two third was recovered in the DnOP phase.

## Acknowledgements

The authors wish to thank the Netherlands Technology Foundation (STW) for financial support and Prof.Ir. K.Ch.A.M. Luyben and Prof.Dr.Ir. K. van 't Riet for helpful discussions.

## Nomenclature

DnOP	di-n-octyl phthalate
$k_D$	first-order deactivation parameter ( $s^{-1}$ )
$K_P''$	propene oxide-inhibition parameter ( $\text{mol m}^{-3}$ )
L	number of moles of phase 1, 2 or 3 (mol)
$m_1$	total amount of propene consumed (mol)
$m_P$	total amount of propene oxide accumulated (mol)
M	molecular weight ( $\text{g mol}^{-1}$ )
NADH	nicotinamide adenine dinucleotide
P	propene oxide concentration in the calcium alginate gel phase ( $\text{mol m}^{-3}$ )
$P_T$	total pressure in the experimental system (Pa)
$P_{PO}^0$	vapour pressure of pure propene oxide (Pa)
R	gas constant ( $\text{J mol}^{-1} \text{K}^{-1}$ )
T	temperature of the gas phase (K)
t	time (s)
V	number of moles of gas (mol)
vc	propene oxide-consumption rate ( $\mu\text{mol min}^{-1} (\text{g dry weight})^{-1}$ )
$V_0$	initial propene-epoxidation activity of immobilized cells ( $\mu\text{mol min}^{-1} (\text{g dry weight})^{-1}$ )
X	amount of immobilized biocatalyst (g dry weight)
x	mole fraction of propene oxide in phase 1, 2 or 3
y	mole fraction of propene oxide in the gas phase
$\gamma$	activity coefficient of propene oxide
$\eta$	overall effectiveness factor
$\rho$	specific gravity ( $\text{kg m}^{-3}$ )

## Subscripts

ALG	calcium alginate phase
DnOP	di-n-octyl phthalate phase
HEX	n-hexadecane phase
WAT	water phase
k	phase k
1	phase 1
2	phase 2
3	phase 3

## References

1. Antonini, E., Carrea, G. and Cremonesi, P. *Enzyme Microb. Technol.* 1981, **3**, 291–296
2. Carrea, G. *Trends in Biotechnol.* 1984, **2**, 102–106
3. Lilly, M.D. *J. Chem. Tech. Biotechnol.* 1982, **32**, 162–169
4. Lilly, M.D. and Woodley, J.M. in *Biocatalysts in Organic Syntheses* (Tramper, J., van der Plas, H.C. and Linko, P., eds), Elsevier, Amsterdam, 1985, pp. 179–192
5. Habets–Crützen, A.Q.H., Brink, L.E.S., van Ginkel, C.G., de Bont, J.A.M. and Tramper, J. *Appl. Microbiol. Biotechnol.* 1984, **20**, 245–250
6. Tramper, J., Brink, L.E.S., Hamstra, R.S., de Bont, J.A.M., Habets–Crützen, A.Q.H. and van Ginkel, C.G. in *Third European Congress on Biotechnology*, Verlag Chemie, Weinheim, 1984, vol. 2, pp. 269–276
7. Brink, L.E.S. and Tramper, J. *Biotechnol. Bioeng.* 1985, **27**, 1258–1269
8. Brink, L.E.S. and Tramper, J. *J. Chem. Tech. Biotechnol.* (in press)
9. Brink, L.E.S. and Tramper, J. *Enzyme Microb. Technol.* 1986, **8**, 281–288
10. Fukui, S. and Tanaka, A. *Adv. Biochem. Eng. Biotechnol.*, 1984, **29**, 1–33
11. Brink, L.E.S. and Tramper, J. (unpublished results)
12. Brink, L.E.S. and Tramper, J. *Enzyme Microb. Technol.* 1986, **8**, 334–340
13. Brink, L.E.S., Tramper, J., van 't Riet, K. and Luyben, K.Ch.A.M. *Anal. Chim. Acta* 1984, **163**, 207–217
14. Habets–Crützen, A.Q.H., Carlier, S.J.N., de Bont, J.A.M., Wistuba, D., Schurig, V., Hartmans, S. and Tramper, J. *Enzyme Microb. Technol.* 1985, **7**, 17–21
15. Habets–Crützen, A.Q.H. and de Bont, J.A.M. (submitted)
16. Aarna, A., Melder, L. and Ebber, A. *Zh. Prikl. Khim.* 1979, **52**, 1640–1642 (Russ.)
17. Prausnitz, J.M. in *Molecular Thermodynamics of Fluid–Phase Equilibria*, Prentice–Hall, Inc., Englewood Cliffs, NJ, 1969, pp. 331–336
18. Habets–Crützen, A.Q.H. and de Bont, J.A.M. (unpublished results)
19. Gmehling, J. and Onken, U. in *Vapor–Liquid Equilibrium Data Collection*, Dechema, Frankfurt/Main, 1977, Chemistry Data Series, Vol. I, Part 1, p. 257

## Appendix

The closed recirculation reactor system consists of at most four different phases: calcium alginate gel (1), n-hexadecane (2), DnOP (3) and a gas phase. The alginate phase (4%, w/v) will be treated here as a water phase ( $\gamma_{\text{ALG}} \sim \gamma_{\text{WAT}}$ ). In view of the high circulation rates of n-hexadecane and gas, it can be assumed that phase 1 and 2 and the gas phase are in thermodynamic equilibrium at 30°C, DnOP is in equilibrium with the gas at 0°C and, finally, there are uniform propene oxide mole fractions in the solid, liquid and gaseous phases ( $x_1$ ,  $x_2$ ,  $x_3$ , and  $y$ ). The total amount of produced epoxide (mP) is distributed among the three or four (the latter in case of absorption in DnOP) phases present in the experimental set-up. This can be expressed mathematically in the following propene oxide balance:

$$x_1L_1 + x_2L_2 + x_3L_3 + yV = \text{mP} \quad (\text{A-1})$$

with  $L_k$  the number of moles of phase  $k$  and  $V$  the number of moles of gas. Assuming ideal gas–phase behaviour ( $P_T = 10^5$  Pa), the following two equations can be used to describe the phase equilibria between phase 1 and 2 and the gas phase:

$$\gamma_1(30^\circ\text{C}) x_1 \text{PPO}^\circ(30^\circ\text{C}) = y \text{P}_T \quad (\text{A-2})$$

$$\gamma_2(30^\circ\text{C}) x_2 \text{PPO}^\circ(30^\circ\text{C}) = y \text{P}_T \quad (\text{A-3})$$

Similarly, the equilibrium between phase 3 and the gas phase is characterized by:

$$\gamma_3(0^\circ\text{C}) x_3 \text{PPO}^\circ(0^\circ\text{C}) = y \text{P}_T \quad (\text{A-4})$$

In addition to the temperature dependency, the activity coefficients in equations A-2 to A-4 are also functions of the epoxide mole fractions of the pertinent phases. However, at low concentrations,  $\gamma_1$  was found not to be dependent on the mole fraction in the aqueous phase ( $\gamma_1 \sim 17.6$  for  $x_1 < 3 \times 10^{-4}$  or  $P < 17$  mM [13]). It is assumed here that  $\gamma_2$  and  $\gamma_3$  (both much nearer to unity than  $\gamma_1$ ) can also be considered not to be related to  $x_2$  and  $x_3$ , respectively. The mole fraction of propene oxide in the immobilized-cell phase,  $x_1$ , can be obtained by rearranging equations A-1 to A-4:

$$x_1 = \text{mP} \left( L_1 + \frac{\gamma_1(30^\circ\text{C})}{\gamma_2(30^\circ\text{C})} L_2 + \frac{\gamma_1(30^\circ\text{C}) \text{PPO}^\circ(30^\circ\text{C})}{\gamma_3(0^\circ\text{C}) \text{PPO}^\circ(0^\circ\text{C})} L_3 + \frac{\gamma_1(30^\circ\text{C}) \text{PPO}^\circ(30^\circ\text{C})}{\text{P}_T} V \right)^{-1} \quad (\text{A-5})$$

The following numerical values were applied in this work:  $\text{P}_T = 10^5$  Pa,  $\text{PPO}^\circ(30^\circ\text{C})$  and  $\text{PPO}^\circ(0^\circ\text{C})$  about  $0.857 \times 10^5$  and  $0.241 \times 10^5$  Pa [19], respectively,  $L_k = (\text{cm}^3 \text{ of phase } k) \times \rho_k / M_k \text{ mol}$ ,  $\rho_1$ ,  $\rho_2$  and  $\rho_3$  equal to 1, 0.77331 and 0.985 g  $\text{cm}^{-3}$ , respectively,  $M_1$ ,  $M_2$  and  $M_3$  equal to 18, 226.45 and 390.54 g  $\text{mol}^{-1}$ , respectively,  $V = (\text{m}^3 \text{ of gas}) \times \text{P}_T / (\text{RT}) \text{ mol}$ ,  $\text{P}_T = 10^5$  Pa,  $R = 8.314$  J  $\text{mol}^{-1} \text{K}^{-1}$  and  $T = 303.15$  K. The gas volume of the experimental set-up was about  $1.5 \times 10^{-3} \text{ m}^3$  ( $1.5 \times 10^{-2} \text{ m}^3$  in case of the propene oxide production with 50 g dry weight of cells). The epoxide concentration in the biocatalyst phase,  $P$ , is easily calculated as follows:

$$P = 10^6 \rho_1 x_1 / (M_1 (1-x_1)) \quad (\text{A-6})$$

with  $P$  in mM. Equations A-5 and A-6 can also be used to estimate the product concentration in the biocatalyst phase if the epoxide is not absorbed in DnOP (i.e.  $L_3 = 0$  in equation A-5).

## 8. DISCUSSION

### 8.1 Microbial Propene Epoxidation as Model Reaction

The specific epoxidation activity of the mono-oxygenase of freely suspended (or gel-entrapped) *Mycobacteria* is very low. This can be comprehended, when propene-consumption rates of suspensions of resting, ethene-grown cells ( $\sim 0.01$  to  $0.03 \mu\text{mol min}^{-1} (\text{mg cell protein})^{-1}$  [1]), are compared to typical specific activities of enzymes ( $1$  to  $10^4 \mu\text{mol min}^{-1} (\text{mg protein})^{-1}$  [2]). The inadequate activity is one of the main reasons for the unfavourable economics of the microbial epoxidation process under investigation. Other factors are the low stability of the biocatalyst (chapter 7), the narrow cost difference between substrate and product (though higher in case of stereospecific propene oxide) and, finally, the existence of established, chemical epoxidation routes (section 1.4). The latter probably also have played a role in the decision to abandon the multi-enzyme process for alkene epoxidation (see references 63 en 64 in chapter 1) developed to pilot-plant scale by Cetus Corporation [3].

The low cell activity is also an explanation for the observation that the measured, volumetric epoxide productivity by classical fermentation ( $\sim 0.4 \text{ mol m}^{-3} \text{ h}^{-1}$  [4]), using suspended cells in an aqueous reaction medium, is comparable to that of a 'high-tech' reactor as described in chapters 6 and 7 ( $\sim 0.3 \text{ mol m}^{-3} \text{ h}^{-1}$ , chapter 7), using immobilized cells in a packed-bed bioreactor and an organic solvent as substrate and product reservoir. The disappointing performance of the latter reactor type is illustrated in Figure 1, which is adopted from Cooney [5]. The volumetric

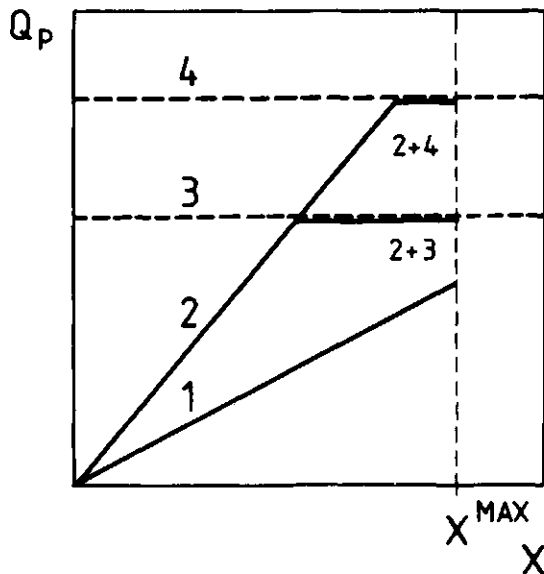


**Figure 1.** Volumetric epoxide productivity,  $Q_p$ , as a function of the biocatalyst concentration,  $X$ , for two values of the specific epoxidation activity,  $V_M$ , of the biocatalyst (low (1) and high (2)); mass-transfer limitations: fermentor (3), packed-bed organic-liquid-phase/immobilized-cell reactor (4); see text for discussion.

epoxide productivity,  $Q_p$ , is given as a function of the biocatalyst concentration,  $X$ , for two values, low (1) and high (2), of the specific epoxidation activity,  $V_M$ , of the biocatalyst. The vertical dashed line represents the maximal catalyst concentration, while the horizontal lines represent the mass-transfer restrictions to production rates of the two bioreactor types (fermentation (3) and the packed-bed reactor used in this work (4)). The lines are arbitrarily chosen. Due to the present low cell activities (1), mass-transfer rates in both reactor types (3 and 4) are not constraining the epoxide production even with cell concentrations (in suspension or in alginate beads) close to the maximal value. Only when large gel particles (2 to 3 mm) in combination with low substrate concentrations ( $< \sim 100 \mu\text{M}$  in gel phase) are employed, internal diffusion in the immobilized-cell particles (chapters 4, 5 and 6) becomes manifest (i.e. line 4 is so far lowered that it crosses line 1). Therefore, conventional fermentation would be the most economical process scheme (though still unattractive, see above), especially as the product, propene oxide, is volatile enough to be stripped out of the cell suspension by the propene/air mixture. The latter would facilitate recovery of the epoxide and reduce product inhibition. Fermentation with immobilized cells may be applied as a possible way to increase the maximal cell concentration,  $X^{\text{MAX}}$ , and, thus, the productivity [6, 7]. However, besides prolonging the half-live of the cells (chapter 7, [8]), enhancing the epoxidation activity of the cells would be the most rational procedure to attain higher productivities (1 $\rightarrow$ 2). The use of an organic solvent as substrate reservoir might in that case become essential for sufficient supply of the sparingly water-soluble substrates to the (immobilized) cells and, accordingly, to improve the productivity of the epoxide (2+3 $\rightarrow$ 2+4).

The above-mentioned considerations of the low cell activity do not automatically imply that the epoxidation of propene by *Mycobacterium* cells is not suited for use in a fundamental study of the application of water-immiscible organic solvents in biotechnological processes. Several basic concepts of organic-liquid-phase/immobilized-cell systems, like choice of solvent type, modelling of mass-transfer to and in the support material and design of a packed-bed organic-liquid-phase bioreactor, have been worked out, using substrate-consumption and epoxide-production data. The found principles and proposed diffusion and reactor models are believed to be useful for a broad range of bioconversions in biphasic media. In the next paragraphs a discussion of these phenomena will be presented.

## 8.2 Choice of the Organic Solvent

The simple question: 'which solvent should be used in two-liquid-phase biocatalysis' requires a not so simple answer. Many conflicting, experimental findings have been reported. For example, for the conversion of cholesterol to cholestenone by *Nocardia* cells toluene proved to be superior to e.g. cyclohexane and chloroform [9], while toluene was found to be poisonous for the '*Methanobac*' cells used by Playne and Smith [10] and also for the *Mycobacteria* used in this work (chapter 3). Further, application of tetrachloromethane did not affect the activity of a dehydrogenase enzyme [11] and resulted in reasonable rates of cholesterol oxidation by *Nocardia* cells [9, 12], but gave a low activity in case of propene-epoxidizing cells (chapter 3) and also in case of epoxidation by *Pseudomonas putida* cells [13]. In the latter investigation cyclohexane was found to be the optimal solvent. Part of these apparently contradictory results may be understood, if it is recognized, that solvent

effects can be divided in two groups:

- effects related to inhibition and/or denaturation of the enzyme or of enzyme systems (in case of whole cells solvent effects on cell organelles, notably leakage of membranes, could also be important)
- effects related to the solubilities of substrates and products in the solvent and to the partitioning of these compounds between the phases of interest

Thus, a solvent reported to be biocompatible could still lead to low productivities, if the solvent capacity for substrates and/or products is insufficient. As an illustration, Cremonesi et al. [11] observed that *n*-hexane did not decrease activity and stability of a dehydrogenase enzyme used for the reduction of cortisone. However, due to the low solubility of cortisone in *n*-hexane, the conversion was found to be very low. In contrast, the use of ethyl acetate and butyl acetate resulted in lower activities and stabilities, but yielded the highest conversions, as a result of the high substrate solubilities in these two solvents. From the above, it can be concluded that many factors affect the choice of the organic solvent and that experimental testing of a series of possibly suitable solvents remains necessary. However, general rules for solvent optimization would be very helpful to facilitate this laborious work.

Some correlations between biocatalyst activities in biphasic systems and solvent properties have been reported. Duarte and Lilly [12] found that the rate of cholesterol oxidase by non-growing cells seemed to be influenced by the solubility in water of the solvents tested (ethers and chloro derivatives of methane and ethane), but no clear relation emerged. A weak correlation between the solvent solubility in water and activity retention was also noted in this work (chapter 3). Mostly, however, some measure for the polarity of the solvent has been used. Omata et al. [14] could relate high steroid-transformation activities of free *Nocardia* cells to low values of the dielectric constant of the employed organic solvents. In this work the Hildebrand solubility parameter,  $\delta$ , of the solvent, in combination with the molecular weight, was successfully used to explain not only the measured differences in propene-epoxidation activities of the immobilized cells, but also the comprehensive results of Playne and Smith [10] (chapter 3). Low polarities ( $\delta < \sim 8$ ) and high molecular weights ( $M > \sim 200$ ) were favorable for a high retention of cell activity. Laane et al. [15] recently showed, however, that the logarithm of the partition coefficient,  $\log P$ , of a given solvent in the standard octanol-water two-phase system is a more accurate parameter for the polarity than  $\delta$ , especially for apolar solvents. High values of the epoxidation activities of immobilized *Mycobacterium* cells and of the gas production rates of free '*Methanobac*' cells [10], both used in chapter 3, clearly related to high  $\log P$ -values (low polarity,  $\log P > 4$ ). In this case the molecular weight of the solvent appeared not necessary.

The polarity of the organic solvent, preferably expressed by the  $\log P$  parameter, is, thus, suited to make a first selection from the vast list of possible solvents. Non-polar solvents generally are more biocompatible than more polar solvents. However, as discussed above, biocompatibility is not the only determining factor. The capacity of the solvent to dissolve substrates and products is also of importance. The polarity can also in this case be used to facilitate the choice of an optimal solvent, as the solubility of a compound in an organic solvent can often be related to the polarity of that solvent (chapter 3). Optimization of the solvent polarity will be likely, as a high solvent capacity may well conflict with biocompatibility requirements. For example, many common solvents, known for their high extraction capacities, like 1-hexanol, chloroform, benzene, toluene, tetrachloromethane and diisopropylether, may lead to low retentions of biocatalytic activity, as these solvents



all possess more or less polar characteristics ( $\log P$  values  $\leq 2.8$  [16],  $\delta$  values  $\geq 8.6$ , except diisopropylether:  $\delta = 7.1$ ). Rules for the optimization of solvent polarity were recently given by Laane et al. [16]. The polarity of the interphase between biocatalyst and the organic solvent was also considered. The authors argued that in general an optimal situation would be approached, when the solvent polarity (expressed by  $\log P$ ) was close to the polarity of the product, while the difference between solvent and substrate polarity should be as large as possible. For biocompatibility the  $\log P$  value of the solvent must, however, be larger than 2, preferably 4. Furthermore, for the polarity of the interphase these rules are the other way round: interphase polarity close to substrate polarity and a large difference between interphase and product polarity. These rules were supported by experimental measurements of enzymatic reaction rates in a reversed-micelle system.

The following two comments can be made with respect to the work of Laane et al. [16]. Firstly, enhancement of the difference in polarity between organic solvent and substrate could in certain cases increase the partition coefficient of the substrate between the interphase and the organic solvent phase and, hence, would lead to higher substrate concentrations near the biocatalyst in the interphase (see Figure 2).

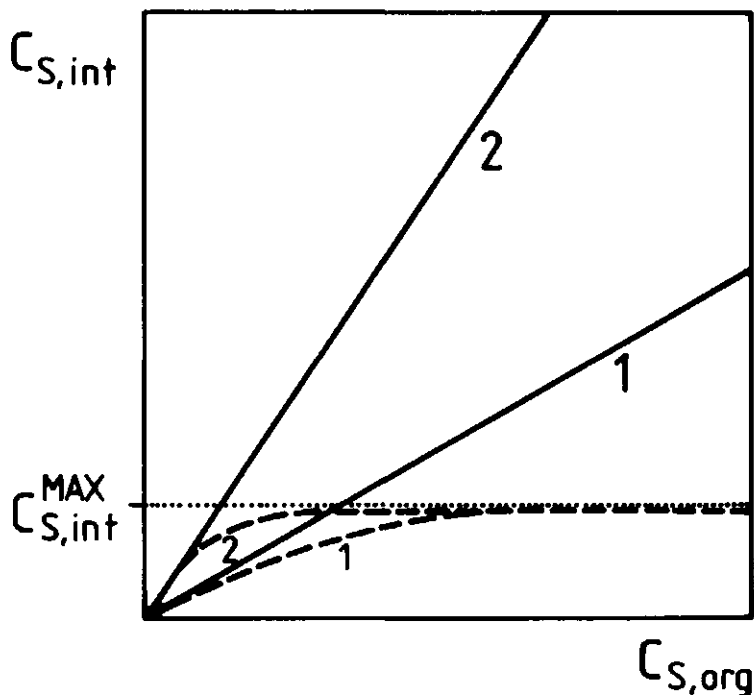


**Figure 2.** Substrate concentration in the interphase ( $C_{S, int}$ ) versus substrate concentration in the organic solvent phase ( $C_{S, org}$ ). Effect of solvent polarity on partitioning of a (non-polar) substrate between the interphase and the solvent; 1: small difference between substrate and solvent polarity, 2: large difference between substrate and solvent polarity; substrate miscible in all proportions with interphase (—), substrate with a limited solubility in an aqueous interphase (---).

A similar phenomenon was observed by Omata et al. [14], who found that increasing the solvent polarity facilitated the permeability of hydrophobic compounds in a hydrophilic gel. In many biphasic, biocatalytic conversions, however, the interphase will be water or a hydrophilic phase (see e.g. Figure 2 in chapter 1). The concentration of a non-polar substrate in an aqueous interphase will often be mainly determined by the maximal, usually very low solubility of that compound in water (Figure 2), and hardly by the polarity of the water-immiscible solvent adjacent to the interphase. Maximizing the difference between solvent and substrate polarity would in that case be irrelevant. Furthermore, the polarity of the interphase in a reversed-micelle system is relatively easy to adopt by varying surfactants and cosurfactants. In case of an aqueous interphase the possibilities of changing the polarity of the microenvironment of the biocatalyst are, however, limited.

Secondly, one should not only consider bipartitioning of the substrate between the solvent and the interphase, but also the absolute substrate concentration possible in the solvent, which will determine the storage capacity of the solvent for the reactant. High substrate concentrations in the solvent are in this respect desirable for minimizing the volume of the reaction mixture. The latter could conflict with the above proposed rule of maximizing the difference in polarity between solvent and substrate.

### 8.3 Hydrophilic versus Hydrophobic Matrices

The propene-epoxidizing cells used in this work were entrapped in calcium alginate, a hydrophilic gel. This natural support, a linear copolymer of D-mannuronic acid and L-guluronic acid, is one of the most widely employed materials to immobilize (high-molecular weight) enzymes and cells [17]. It can be considered as a typical example of the broad class of hydrophilic gels, to which agar, agarose, collagen, chitosan,  $\kappa$ -carrageenan, gelatin and some acrylic copolymers also belong. The propene-consumption rate and epoxide-accumulation rate of the *Mycobacterium* cells in calcium alginate strongly resembled that of the  $\kappa$ -carrageenan gel-entrapped cells (chapter 3). Apart from many advantages (see below), immobilization in alginate (or more general in hydrophilic carriers) possesses one significant drawback: the solubility of reactants in the gel is of the same order of magnitude as that in water. Especially for sparingly water-soluble substrates, this could lead to a serious internal mass-transfer limitation in hydrophilic beads. Decreasing the size of the gel particles is only of limited use, as particle diameters smaller than about 0.5 mm are difficult to produce and will cause operating problems in large-scale reactors. The effects of mass transfer were quantified in chapters 4 and 5. Despite the low epoxidation activities, internal diffusion could limit the reaction rate, if large particles were used (2 to 3 mm).

In principle, the problem of low solubility of apolar compounds in hydrophilic gels could be avoided by employing more hydrophobic supports. This was achieved by Fukui and Tanaka [18], who developed methods for entrapping biocatalysts in synthetic gels of different degrees of hydrophilicity/hydrophobicity (e.g. photo-cross-linkable resin prepolymers and urethane prepolymers). These authors demonstrated the feasibility of this approach for converting non-polar compounds in various organic-liquid-phase/immobilized-biocatalyst systems. It was shown that the reaction rate of prepolymer-entrapped biocatalysts could be enhanced by using more hydrophobic gels. This increase could be related to higher partition coefficients

of the substrates between the gel and the solvent. The work of Fukui and Tanaka thus corresponds to the in the previous section mentioned optimization rules suggested by Laane et al. [16], who proposed matching the interphase (in this case gel) polarity to the substrate polarity. Propene-epoxidation experiments were also carried out with *Mycobacterium* cells immobilized in a hydrophobic urethane prepolymer (PU-3). The by Omata et al. [19] described procedure of immobilization was followed. The half-live of the cells in PU-3 (~2 h) appeared much lower than that of alginate gel-entrapped cells (~2 days) [20]. Therefore, prepolymer methods were not applied in the work described in this thesis. In general, however, entrapment in hydrophobic gels seems to be a very promising technique, especially for the conversion of non-polar reactants. Below the pros and cons of hydrophilic and hydrophobic matrices will be examined in more detail.

The two types of biocatalyst entrapment, hydrophilic gels and hydrophobic gels (especially the prepolymer methods proposed by Fukui and Tanaka [18]), are compared in Table 1. Emphasis is placed on the use of these gels in water/organic solvent biphasic systems.

**Table 1.** Characteristics of hydrophilic and hydrophobic gels. See text for discussion

	hydrophilic	hydrophobic
biocompatibility of support material	++	+/-
convenience	++	-(?)
protection against harmful solvent effects	++	-
solubility of non-polar substrates	--	++
effective diffusion coefficients	+	?
modelling of mass-transfer effects	++	-(?)
use in slurry reactors	--	+
use in fixed-bed reactors	+/-	+(?)

#### *Biocompatibility of support material*

Hydrophilic gels are often isolated from natural materials (e.g. marine algae). This, the high water content (high water activity) and the mild immobilization procedure could explain why so many biocatalyst have been successfully immobilized in these gels. The entrapment of *Mycobacterium* cells in calcium alginate and in  $\kappa$ -carrageenan also resulted in almost no activity loss (chapter 3). In contrast, hydrophobic materials are often synthetic and usually contain less water. Thus, it can be expected that the number of biocatalysts, that can be entrapped in hydrophobic matrices with high retention of activity, is significantly smaller than in the case of hydrophilic supports.

### *Convenience*

The technique of immobilization in hydrophilic gels is usually very convenient. Only practical experience can make this fully understood. The procedure is mild, flexible, reproducible and permits a high loading of biocatalyst. If desired for modelling purposes, the shape of the particles can be made almost spherical. Also, successful scale-up techniques of the immobilization process have been reported [21, 22, 22a]. Thus, if needed, larger quantities of immobilized biocatalyst can be produced. Scale-up methods for hydrophobic gels have not been developed yet. Furthermore, the gels prepared by prepolymer methods are usually cut into (cubic) particles. This makes modelling inconvenient and excludes the use of very small particles (< 1 mm).

### *Protection against harmful solvent effects*

The employed water-immiscible solvent may inactivate the biocatalyst and interfere with the mechanical and/or chemical stability of the support material. In case of hydrophilic gels these effects will be minimized as a result of the low solvent concentration in the aqueous gel. For hydrophobic gels the situation could be different. Like the solubility of a non-polar substrate, the solvent solubility in the gel is probably also relatively high, thereby increasing the risk of damage to the biocatalyst or to the carrier.

### *Solubility of non-polar substrates*

As discussed already above, the characteristic advantage of hydrophobic gels is their high capacity for water-insoluble substrates. The gel hydrophobicity can even be adopted to that of the substrate to be converted. This could reduce any internal-diffusion limitations, often found when using aqueous gels (chapters 4 and 5). The picture becomes, however, more complicated if the product concentration in the gel is also determining the production rate (e.g. product inhibition). In case of apolar products, a large difference in polarity between gel and product [16] would be easier achieved with hydrophilic gels.

### *Effective diffusion coefficient*

The degree of internal-diffusion limitation is also determined by the effective diffusivities of substrates and products in the support material. The availability of accurate estimates for effective diffusion coefficients is, thus, of importance for the design of immobilized-biocatalyst reactors. Apparently, this observation has become more recognized in recent years, as the number of papers dealing with the determination of effective diffusion coefficients is steadily growing. A general trend in the findings of these reports is that effective diffusion coefficients of low-molecular weight compounds (e.g. oxygen, ethanol and glucose) in hydrophilic gels (often 1 to 4% calcium alginate) are usually not much lower than the corresponding diffusion coefficients in water [23-26]. This observation was used in the modelling of (internal) diffusion effects on the epoxidation kinetics of the alginate-entrapped cells (chapters 4 and 5). From the agreement between predicted and experimental substrate-consumption rates, it was among others concluded that the assumed effective diffusion coefficients were reasonably accurate. Not only the relatively high value of the effective diffusion coefficient in hydrophilic matrices, but also the fact that rather reliable estimates are available for this case, can be considered as additional advantages of using hydrophilic gels. For hydrophobic gels values for effective diffusion coefficients seem not to be available yet.

### *Modelling of mass-transfer effects*

In chapters 4 and 5 it was shown that modelling of coupled reaction and diffusion phenomena in calcium alginate beads is relatively straightforward. Other, similar examples, using hydrophilic gels as the support material, have been reported (e.g. see references 14, 19, 20 to 24 in chapter 4). Again, little is known with respect to the description of reaction and diffusion in hydrophobic gels. The fact that spherical particles cannot easily be obtained seems to be a drawback.

### *Use in slurry reactors*

Like the bulk of described two-liquid-phase biocatalytic reactions, bioconversions in biphasic systems using biocatalysts entrapped in hydrophilic gels are often carried out in small, shaken or stirred laboratory vessels (e.g. [27]). Accordingly, little is known about the hydrodynamics of these systems, especially about how to obtain a well-defined suspension of the hydrophilic beads in a hydrophobic solvent in case of class B2 and C3 systems (Figure 2, chapter 1). If special measures are not taken, e.g. coating of the gel particles with a hydrophobic substance, the creation of a sufficient solvent/gel contacting efficiency may be very cumbersome as a result of the high surface tension between particles and solvent. For this reason, we employed a fixed bed to contact the alginate beads with the solvent, n-hexadecane, as described in chapter 6. Surface tensions between beads and solvent will be lower in case of entrapment in a hydrophobic matrix. This probably makes slurry reactors easier to operate.

### *Use in fixed-bed reactors*

It is well-known that the compressibility of hydrophilic-gel materials is often high. This could lead to poor flow properties and high pressure drops, in case these gels are used as the packing material in fixed-bed reactors of a technical scale [28]. The rigidity of the particles may be enhanced by increasing the concentration of the support material or by partial shrinkage of the particles by gel drying [29], but in these cases lower values for effective diffusion coefficients can be expected. As reported in chapter 6, mixing of the alginate particles with small glass beads had to be used to improve the contacting efficiency between the alginate gel and the solvent and to prevent bed compaction. Few data exist concerning the flow characteristics of fixed beds of hydrophobic particles. The situation does not seem to be fundamentally different with respect to bed compaction. The lower surface tensions may, however, improve the contacting efficiency between the hydrophobic particles and the organic solvent.

From Table 1 it can be concluded that, if the solubility of a non-polar substrate in the gel material is severely limiting the conversion rate and/or a slurry reactor is essential, hydrophobic gels should be carefully considered when choosing the technique of immobilization. In case the other aspects of Table 1 are also of importance, the use of hydrophilic gels may be more advantageous, even for the conversion of apolar substrates. However, many characteristics of hydrophobic supports have to be worked out systematically and, thus, are subject to improvement.

## 8.4 Design of Fixed-Bed Organic-Liquid-Phase Bioreactors

In the previous two sections various factors determining the suitability of an organic solvent and of the polarity of the immobilized-biocatalyst phase for use in a water/organic solvent two-phase system have been discussed. The main design criteria were high retention of biocatalytic activity and the need for high mass-transfer rates between the liquid phase(s) and the solid immobilized-biocatalyst phase. However, if gaseous substrates are to be converted, as is the case in the work described in this thesis, mass transfer from the gas phase to the liquid phase(s) also has to be considered and could play a decisive role in the design of an optimal bioreactor. This situation will be examined in more detail below.

In chapter 6 it was argued that the fixed-bed reactor is an obvious reactor type for contacting hydrophilic-gel particles with an organic solvent in case of a class C3 system (no discrete aqueous phase, Figure 2 in chapter 1). This is a result of the very high surface tension between the gel material and the hydrophobic solvent. If supply of gaseous substrates is necessary, two contact schemes can be distinguished. One approach, adopted in chapter 6, is to separate the gas/liquid and liquid/solid contacting processes (e.g. see Figure 1 in chapter 6). Thus, one gas/liquid contactor and one two-phase fixed-bed reactor (or packed-bed reactor) are in that case needed. The other possibility is to establish the required phase contact between the three phases (gas, liquid and solid) in one three-phase fixed-bed reactor (or trickle-bed reactor). The first approach offers certain distinct advantages. Mass transfer between gas and liquid can be carried out in standard gas/liquid contactors (e.g. stirred vessel, bubble column, packed column, spray tower), which are relatively easy to design. Modelling of the transport processes in the packed bed, liquid/solid mass transfer and coupled diffusion and reaction in the immobilized-biocatalyst beads, is also straightforward (chapter 6). In contrast, the design of a three-phase fixed-bed reactor is much more complex (e.g. [30]). A complication, that may arise with separation of the liquid/solid contacting process from the gas/liquid contacting process, is depletion of gaseous substrates at the end of the packed-bed bioreactor. The use of an organic reaction medium could then be beneficial (chapter 6), as the solubilities of many gases in solvents are markedly higher than those in water. With aerobic processes oxygen exhaustion will probably be the main design criterium of the packed bed. The solubilities in organic solvents of any other, gaseous (non-polar) substrates are likely to be much higher than that of oxygen. Using in this work obtained, experimental reactor data (chapter 6), the design of a packed-bed organic-liquid-phase/immobilized-biocatalyst reactor, with oxygen as the limiting substrate, will be quantified below.

Suppose that the required volume,  $V_R$ , of a packed-bed immobilized-cell reactor is  $10 \text{ m}^3$  in order to meet a certain productivity ( $\text{mol h}^{-1}$ ) of stereospecific propene oxide. This volume can be determined from the specific epoxide production rate (taking into account product inhibition and epoxide consumption, chapter 7), the fraction of biocatalyst particles (calcium alginate) in the reactor ( $\epsilon_A \sim 0.3 \text{ m}^3 \text{ particle} (\text{m}^3 \text{ reactor})^{-1}$ , chapter 6), the cell density in the beads ( $X \sim 70 \times 10^3 \text{ g dry weight} (\text{m}^3 \text{ particle})^{-1}$ ) and, finally, using the assumption that the overall biocatalyst effectiveness of the consumption of the limiting substrate (oxygen, see above) is near unity. Internal-diffusion limitation can be shown to be negligible (chapter 4), if oxygen concentrations in the bulk of the used reactor medium are higher than  $\sim 200 \mu\text{M}$  (aqueous phase concentration, oxygen-consumption rate  $V_M \sim 5 \mu\text{mol min}^{-1} (\text{g}$

dry weight)<sup>-1</sup>, particle diameter  $d_p \sim 1$  mm). For simplification external-diffusion limitation is neglected (chapters 4 to 6).

The height to diameter ratio ( $H/D$ ) of the packed-bed bioreactor and the flow rate ( $\phi_v$ ) of the reaction medium are the two basic design parameters. The flow rate of the liquid, pre-saturated with a propene/(~20 vol%) oxygen mixture, should be large enough to assure high oxygen levels over the entire bed length. Oxygen concentrations in the reactor higher than ~200  $\mu\text{M}$  (aqueous phase concentration), and hence a biocatalyst effectiveness of about unity, can be obtained by keeping the oxygen conversion below ~20%. The latter can also be formulated mathematically as:

$$0.20 C_o \phi_v > \sim 5 \epsilon_A X V_M V_R \text{ (mol s}^{-1}\text{)} \quad (1)$$

in which  $C_o$  is the oxygen solubility in the reactor-inlet stream (at 1 atm oxygen).

**Table 2.** Properties of the three reaction media

reaction medium	$C_o$ (mM)	$\rho_L$ (kg/m <sup>3</sup> )	$\eta_L$ at 30°C (10 <sup>-3</sup> Ns/m <sup>2</sup> )
water	1.2	1000	0.8
n-hexadecane	5.9	773	3.1
perfluoro hydrocarbon (FC-72)	27	1680	0.7

This value is dependent on the type of reaction medium. Three biocompatible media (chapter 3) will be considered here: water, n-hexadecane and a perfluoro compound (FC-72, obtainable from 3M). The oxygen solubilities, densities ( $\rho_L$ ) and dynamic viscosities ( $\eta_L$ ) of these solvents are given in Table 2. Equation 1 can also be written as:

$$U > \sim 5 \epsilon_A X V_M H / (0.20 C_o) \quad (2)$$

in which  $U$  is the superficial velocity of the liquid. Equation 2 provides a lower limit for  $U$  as a function of the bed height,  $H$ . However, there is also an upper limit for the liquid velocity, as the latter is related to the pressure drop over the packed bed. To facilitate the calculations the well-known Ergun equation [31] will be applied here. Despite the dilution of the bed with small glass particles ( $d_p \sim 1$  mm, chapter 6), pressure drops may be higher than the thus calculated values due to the compressible nature of the alginate particles ( $\epsilon_A \sim 0.3$ , void fraction  $\epsilon \sim 0.35$ , fraction of glass beads  $\sim 0.35$ ). This effect will not be considered here. Using the Ergun relation, the pressure drop in a packed bed with height  $H$  can be estimated as:

$$\Delta P = 170 (1-\epsilon)^2 \eta_L U H / (\epsilon^3 d_p^2) + 1.75 (1-\epsilon) \rho_L U^2 H / (\epsilon^3 d_p) \text{ (Nm}^{-2}\text{)} \quad (3)$$

The pressure drop should always be less than the maximal, allowable pressure drop,  $\Delta P^{\text{MAX}}$ , over the bed:

$$\Delta P < \Delta P^{\text{MAX}} \text{ (Nm}^{-2}\text{)} \quad (4)$$

A reasonable value for  $\Delta P^{\text{MAX}}$  is 10<sup>5</sup> Nm<sup>-2</sup> (1 bar). The upper limit for the

superficial velocity as function of the bed height can be obtained by combining equations 3 and 4.

For facilitating the distribution of liquid over the bed and for other, practical reasons, the bed height to diameter ratio should not be too small:

$$(H/D) > \sim 1 \quad (5)$$

or with  $V_R = 10 \text{ m}^3$ :

$$H > \sim 2.3 \text{ (m)} \quad (6)$$

The lower limits of the superficial velocity (equation 2) and the bed height (equation 6) and the upper limit of  $U$  (equations 3 and 4) are visualized in a graph of  $U$  versus  $H$  (Figure 3). Using water as the reaction medium (Figure 3a), it can be observed that no combination of  $U$  and  $H$  can be found, which fulfills all of the above formulated requirements. The same applies with  $n$ -hexadecane as the transport medium, though this is not as clear as with water as the substrate reservoir. The higher oxygen solubility (Table 2) lowers the oxygen-depletion line, but the maximal-pressure line is also lowered due to the higher viscosity of  $n$ -hexadecane. Only in case of the perfluoro compound, with its high capacity for oxygen, as the transport medium, an area of combinations of  $U$  and  $H$  can be distinguished, which satisfies the three mentioned conditions. Thus, assuming the validity of the used reactor data, the above calculations demonstrate that the application of a biocompatible, organic reaction medium with a high capacity for oxygen could make a technical-scale packed-bed reactor for propene epoxidation possible, and, furthermore, that separation of the gas/liquid and liquid/solid contacting processes is feasible. However, as discussed in section 8.1, much higher epoxidation rates are necessary for improving the process economics. In Figure 3c it can be seen that in that case the related, higher oxygen-consumption rates ( $V_M$ ) of the gel-entrapped cells could make even operation with a solvent with a very high capacity for oxygen, like perfluoro hydrocarbons, not feasible. A trickle-bed reactor might then be required for sufficient supply of oxygen at acceptable pressure drops.



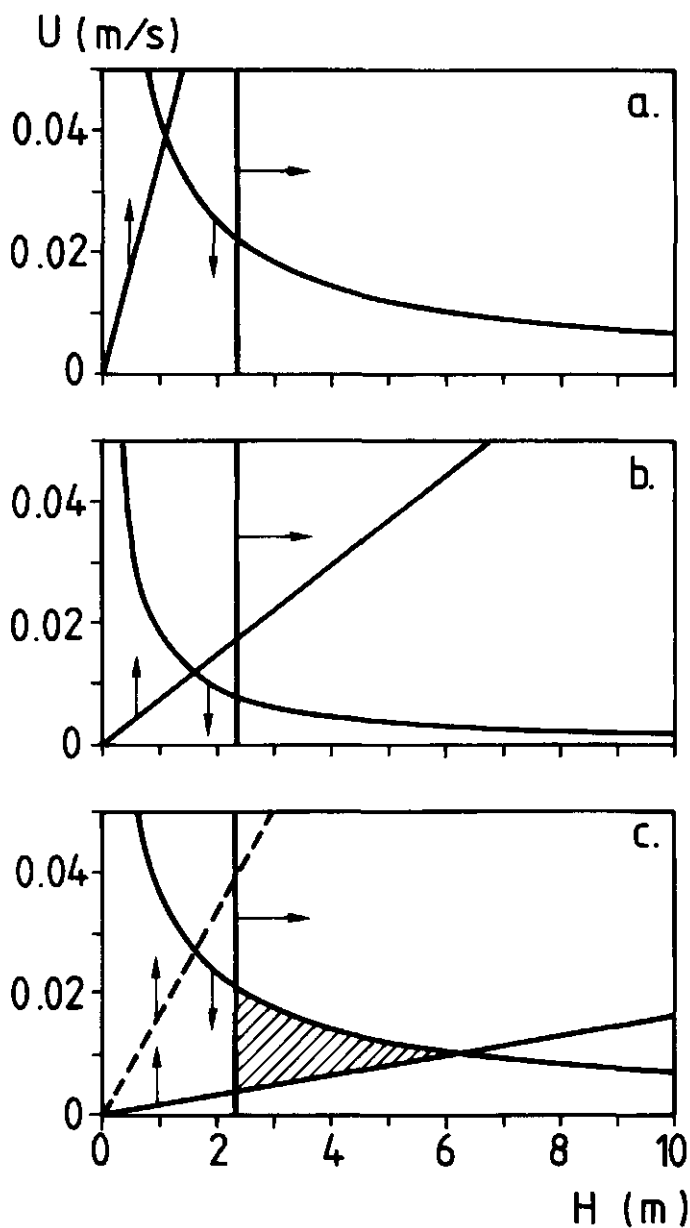


**Figure 3.** Three design criteria of a packed-bed immobilized-cell reactor (oxygen depletion ( $\uparrow$ ), pressure drop ( $\downarrow$ ), height to diameter ratio ( $\rightarrow$ )) visualized in a graph of the superficial velocity,  $U$ , versus the bed height,  $H$ ; reaction medium: water (a), *n*-hexadecane (b), perfluoro hydrocarbon (c). The hatched area represents combinations of  $U$  and  $H$ , which satisfy the three design criteria (see text). The dashed line represents the oxygen-depletion criterium in case of a higher oxygen-consumption rate ( $V_M \sim 50 \mu\text{mol min}^{-1} (\text{g dry weight})^{-1}$ ).

## 8.5 References

1. Habets-Crützen, A.Q.H., Brink, L.E.S., van Ginkel, C.G., de Bont, J.A.M. and Tramper, J. *Appl. Microbiol. Biotechnol.* 1984, **20**, 245-250
2. Barman, Th.E. in *Enzyme Handbook*, Springer Verlag, New York, 1969, vols. 1 and 2
3. Linko, P. and Linko, Y.-Y. in *CRC Critical Reviews in Biotechnology*, CRC Press, Inc., Cleveland, OH, 1984, vol. 1, pp. 289-338
4. Habets-Crützen, A.Q.H., Carlier, S.J.N., de Bont, J.A.M., Wistuba, D., Schurig, V., Hartmans, S. and Tramper, J. *Enzyme Microb. Technol.* 1985, **7**, 17-21
5. Cooney, C.L. *Science* 1983, **219**, 728-733
6. Radovich, J.M. *Enzyme Microb. Technol.* 1985, **7**, 2-10
7. Karel, S.F., Libicki, S.B. and Robertson, C.R. *Chem. Eng. Sci.* 1985, **40**, 1321-1354
8. Habets-Crützen, A.Q.H. and de Bont, J.A.M. (submitted)
9. Buckland, B.C., Dunnill, P. and Lilly, M.D. *Biotechnol. Bioeng.* 1975, **17**, 815-826
10. Playne, M.J. and Smith, B.R. *Biotechnol. Bioeng.* 1983, **25**, 1251-1265
11. Cremonesi, P., Carrea, G., Ferrara, L. and Antonini, E. *Biotechnol. Bioeng.* 1975, **17**, 1101-1108
12. Duarte, J.M.C. and Lilly, M.D. in *Enzyme Engineering* (Weetall, H.H. and Royer, G.P., eds), Plenum Press, New York, 1980, vol. 5, pp. 363-367
13. Harbron, S., Smith, B.W. and Lilly, M.D. *Enzyme Microb. Technol.* 1986, **8**, 85-88
14. Omata, T., Tanaka, A. and Fukui, S. *J. Ferment. Technol.* 1980, **58**, 339-343
15. Laane, C., Boeren, S. and Vos, K. *Trends in Biotechnol.* 1985, **3**, 251-252
16. Laane, C., Boeren, S., Vos, K. and Veeger, C. *Biotechnol. Bioeng.* (in press)
17. Tramper, J. *Trends in Biotechnol.* 1985, **3**, 45-50
18. Fukui, S. and Tanaka, A. *Adv. Biochem. Eng.* 1984, **29**, 1-33
19. Omata, T., Iida, T., Tanaka, A. and Fukui, S. *Eur. J. Appl. Microbiol. Biotechnol.* 1979, **8**, 143-155
20. Brink, L.E.S. and Tramper, J. (unpublished results)
21. Klein, J., Stock, J. and Vorlop, K.-D. *Eur. J. Appl. Microbiol. Biotechnol.* 1983, **18**, 86-91
22. Hulst, A.C., Tramper, J., van 't Riet, K. and Westerbeek, J.M.M. *Biotechnol. Bioeng.* 1985, **27**, 870-876
- 22a. Rehg, T., Dorger, C. and Chau, P.C. *Biotechnol. Lett.* 1986, **8**, 111-114
23. Sato, K. and Toda, K. *J. Ferment. Technol.* 1983, **61**, 239-245
24. Tanaka, H., Matsumura, M. and Veliky, I.A. *Biotechnol. Bioeng.* 1984, **26**, 53-58
25. Adlercreutz, P. *Biotechnol. Bioeng.* 1986, **28**, 223-232
26. Hannoun, B.J.M. and Stephanopoulos, G. *Biotechnol. Bioeng.* 1986, **28**, 829-835
27. Duarte, J.M.C. and Lilly, M.D. in *Enzyme Engineering* (Weetall, H.H. and Royer, G.P., eds), Plenum Press, New York, 1984, vol. 7, pp. 573-576
28. Buchholz, K. and Gödelmann, B. in *Characterization of Immobilized Biocatalysts* (Buchholz, K., ed.), Dechema Monograph No. 1724-1731, Verlag Chemie, Weinheim, 1979, vol. 84, pp. 127-135
29. Klein, J. and Wagner, F. in *Biotechnology*, Dechema Monograph No. 1693-1703, Verlag Chemie, Weinheim, 1978, vol. 82, pp. 142-150
30. Sweed, N.H. in *Multiphase Chemical Reactors* (Rodrigues, A.E., Calo, J.M. and Sweed, N.H., eds), Sijthoff and Noordhoff, Alphen aan den Rijn, The Netherlands, 1981, vol. 2, pp. 135-155
31. Beck, W.J. and Muttzall, K.M.K. in *Transport Phenomena*, John Wiley and Sons, London, 1975, pp. 112-120

## SUMMARY

Replacement of a considerable part of the traditional, aqueous reaction medium in biotechnology by an organic medium is a promising technique to broaden the scope and range of biotechnological processes. This seems especially to be true for the conversion of non-polar substances. The high capacity of solvents for sparingly water-soluble substrates and products could reduce the required volume of the reaction mixture significantly, and may also lead to less substrate and/or product inhibition in the aqueous biocatalyst phase, when these mechanisms are involved. Furthermore, the use of an organic solvent could shift reaction equilibria favourably and facilitate down-stream processing. In chapter 1 a general review is presented of non-aqueous solvent systems in biocatalytic processes. Special attention is paid to two-liquid-phase systems, involving water-immiscible solvents. Several facets of these biphasic systems have been studied in this thesis using the epoxidation of propene by gel-entrapped *Mycobacterium* cells as a model.

After the description of the throughout this work employed techniques of gas-analysis automatization and of substrate-level control (chapter 2), the far-reaching consequences of the solvent choice are treated in chapter 3. Many solvents cause rapid inactivation of the free, propene-epoxidizing cells. This appears also to be the case if the cells are immobilized in calcium alginate. However, the support material prevents direct cell-organic solvent contact and the associated aggregation and clotting of cells, mostly accompanied with loss of activity. High activity retentions of the immobilized cells relate to low polarities and high molecular weights of the used solvents. The polarity, as expressed by the Hildebrand solubility parameter, is also useful for describing the solvent capacity for one of the two substrates, oxygen, and for the product, propene oxide. The capacity for propene is less well described by the Hildebrand solubility parameter, but also less relevant, as the capacity of the solvents for propene is always about two orders of magnitude higher than that of water, and thus limitation of the rate by insufficient supply of propene is less likely to occur. It is stressed that optimization of the solvent polarity is necessary, as the requirement of a high activity retention conflicts with the need for a high solvent capacity for the polar propene oxide. Optimization of the polarity will also be likely in case of other types of two-liquid-phase bioconversions.

External and internal-diffusion limitations, which are to be expected when using cells entrapped in a hydrophilic gel, are quantified in chapters 4 and 5. With negligible product inhibition, satisfactory predictions of the mass-transfer effects on the intrinsic Michaelis-Menten kinetics of the immobilized cells are obtained by using a simple pore-diffusion model (chapter 4). Internal diffusion is found to severely limit the epoxidation rate. A more complex model for the intrinsic epoxidation kinetics has been derived for modelling of mass-transfer rates in case of product inhibition (chapter 5).

The microkinetic model defined in chapter 4 is integrated in a macrokinetic model to describe the behaviour of a packed-bed immobilized-cell reactor (chapter 6). Depletion of the limiting substrate, oxygen, along the length of the bioreactor can be prevented by using an organic solvent, n-hexadecane, as the transport medium. It is argued that this finding may eliminate the need for a separate gas phase in the fixed-bed reactor. Model predictions of the oxygen conversion in the bioreactor at various degrees of external and internal-diffusion limitation, at various liquid space times and with water or n-hexadecane as the continuous phase are in good

agreement with experimentally obtained values. In chapter 7 some other, main limitations of the epoxide production in the packed-bed organic-liquid-phase/immobilized-cell reactor are quantified. Product inhibition is reduced by absorption of the inhibitory epoxide in a cold di-n-octyl phthalate phase. The stability of the immobilized cells is increased by supplying the cells alternately with propene and a co-substrate (ethene). About 50 g dry weight of cells in a 1.7 dm<sup>3</sup> packed-bed reactor were used, which produced ~1.5 g chiral propene oxide; two third of the epoxide was absorbed in the octyl phthalate phase.

Finally, in the last chapter of this thesis a general discussion is presented. The significance of optimization of the solvent polarity and of the interphase polarity, i.e. the polarity of the phase between biocatalyst and organic solvent is underlined. In case of entrapment in prepolymers, the hydrophobicity/hydrophilicity balance of the gel can be optimized with respect to polarities of substrates and products. Several features of hydrophilic and hydrophobic gels are compared. A quantitative illustration is given concerning the design on a technical scale of a fixed-bed organic-liquid-phase/immobilized-cell reactor. The advantages of using solvents with a high substrate capacity (often oxygen in case of aerobic processes) are demonstrated.

## SAMENVATTING

Vervanging van een aanzienlijk deel van het traditionele, waterige reactiemedium in de biotechnologie door een organisch medium is een veelbelovende techniek om het aantal toepassingsmogelijkheden van biotechnologische processen te verhogen en/of de economische haalbaarheid van deze processen te verbeteren. Dit lijkt vooral te gelden voor de omzetting van apolaire stoffen. De hoge capaciteit van organische oplosmiddelen voor slecht in water oplosbare substraten en producten kan het benodigde reactievolume sterk verkleinen en kan tevens de invloed van eventuele substraat- en/of productremming verminderen. Het gebruik van een geschikt organisch solvent zou ook reactie-evenwichten in gunstige zin kunnen doen verschuiven en de productopwerking kunnen vergemakkelijken. Een algemeen overzicht van niet-waterige oplosmiddelsystemen in biokatalytische processen is gegeven in hoofdstuk 1. Speciale aandacht wordt daarbij geschonken aan water/organisch solvent twee-fase systemen. De epoxidatie van propeen door geïmmobiliseerde *Mycobacterium* cellen is in dit proefschrift als model gebruikt bij de bestudering van de verschillende facetten van deze twee-fase systemen.

Na de beschrijving van de belangrijkste, in dit werk gebruikte experimentele technieken, automatische gasanalyse en regeling van de substraatconcentraties, in hoofdstuk 2, worden de verstrekkende gevolgen van de keuze van het organisch solvent behandeld in hoofdstuk 3. Veel solvents veroorzaken een snelle afname van de epoxidatie-activiteit van vrije en van in calcium alginaat gel ingesloten cellen. Gelinsluiting voorkomt echter direct contact tussen cellen en organisch solvent en de daarmee gerelateerde aggregatie en klontervorming van cellen, veelal gepaard gaand met verlies van activiteit. Hoge activiteitsretenties van de geïmmobiliseerde cellen worden aangetroffen bij gebruik van solvents met lage polariteiten en hoge molecuulgewichten. De polariteit, zoals uitgedrukt door de Hildebrand oplosbaarheidsparameter, kan ook bruikbaar zijn bij de beschrijving van de capaciteiten van de solvents voor zuurstof en voor het product, propeenoxide. De capaciteit voor propeen wordt minder goed beschreven door de Hildebrand oplosbaarheidsparameter, maar is ook minder relevant, aangezien de solventcapaciteit voor propeen vrijwel steeds ongeveer twee orden van grootte hoger is dan de capaciteit van water, en limitatie van de reactiesnelheid door onvoldoende toevoer van propeen dus onwaarschijnlijk is. Optimalisering van de solventpolariteit is noodzakelijk, aangezien solvents met een hoge extractiecapaciteit voor het polaire propeenoxide tevens celinactivering zullen veroorzaken. Ook bij andere water/organisch solvent biokatalytische reacties zal optimalisering van de polariteit in veel gevallen nodig zijn.

Insluiting van de cellen in het hydrofiele calcium alginaat kan aanleiding geven tot externe en interne diffusielimitering. In hoofdstukken 4 en 5 zijn deze limitaties gequantificeerd. Bevredigende voorspellingen van de stoftransporteffecten op de intrinsieke Michaëlis-Menten kinetiek van de geïmmobiliseerde cellen worden verkregen door gebruik te maken van een eenvoudig poriediffusiemodel (hoofdstuk 4). Interne diffusie in het geldeeltje blijkt de epoxidatiesnelheid sterk te kunnen limiteren. In hoofdstuk 5 wordt een uitgebreider model voor de intrinsieke epoxidatiekinetiek afgeleid om ook in het geval van productremming door het gevormde propeenoxide modellering van de stoftransportsnelheden mogelijk te maken.

Het in hoofdstuk 4 opgestelde model voor de microkinetiek is toegepast in een

macrokinetisch model van een gepakt-bed, geïmmobiliseerde-cel reactor (hoofdstuk 6). Uitputting van het limiterende substraat, zuurstof, aan het einde van de bioreactor kan worden voorkomen door gebruik te maken van een organisch solvent, n-hexadecaan, als het transportmedium. Dit kan de aanwezigheid van een afzonderlijke gasfase in de gepakt-bed reactor overbodig maken.

Modelvoorspellingen van de zuurstofconversie in de bioreactor bij verschillende niveau's van externe en interne diffusielimitering, bij verschillende verblijftijden van het reactiemedium en met water of n-hexadecaan als de continue fase blijken goed in overeenstemming te zijn met experimenteel verkregen waarden. In hoofdstuk 7 worden andere, belangrijke limiteringen van de epoxideproductie in een gepakt-bed, organisch-solvent/geïmmobiliseerde-cel reactor beschreven en gemodelleerd. De invloed van productremming kan worden verminderd door absorptie van het toxische epoxide in een koude di-n-octyl ftalaat fase. De stabiliteit van de geïmmobiliseerde cellen verbetert door de cellen afwisselend propeen en een co-substraat (etheen) aan te bieden. Ongeveer 1.5 g stereospecifiek propeenoxide is geproduceerd door gebruik te maken van 50 g (drooggewicht) cellen in een 1.7 dm<sup>3</sup> gepakt-bed reactor. Twee derde gedeelte van het gevormde epoxide is daarbij geabsorbeerd in de octyl ftalaat fase.

Dit proefschrift wordt tenslotte afgerond met een algemene discussie in het laatste hoofdstuk. Het belang van optimalisering van de solventpolariteit en van de polariteit van de fase tussen de biokatalysator en het organisch solvent wordt aangegeven. De hydrofoob/hydrofiel balans van deze 'tussenfase' kan bij insluiting in prepolymere geoptimaliseerd worden met betrekking tot de polariteiten van substraten en producten. De verschillende aspecten van hydrofobe en hydrofiële gelen worden met elkaar vergeleken. Het ontwerp van een gepakt-bed, organisch-solvent/geïmmobiliseerde-cel reactor op industriële schaal wordt geïllustreerd met behulp van een quantitatie voorbeeld, waarin duidelijk de voordelen van het gebruik van solvents met een hoge capaciteit voor het substraat (vaak zuurstof bij aerobe processen) naar voren komen.

## DANKWOORD

Bij de totstandkoming van dit proefschrift ben ik in het bijzonder dank verschuldigd aan de volgende personen en ondersteunende afdelingen:

Allereerst, Hans Tramper, die door zijn vele adviezen en opbouwende kritieken voor mij een ware leermeester in de kunst van de wetenschap is geweest. Karel Luyben en Klaas van 't Riet, voor de frequente, nuttige discussies. Ans Habets-Crützen, Sybe Hartmans en Jan de Bont, voor microbiële bijscholing. Tevens, Ido Wolters, voor praktische hulp (en niet alleen op technisch-wetenschappelijk gebied). Gerard van de Venne (HTS-Amsterdam), voor het bepalen van extractiecapaciteiten van lange series organische solvents. De Centrale Dienst in het Biotechnion, en dan denk ik met name aan de vakmensen van de technische werkplaats, de tekenkamer, de electronische en fotografische afdelingen en de instrumenten- en glaswerkmagazijnen. De glasinstrumentmakerij van de vakgroep Organische Chemie mag niet onvermeld blijven. Tenslotte, de leden van de STW-gebruikerscommissie, voor een kritische evaluatie van de onderzoeksresultaten.

Dit onderzoek werd mogelijk gemaakt door financiële steun van de Stichting voor de Technische Wetenschappen.

## CURRICULUM VITAE

Op 25 juni 1959 werd ik geboren in het in West-Friesland (N.-H.) gelegen Enkhuizen. Het voorbereidend wetenschappelijk onderwijs (VWO-B) werd gevolgd aan het St. Werenfridus Lyceum in het tevens in genoemde streek gesitueerde Hoorn. In 1977 nam mijn wetenschappelijke carrière echter werkelijk een aanvang met een studie in de Scheikundige Technologie aan de TU Delft. Het afstudeeronderwerp werd uitgevoerd bij de vakgroep Chemische Technologie (Laboratorium Apparatenbouw voor de Procesindustrie) en behelsde de modellering van een continue suikerkristallisator op pilot-plant schaal. Verder hadden vooral toegepaste thermodynamica (scriptie) en automatisering in de chemie mijn speciale interesse. Een stage in Zuid-Afrika bleek voor mij in allerlei opzichten een 'eye-opener' te zijn. Kort na de afronding van mijn studie (augustus 1982) ben ik gestart met een vierjarig, door ZWO (STW) gefinancierd promotie-onderzoek bij de sectie Proceskunde (vakgroep Levensmiddelentechnologie) van de LU Wageningen.